A Continuous Authentication Approaches for Data Security Services against Reconstruction Attacks using Multiple Biometric	S. Gunasundari	Computer Science	International Journal of Advanced Research in Computer and Communication Engineering	2017	ISSN (Online) 2278-1021 ISSN (Print) 2319 5940	h-indexed https://ijarcce.com/upload/2017/february-17/IJARCCE%20109.pdf

IJARCCE

ISSN (Online) 2278-1021
ISSN (Print) 2319 5940

International Journal of Advanced Research in Computer and Communication Engineering
ISO 3297:2007 Certified
Vol. 6, Issue 2, February 2017

A Continuous Authentication Approaches for Data Security Services against Reconstruction Attacks using Multiple Biometric

Mrs. S. Gunasundari M.Sc., M.Ed., M. Phil[1], Miss. R. Punitha[2]

Assistant Professor, Department of Computer Science, Sakthi college of Arts and Science for Women, Oddanchatram[1]

M. Phil Scholar, Department of Computer Science, Sakthi college of Arts and Science for Women, Oddanchatram[2]

Abstract: Internet Security and data privacy is preserved by the appropriate authentication schemes. User name and password based authentication is the fundamental step to access internet services. The conventional authentication system follows initial session verification rather than continuous verification. The continuous authentication is referred as the detection of authorized users and authenticating them even after successful login. This type of continuous authentication technique plays vital role in internet security as it performed by various types of authentication schemes. In this paper, a complete authentication protocol is used, which focuses on the throughout authentication scheme that is from login to logout time. This system about the authorized person's face detection for throughout session (From login time to logout time).The Web camera placed in front of the system in which they are working that camera will capture the face of the authorized person if the person start to move from the camera the capturing process will struck and the transaction will not allow the unauthorized persons to work. This application is fully applied with the camera. Once the person wants to do the transaction then he should sit in front of the camera and the face is authenticated for further steps. The camera will continuously monitor the face to avoid in authenticate transactions. If the user tries to move from the camera then the transaction will not be continued. It will get struck. So, user should be there until he/she finishes the transactions. This project utilizes face matching algorithm and canny and sobal algorithm for edge detection.

Keywords: Face matching, Finger print recognition, authentication, Internet Security, biometric techniques, continuous authentication.

I. INTRODUCTION

Data security and secure User authentication is an ultimate goal of almost all applications. All application has the aim to authenticate user for secure data access. This yearned lots of attention due to the recent boosting in the frequency and complexity of cyber-attacks. Nowadays authentication systems are grown with different types of working procedures and attribute against those attacks. In traditional authentication system, username and passwords are used for authentication. All authentication techniques such as biometric, device based and graphical passwords are used at the time of login, there is no verification performed during the session. In some traditional web mail servers such as Yahoo, used active screen monitoring technique [1]. This allows the users to logout the session if they are inactive. This type of traditional method avoids unauthorized access in the website. The services will be provided after successful authentication and the resources will be available for a fixed period of time. This kind of authentication is typically based on single session verification. This approach believes that a single verification, when performed at the beginning of the session is sufficient, and that the identity of the user is constant during the whole session. So there is a need to develop a continuous verification for secure throughout the session. In this paper, we surveyed various techniques and tools used for web security.

Internet security consists of the procedures adopted to monitor and prevent authorized entry in remote a computer network. Internet security involves the authorization of access to data in a distributed manner, which has more challenges in the real time phenomenon. Internet security begins with basic username and password verification. This type of verification only consist the password field, this type of authentication is known as single factor authentication. Security management for internet is different from the normal desktop security application [2]. A desktop application security only requires basic security when comparing with the internet applications, this type of applications needs strong techniques along with new hardware support to thwart hacking and other types of attacks [3]. To resolve this issue, we need continuous user authentication methods that continuously monitor and authenticate users based on some biometric elements. Earlier mechanisms for continuous user authentication cannot authenticate users without biometric observation, so biometric authentication is useful for continuous authentication. In such application, the continuous user authentication to be easy

IJARCCE
ISSN (Online) 2278-1021
ISSN (Print) 2319 5940
International Journal of Advanced Research in Computer and Communication Engineering
ISO 3297:2007 Certified
Vol. 6, Issue 2, February 2017

to use, passive authentication is desirable because the system should not require users' active cooperation to authenticate users continuously. The passive authentication is using faces as default continuous verification.

Need for Authentication

Authentication is the process which allows a user to validate their self before accessing their data. If the server and client cannot properly authenticate, there is no belief in the actions on information provided by their part. Authentication can involve highly hard and tricky methods to provide high level security. The simplest form of authentication is the one factor authentication, which stated above.

1. **Frequency of security contravention:** in real time internet applications and social networks such as twitter, Facebook and linked in have R&D departments, which captures and monitors the authentication and access activities [4].

2. **Enhanced methods of authentication** have "morphed from traditional tokens to USB devices to smart cards to fingerprint readers, soft tokens and scanning devices." Contextual authentication, based on analytics of behavior patterns and device patterns, is growing in importance and more vendors are offering it with their core user authentication products. In addition, there is an increased interest in using biometrics for a higher level of assurance with improved user experience, including form factors like voice recognition, iris matching, finger and other biometric features [5].

1.1 Role of Continuous Authentication

Continuous authentication is important not only for high security systems, but also low security systems. For example, an average user typically walks away from the computer for short breaks without logging out of the system. This opens up an opportunity for unauthorized users to access the computing resources easily. We evaluate the following three criteria for continuous user authentication [6].

1. Usability: The system should not require any additional verification for second time as long as the users are in front of the device. In such cases the system can't re-authenticate the user with any other biometric observations other than the face and posture. For example, it would be inconvenient for the user to meet the requirement of entering a password or provide his fingerprint whenever he takes a break to read a book or consult notes.

2. Security: The system should require active re-authentication of the user every time the user walks away from the application or system. This requirement will ensure that unauthorized users cannot access the resources after the legitimate user moves away.

3. Cost: In continuous authentication, cost is the important factor, because the remote system should possess proper hardware to complete the multi factor authentication and continuous authentication schemes. For this reason, the authentication system should use only the standard devices and avoid the use of high cost devices.

3. Internet Security through Biometrics:

Biometrics is the science of establishing identity of an individual based on the physical or behavioral attributes of the human. The relevance of biometrics in modern society has been reinforced by the need for large-scale identity management systems whose functionality relies on the accurate determination of an individual's identity in the context of several different applications over internet. Additionally, biometric authentication systems can be more convenient for the user which doesn't need to memorize, it achieves the privacy and a single biometric component can be used to access several accounts [7]. Some types of biometric data are illustrated below.

a. Physical biometrics based authentication
b. Behaviour based authentication

a. Physical biometrics based authentication

Face Biometrics:

Face detection and recognition includes many complementary elements, each part has its own. Depending on regular system each part can work individually. Face detection is an image processing concept that is based on learning algorithms to allocate human faces in digital images [8]. The biometric data's such as face matching and finger matching application need to be performed the following steps

- Face ,finger Recognition
- Feature extraction, and
- Face and finger matching
- Authentication.

Fingerprint Scan Biometrics:

Fingerprints are the common and widely used biometric component for almost all application. Due to it reliable nature, it is used in all application. When comparing with other biometric components such as iris, palm print or voice biometric the finger prints are easy to scan and match. So this is very useful with fast matching. The advancement of fingerprint can be recognition of veins and nerves with the help of high quality scanners [8]. This is unique and also we have numerous choice i.e., human have ten fingers. The user can use any finger among ten.
The following fig 1.0 shows the basic process associated with the biometric scanner system. The initial process of this system is feature extraction, there are several feature extracting techniques are available in the current research. We left the comparison of those techniques for future work. We examined different techniques and methods used in continuous verification.

IJARCCE
ISSN (Online) 2278-1021
ISSN (Print) 2319 5940
International Journal of Advanced Research in Computer and Communication Engineering
ISO 3297:2007 Certified
Vol. 6, Issue 2, February 2017

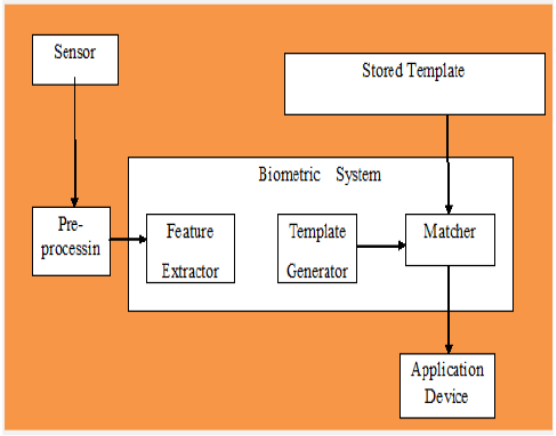

FIG 1.0 fingerprint scanning system architecture

In literature [9] there are several authors from the papers [10][11] have highlighted several security threats in biometric authentication, in order to eliminate the fake entry in biometric based authentication, Derakhshani et al. Proposed two software-based for fingerprint liveners detection, this also includes the other active parameters to match the fingerprint [12]. Soutar proposed a "hill-climbing" attack for a simple image recognition system based on filter based correlation. Using the matching scores returned from the matcher that was generated for each of the successive face images, this initial image is modified.

b. Behavior based authentication:

Keystroke Biometrics:
Keystroke biometrics or monitoring keystroke dynamics is considered to be an effortless behavioral based method for authenticating users which employs the person's typing patterns for validating his identity [13]. Keystroke dynamics is "not what you type, but how you type." In this approach, the user types in text, as usual, without any kind of extra work to be done for authentication. Moreover, it only involves the user's own keyboard and no other external hardware. All keystroke dynamics studies involve conducting five main experiment parts in the following order: recruiting participants, requesting a typing task to be done by the Participants, collecting the timing data of keystrokes, obtaining timing features from the raw keystroke data, training the classifier using part of the keystroke data and using the other part for testing the classifier [14].

c. Device based authentication
User authentication using devices are referred as more flexible and reliable way of verification, which fights against keylog and other types of attacks. Initially the devices such as mobile phones are used to fight against these password threatening attacks. Users should carry and have their mobile phones at the time of authentication. The OTP (one Time Passwords) are the popular technique, where user should poses their phones. The received keys will be taken for authentication. This types of authentication is known as device based authentication [15].

II. LITERATURE

The idea of continuous authentication is not novel approach. But the criteria and components are different and innovative. The differences are identified between biometrics and traditional passwords are discussed by Klosterman and Ganger in [16], they have also examined the proved biometrics are the most appropriate way to achieve continuous authentication. In order to prove, that Linux Pluggable Authentication Module (PAM) [17] has been proposed. This technique increased the computational cost, the authentication decision became very slow and face was used for verification.

Later from biometric components, voice, face and fingerprints are used for continuous verification [18]. The author found two key issues in continuous authentication such as the integration of time and modality, and the authenticity certainty at any time. But the work only focused the multi component fusion and they didn't study the consequences of detection process. And the approach is failed to satisfy the cost criteria.

Later the first implementation of a continuous verification system integrated into an operating system (OS) is proposed in [19], in this paper the author integrated the OS and biometric verification components. They have used camera and fingerprint component. The integrated portion of finger with mouse increases the reliability, however this method is not satisfied the scalability oriented implementation. The above modalities are very accurate; but they might be inherently limited in their sampling rate.

By continuous verification, the identity of the human operating the computer is continually verified at every session [20]. Verification is computationally simpler than identification and attempts to determine how "close" an observation is to a known value, rather than finding the closest match in a set of known values. Verification is a realistic operation in the normal usage of a computer system because we can assume that the user's identity has been incontrovertibly established by a preceding strong authentication mechanism. It is also appealing because it can conceivably be offloaded to a hardware device that is properly initialized with user specific data upon successful login.

A model-based evaluation of scalability and security tradeoffs of a multi-service web-based platform has been proposed. This utilizes the continuous evaluation of security mechanism, this degrades the performance properties. The different configurations are assessed and the security counter measures are introduces in this paper [21].This paper highlights one emerging application of stochastic modeling, i.e., the evaluation of the impact of

IJARCCE
ISSN (Online) 2278-1021
ISSN (Print) 2319 5940
International Journal of Advanced Research in Computer and Communication Engineering
ISO 3297:2007 Certified
Vol. 6, Issue 2, February 2017

security countermeasures on the performance of a service-based architecture such as SAAS (software as a service). This paper left several process as future work. Such processes are handling attack models, providing balanced security and the performance criteria's. The author failed to evaluate the proposal based on the above scenario.

D.M. Nicol, W.H. Sanders, and K.S. Tridevi [22] surveyed existing model-based techniques for evaluating system steadiness, and summarized the need of system security. The authors found that many techniques from dependability evaluation can be applied in the security domain later however that significant challenges should made appropriately. The system concentrated on the cyber attacks and the impact of those attacks in the continuous verification. But still there is no solution for unknown vulnerabilities.

III. PROPOSED SYSTEM

1. Enrollment Module

The registration module contains all the information about the person. It actually captures image of the person through Webcam and stores all the relevant details of the person such as name, phone number along with the fingerprint. The following figure describes an access control system based on fingerprint authentication. In this model, each user has an account and a corresponding ID in the Database.

2. User authentication:

User credentials are registered and stored with the fingerprint images. The registered user is the valid person to do the application. Other persons cannot access the application even they steal the credentials of the valid persons.

3. Biometric data Identification and Verification Module

Users are identified by their measurable human characteristics, such as fingerprint. Biometric characteristics are believed to be a reliable authentication factor since they provide a potential source of high-entropy information and cannot be easily lost or forgotten. Despite these merits, biometric authentication has some imperfect features. Un-like password, biometric characteristics cannot be easily changed or revoked. Some biometric characteristics (e.g., fingerprint) can be easily obtained without the awareness of the owner and it will forward and stored in database.

a. Fingerprint Matching:

Fingerprint matching algorithm that initially identifies the candidate common unique (minutiae) points in both the base and the input images using ratios of relative distances as the comparing function. A tree like structure is then drawn connecting the common minutiae points from bottom up in both the base and the input images. Matching score is obtained by comparing the similarity of the two tree structures based on a threshold value. Fingerprint based biometric authentication and verification systems have gained immense popularity and acceptance ever since their inception. Matching two fingerprints can be unsuccessful due to various reasons and also depends upon the method that is being used for matching. Very popular methods include minutiae based matching, correlation based matching, pattern matching etc…

Matching Techniques:

The three matching techniques are

- direct matching
- minutiae matching

A fingerprint is the pattern of ridges and valleys on the surface of a fingertip. The endpoints and crossing points of ridges are called minutiae. A ridge ending is defined as the ridge point where a ridge ends abruptly. A bifurcation is defined as the ridge point where a ridge bifurcates into two ridges. It is a widely accepted assumption that the minutiae pattern of each finger is unique and does not change during one's life.

b. Face recognition and matching

In face identification module, if the person enters the image of that person is compared with the image that are stored already in the database. In face verification module, if a person enters User will be verified whether they are authorized user or an unauthorized user. This is very useful to monitor who visited often. Face recognition systems in general, and access control systems based on face authentication in particular, use a "learning" mechanism to collect data on facial characteristics if users. Hence, the first important point to care about in a face recognition model is the Face Database storing this information. When the system finishes scanning a video or photo of a user's face, the digitalized information will go through these following modules one after another:

- Face Detection: locating the face in the photo or video and removing unnecessary details on the background.
- Feature Extraction: extracting facial characteristics needed for recognition.
- Feature Match: comparing scanned information with database to decide if it matches some user's face. If the face matched, the ID of the corresponding is returned.

Edge detection –canny sobal algorithm

4. Continuous Verification for security:

The camera will continuously monitor the face to avoid in authenticate transactions. If the user try to move from the camera then the transaction will not be continued. It will get struck. So, user should be there until he/she finish the transactions.

a. Face monitoring using camera:

This application is fully applied with the camera. Once the person wants to do the transaction then he should sit in front of the camera and the face is authenticated for further steps.

IJARCCE
ISSN (Online) 2278-1021
ISSN (Print) 2319 5940
International Journal of Advanced Research in Computer and Communication Engineering
ISO 3297:2007 Certified
Vol. 6, Issue 2, February 2017

5. Transaction maintenance and Report:

In this transaction maintenance all the transaction details will be updated and monitor in a secure manner. So the information will not misuse by other persons.

In accessibility module, if a person is an authorized user, then User will be permitted to access the resources. Otherwise, User will not be permitted. This provides more security and prevents from unauthorized user by providing face recognition.

In this report "Login to Logout authentication for all online Transactions "all the information are in secure way and information are updated ,final report is generated.

6. Intruder alert Process:

If the authentication fails, the system automatically finds the system details and captures the faces of users. These details will be send to the user via email.

Architecture:

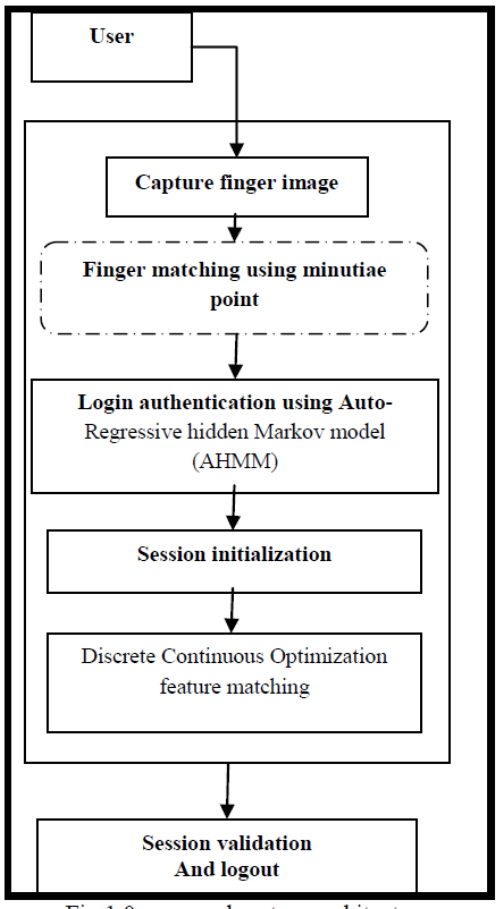

Fig 1.0 proposed system architecture

III. CONCLUSION

In this paper we presented an empirical study about the continuous authentication in internet services. From this survey we could identify different problems and issues associated with the continuous verification. Many authors proposed different modality and biometric components to achieve continuous verification, but only few concentrated on the cost criteria. And such studies are size limited and created many scalability issues. From this survey we have found several future directions to improve the authentication system in real-time internet services.

REFERENCES

[1] A. Klosterman and G. Ganger, "Secure Continuous Biometric-Enhanced Authentication," Technical Report CMU-CS-00-134, Carnegie Mellon Univ., May 2000.

[2] A.G. Morgan, "The Linux-PAM System Administrators' Guide," documentation distributed with Linux-PAM, http://www.kernel.org/pub/linux/libs/pam/pre/library/, 2006.

[3] A. Altinok and M. Turk, "Temporal Integration for Continuous Multimodal Biometrics," Proc. Workshop Multimodal User Authentication, pp. 131-137, 2003.

[4] S.Kumar, T.Sim, R.Janakirman, and S.Zhang, ''Using Continuous Biometric Verification to Protect Interactive Login Sessions,'' Proc. 21st Ann Computer Security Apllications Conf. (ACSAC' 05), pp.441-450, 2005.. Continuous Verification Using Multimodal Biometrics

[5] L. Montecchi, N. Nostro, A. Ceccarelli, G. Vella, A. Caruso, and A. Bondavalli, ''Model-based Evaluation of Scalability and Security Tradeoffs: a Case Study on a Multi-Service Platform'' Electronic Notes in Theoretical Computer science, vol.310, pp.13-133, 2015.

[6] D.M.Nicol, W.H. Sanders, and K.S. Tridevi, ''Model-Based Evaluation: From Dependability to Security,''IEEE Trans. Dependable and Secure Computing, vol. 1, no.1, pp.48-65, Jan. – Mar. 2004.

BIOGRAPHIES

Mrs. S. Gunasundari M.Sc., M.Ed., M Phil. is working as Assistant Professor of Computer Science department in Sakthi college of Arts & Science for women. Her teaching experience in 4 years and her area of interest is Digital image processing.

Miss. R. Punitha completed MCA in PSNA College of Engineering and technology and currently pursuing M. Phil in computer science in Sakthi college of Arts & Science for women. She worked two years programmer in Neolysi Technology, Chennai. Her area of interest is Network security and web mining.

Reliable Multi Authority Authentication and Attribute-Based Encryption System for Distributed Data Security	S. Yoga	Computer Science	International Journal of Advanced Research in Computer and Communication Engineering	2017	ISSN (Online) 2278-1021 ISSN (Print) 2319 5940	h-indexed https://ijarcce.com/upload/2017/february-17/IJARCCE%20110.pdf

IJARCCE
ISSN (Online) 2278-1021
ISSN (Print) 2319 5940
International Journal of Advanced Research in Computer and Communication Engineering
ISO 3297:2007 Certified
Vol. 6, Issue 2, February 2017

Reliable Multi Authority Authentication and Attribute-Based Encryption System for Distributed Data Security

Mrs. S. Yoga[1], Mrs. Kanagavalli[2]

Assistant Professor, Department of Computer Science, Sakthi college of Arts and Science for Women, Oddanchatram[1]

M. Phil Scholar, Department of Computer Science, Sakthi college of Arts and Science for Women, Oddanchatram[2]

Abstract: Data storing and sharing is an imperative functionality in distributed networks. We propose a secure and reliable multi-owner data sharing scheme in cloud environment. It implies that any user in the group can securely share data with others in the distributed systems. The proposed scheme is able to support dynamic groups efficiently. Specifically, new granted users can directly decrypt data files uploaded before their participation without contacting with data owners directly. The size and computation overhead of encryption are constant and independent with the number of revoked users.

Keywords: Cloud security, Hybrid Cloud, Attribute Based Encryption, Private Cloud.

I. INTRODUCTION

Cloud computing is a paradigm that allows users to access application residing at distant locations especially data centers. NIST definition (Mell and Grance, 2011) of cloud computing states that "Cloud computing is a model for enabling ubiquitous, convenient, on-demand network access to a shared pool of configurable computing resources that can be rapidly provisioned and released with minimal management effort or service provider interaction".

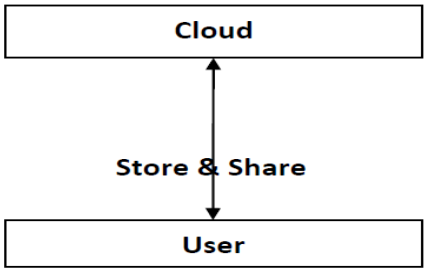

Figure 1.1: Overview of Cloud Computing Paradigm

Fig 1.1 depicts an overview of cloud computing paradigm. Cloud offers vast variety of services in pay-as-you-go manner; in other words it provides services on the basis of utility computing. Amazon Web Services, Google App Engine and Microsoft Azure are some of the current examples of public utility cloud computing services. Amazon Web Services provides a suite of cloud-based services including storage, computation and even human intelligence through the Amazon Mechanical Turk. Further the commercial web service provided by Amazon named Elastic Compute cloud (EC2) allows small companies and individuals to rent computers on which to run their own computer applications. In addition to this Google offers browser-based enterprise applications, through services such as Google Apps. The most important contribution to cloud computing has been the emergence of killer apps from leading technology giants such as Microsoft and Google. As the usage of cloud computing is increasing exponentially, the necessity of providing security and access control has become mandatory.

The primary motivation of our work is the need of security in terms of access control for cloud computing services with multi factor authentication. Several large scale industries and organizations make use of computation solutions and storage infrastructures provided by the cloud service providers (CSP). The affordable and reliable nature of cloud services makes it usage prominent with wider range of organizations. But still the emergence of several security issues by means of attacks and vulnerabilities had created a great scope for security research. The newer ways of using cloud computing for computing, storage and deployment is leading to the development of the cloud domain in different technological perspectives, leading to need of added security. This will motivate the idea of using cloud computing for critical applications.

Privacy preservation and access management forms the two major influences for maintaining cloud data security. The main theme of most of the existing schemes is to make use of cryptographic measures to achieve data security. Each scheme provides solution to specific technical functionality issues, but lags in the provision of complete suitable solution to issues relating to cloud data

IJARCCE
ISSN (Online) 2278-1021
ISSN (Print) 2319 5940
International Journal of Advanced Research in Computer and Communication Engineering
ISO 3297:2007 Certified
Vol. 6, Issue 2, February 2017

access management. The reason is the high level complexity of cryptographic techniques. Existing access control techniques are not designed specifically for a certain application, which can match hardware's and effective signatures. The generality will be a hurdle to achieve fine grained access control and other security properties like fast revocation and access control delegation. In this paper, we present an extensive analysis of existing access control schemes with special importance to Attribute Based Encryption techniques. A complete solution to cloud data access problems with appropriate user access provision methods and improved security establishment techniques are presented in this research work.

CONTRIBUTIONS

In this paper we introduce a set of techniques and frameworks to solve some of the major security challenges associated with cloud computing environment. The key contributions of the thesis were enumerated as follows:

MACP-ABE (Multi Authority Cipher Policy based attribute based encryption)

We introduces a new key aggregation scheme which is named as MASS (Mobile Authentic and Secure Sum up) technique, which collects the keys from all owners and creates an aggregated key for data decryption.

Unlike the previous works, the average size and time of rekeying messages have been avoided. So the communication overhead and time factors are considered here.

The proposal develops a three-step scheme for MASS implementation.

The first one is initial key generation for both single owner data and multi owner data group. The first algorithm can generate a key-tree that corresponds to the optimal key-tree obtained by mathematical analysis.

The second step of the mechanism in MASS is an optimal key-tree maintenance and aggregation algorithm for multi owner data.

The second scheme eliminates the existing re-key and key alteration processes.

The third step of the scheme is the Device based authentication scheme, which helps to gather the encrypted keys from the device and aggregates together for decryption.

Finally this performs the crypto process using the aggregated (sum up) key. This technique is named as **MACP-ABE.**

In order to ensure thesis goals with newly proposed solutions, certain properties relating to better access provision were selected and it has been focused throughout the thesis. The chosen properties were considered to be most important in terms of addressing the issues preventing cloud data access vulnerability. The properties were classified into three categories - security, access control and performance.

II. PROBLEM DEFINITION

Page `Data sharing is an important functionality in cloud domain. This is very important in distributed environment to keep the data more secure and vulnerable less. When considering the flexibility and scalability in data sharing, there are numerous issues arises in the field of security. Efficient data encryption and key sharing schemes have been proposed in the literature, even those schemes were not completely secure in the multi owner data sharing environment. For both security and efficiency, a group key which is shared only by a group of users has been employed for access control. A message for the group is encrypted by the group key which is provided by the group manager. The encrypted group key is transmitted only once to the owner of the file.

Then the transmitted message can be decrypted by only group members having the group key. However, the group key is updated whenever the group membership changes for forward and backward secrecy, which can cause a serious problem with rekeying overhead. And key should be created for every file separately. So the communication and key overhead was high. The challenging problem is how to effectively share encrypted data with effective authentication and minimum key generation overhead. The several applications suffer from in efficient key authentication and key management problems.

Transferring the secret keys inherently requires a protected way, and storing these keys requires rather expensive secure storage. The keys should be unique for every owner for a single file. The costs and complexities involved generally increase with the number of the decryption keys to be shared. The problem occurs when the user try to send the decrypted keys to the unknown multiple users. The user who receives the key need to combine with their group key which is provided by the group manager. The group manager is common to the entire user in the particular group. However the user who sends the encrypted message with their group key only allowed receiving the file.

III. PROPOSED SYSTEM

In modern cryptography, a fundamental problem the literature often says is about leveraging the secrecy of a small piece of knowledge into the ability to perform cryptographic functions which is sampled as encryption and authentication multiple times. In this research, this introduces the concept of how to make a decryption key more powerful and authentication is reliable in the sense that it allows decryption of multiple cipher texts, without increasing its size. The followings are the major contribution of the proposed system. The research work introduces a set of techniques and frameworks to solve some of the major security challenges associated with cloud computing environment. The key contributions of the thesis were enumerated as follows.

DOI 10.17148/IJARCCE.2017.62110

IJARCCE
ISSN (Online) 2278-1021
ISSN (Print) 2319 5940
International Journal of Advanced Research in Computer and Communication Engineering
ISO 3297:2007 Certified
Vol. 6, Issue 2, February 2017

1. A novel scheme called MACP- ABE scheme collective advancement on access control and authentication scheme for multi authority cloud storage systems for preventing numerous security breaks and violations which occurs in the hybrid cloud environment.
2. the research introduce a novel cryptographic access control technique named as **M_Key Cryptography** that provides fine-grained data access and storage correctness verification to data users through the use of the dynamic token granting system.
3. To enable seamless, dynamic and secure interaction of cloud services over larger activity, the research design and implement a **MASS(Mobile Authentic and Secure Sum up)** and hardware authentication scheme that solves the problem of user attribute revocation with forward and backward security assurance.
4. This presents a novel ABE scheme that preserves the property of security and privacy over outsourced sensitive information. It is achieved through the process of key aggregation techniques.
5. A new Device based authentication scheme is introduced to avoid key guessing and stealing issues, and this helps to gather the encrypted keys from the device and aggregates together for decryption.
6. A hardware based authentication scheme is additionally proposed to increase the security of the data. This matches the MAC and IP based signatures while decrypting.

In order to ensure thesis goals with newly proposed solutions, certain properties relating to better access provision were selected and it has been focused throughout the thesis. The chosen properties were considered to be most important in terms of addressing the issues preventing cloud data access vulnerability. The properties were classified into three categories - security, access control and performance.

IV. MACP-ABE

MACP-ABE section introduces the process and steps of the proposed system. the MACP-ABE scheme includes different steps and iterations of authentication, which as summarized into three categories.

The following are the steps involved in the proposed system.

1. Key setup and Key generation phase
2. Cryptographic phase
3. Device authentication phase

A. Key Aggregation

Key aggregation chapter introduces a new key aggregation scheme which is named as **MASS** technique, which collects the keys from different sources and creates an aggregated key for data decryption. Unlike the previous works, the average size and time of rekeying messages have been avoided. So the communication overhead and time factors are considered here.

B. The proposal develops a three-step scheme for MACP-ABE implementation.

The first one is initial key generation for both single owner data and multi owner data group. The first algorithm can generate a key-tree that corresponds to the optimal key-tree obtained by mathematical analysis.
The second step of the mechanism in MACP-ABE is an optimal key-tree maintenance and aggregation algorithm for multi owner data.
The second scheme eliminates the existing re-key and key alteration processes.
The third step of the scheme is the Device based authentication scheme, which helps to gather the encrypted keys from the device and aggregates together for decryption.
Finally this performs the crypto process using the aggregated (sum up) key. This technique is named as **M_Key Cryptography (M_KC).** The M_Key is referred the proposed MACP-ABE scheme which is mentioned above.
In **M_KC**, users encrypt a message not only under a public-key, but also under an adjunct of cipher text called class. That means the cipher-texts are further categorized into different classes.

C. Key Distribution

The key owner holds a master-secret called master-secret key, which can be used to extract secret keys for different classes. More importantly, the extracted key can have an aggregate key which is as compressed as a secret key for a single class, but aggregates the power of many such keys, i.e., the decryption power for any subset of cipher-text classes.

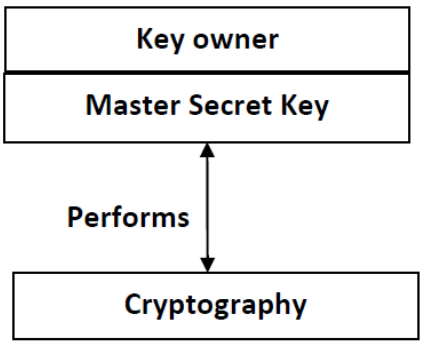

Fig 1.0 key generation process

With the proposed solution, the owners can simply send their private keys via a secure SMS along with the encrypted message. The system will collect and aggregate the keys together. This aggregated key will be used to decrypt the encrypted data's. The sizes of cipher-text, public-key, and master-secret key and aggregate key in the M_KC schemes are all of constant size. Prior outcomes may achieve a similar property featuring a constant-size decryption key, but the classes need to receive the aggregated key via email. The proposed work is flexible in the sense that this constraint is eliminated, that is, no

IJARCCE
ISSN (Online) 2278-1021
ISSN (Print) 2319 5940
International Journal of Advanced Research in Computer and Communication Engineering
ISO 3297:2007 Certified
Vol. 6, Issue 2, February 2017

special relation is required between the classes. All creations can be proven secure in the standard model. To the best of our knowledge, the proposed Mass based aggregation M_KC has not been implemented earlier.

V. RESULTS AND ANALYSIS

A. Implementation Configuration

The implementation is carried out using dotnet cloud framework.. The Cloud model uses the random client generation model. There are 5 clients defined in an implementation with unique identity.

Performance results:

The performance of our proposed work MACP using ABE node scheme is compared with the existing approach ABE. This considered the key size selection on the ABE is compared at the time of verification.

Table 1.0 Encryption Time comparison table

Parameters	Existing (ABE)	Proposed (MACP ABE)
Datasize(512)	8	3
Datasize(1024)	18	7

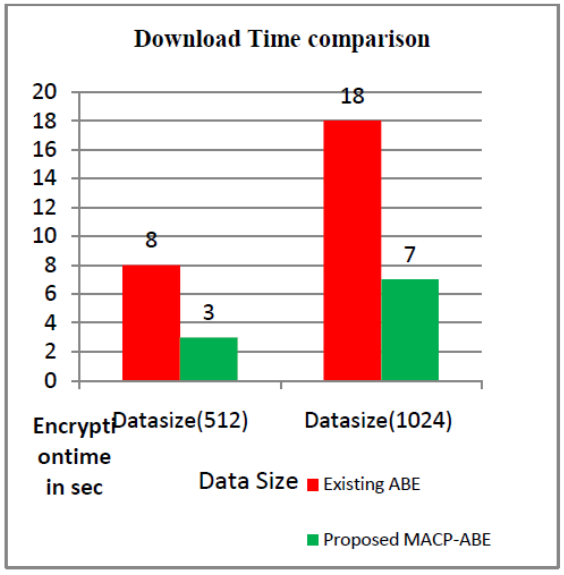

Fig 4.0 comparison chart

Fig. 2.0 presents the encryption overhead costs for different size of data's. The X axis represents the data size, while the Y axis represents the time for encryption. The MACP-ABE compared with the existing ABE method in the form of attribute based encryption.

VI. CONCLUSION

In this paper, a new framework for Cloud data security is proposed, that is named as MACP-ABE .It uses different algorithms and techniques to secure cloud data. With the help of ABE schemes and other device based authentication MACP-ABE effectively secure data in the cloud environment. The major advantage of the system is that, if a user shares a data in the cloud, the data will be more secure than ever.

REFERENCES

[1] H. Wang, "Proxy Provable Data Possession in Public Clouds," IEEE Trans. Services Computing, vol. 6, no. 4, pp. 551-559, http://ieeexplore.ieee.org/stamp/stamp.jsp?tp=&arnumber=6357181, Oct.-Dec. 2012.
[2] Wang, S.S.M. Chow, M. Li, and H. Li, "Storing Shared Data on the Cloud via Security-Mediator," Proc. IEEE 33rd Int'l Conf. Distributed Computing Systems (ICDCS), 2013.
[3] Title: A Break in the Clouds: Towards a Cloud Definition Author: Luis M. Vaquero, Luis Rodero-Merino, Juan Caceres, Maik Lindner Telefonica Investigacion y Desarrollo and SAP Research Madrid, Spain, EU and Belfast, UK, EU
[4] S.S.M. Chow, C.-K. Chu, X. Huang, J. Zhou, and R.H. Deng, "Dynamic Secure Cloud Storage with Provenance," Cryptography and Security, pp. 442-464, Springer, 2012.
[5] M.J. Atallah, M. Blanton, N. Fazio, and K.B. Frikken, "Dynamic and Efficient Key Management for Access Hierarchies," ACM Trans. Information and System Security, vol. 12, no. 3, pp. 18:1-18:43, 2009.
[6] Chu, C., et al. "Key-Aggregate Cryptosystem for Scalable Data Sharing in Cloud Storage." (2014): 1-1.
[7] Kallahalla, Mahesh, et al. "Plutus: Scalable Secure File Sharing on Untrusted Storage." Fast. Vol. 3. 2003.
[8] Goh, H. Shacham, N. Modadugu, and D. Boneh, "Sirius: Securing Remote Untrusted Storage," Proc. Network and Distributed Systems Security Symp. (NDSS), pp. 131-145, 2003.
[9] Liu, Xuefeng, et al. "Mona: secure multi-owner data sharing for dynamic groups in the cloud." Parallel and Distributed Systems, IEEE Transactions on 24.6 (2013): 1182-1191.
[10] S. Kamara and K. Lauter, "Cryptographic Cloud Storage," Proc. Int'l Conf. Financial Cryptography and Data Security (FC), pp. 136- 149, Jan. 2010

BIOGRAPHIES

Mrs. S. Yoga completed MSc (CS&IT) Madurai Kamaraj University. She working as assistant professor of computer science department, sakthi arts and Science College, oddanchatram. Her Teaching experience 4 years. Her area of interest Network Security

Mrs. Kanagavalli completed MSc and currently pursing M.phil computer science at sakthi Arts and science college oddanchatram. Her teaching experience 1years. Her area of interest Network Security.

Structural Boundaries Detection of Ice Floe of Sea Ice using T-Snake GVF	P. Alaguthai	Computer Science	International Journal of Advanced Research in Computer and Communication Engineering	2017	ISSN (Online) 2278-1021 ISSN (Print) 2319 5940	h-indexed https://ijarcce.com/upload/2017/february-17/IJARCCE%20111.pdf

IJARCCE

ISSN (Online) 2278-1021
ISSN (Print) 2319 5940

International Journal of Advanced Research in Computer and Communication Engineering
ISO 3297:2007 Certified
Vol. 6, Issue 2, February 2017

Structural Boundaries Detection of Ice Floe of Sea Ice using T-Snake GVF

P. Alaguthai M.SC., M.Phil.,[1], C. Sindhuja M.SC., M.Phil.[2]

Assistant Professor, Sakthi College of Arts and Science for Women, Dindigul[1]

Research Scholar, Sakthi College of Arts and Science for Women, Dindigul[2]

Abstract: Image processing is one of the upgrading research areas to find out the relevant pattern. It can be applied in many fields of medical, satellite records, analyzing data. Satellite records of image plays an important role in image processing. Satellite view of Sea ice image has been taken to detect the boundaries of the ice floe. Sea ice is a formation of sea water freezing. When the sea ice is broken ice floes were formed from them and ice floe is large pack of floating ice. Detecting the ice floes many Image Processing techniques has proposed. But they prove some of the drawbacks like missing data, inaccurate structural analysis because of difficulties in ice floe identification, separation of boundaries connected ice floes, it is an important issue for the climate and wave and structural ice analysis. To solve these problems here proposed a T-Snake algorithm on GVF, which provide an accurate identification of related pattern and structural boundaries for ice floe.

Keywords: Image processing, Ice floe, Weak boundary solving and T-Snake on GVF.

I. INTRODUCTION

Image processing is any form of signal processing for which the input is an image, such as a photograph or video frame; the output of image processing may be either an image or a set of characteristics or parameters related to the image. Most image-processing techniques involve treating the image as a two-dimensional signal and applying standard signal-processing techniques to it. Image processing usually refers to digital image processing, but optical and analog image processing also are possible. This article is about general techniques that apply to all of them. The acquisition of images (producing the input image in the first place) is referred to as imaging [1]. In every research area they analyze the problem, mostly image analysis involves manipulating the image data to determine exactly the information necessary to help to solve a computer imaging problem. This analysis is typically part of a larger process which involves preprocessing, feature extraction, segmentation, remove noise data, etc. Image processing is done with the help of the digital image, which is captured from the digital format or satellite view, capturing the image are used to identify the problem in any fields. Capturing and analyzing image in image processing is the most important research area. Updating fields of the sea water research is an ongoing process of every research area through image processing sector.

Sea ice is formed with the result of seawater freezing based on the seasonal ice zone. In the seasonal ice zones, there are various types of sea ice floes of which the sizes range from about one meter to a few kilometers. The size distribution of ice floes plays an important role in the dynamical and thermo dynamical process of sea ice area as well as ice concentration and ice thickness [2]. Ice thickness is transferred from atmosphere to ice varies depending on the ice floe size and the melting rate of ice floes depends on the ice floe size because the lateral melting becomes more significant for smaller ice floes. Therefore, it can be said that the ice floe distribution is a key parameter in the seasonal ice zones. The floe size distribution is a basic parameter of sea ice that affects the behavior of sea-ice extent, both dynamically and thermodynamically. Particularly for relatively small ice floes, it is critical to the estimation of melting rate. Hence, estimating floe size distributions contributes to the understanding of the behavior of the sea-ice extent on a global scale. In addition to this, the floe size distribution is also important min ice management for Arctic offshore operations. In addition, the size distribution and shape of ice floes possibly provide a clue to the understanding of ice floe formation processes [3]. It is generally noticed that the distribution of ice floe sizes does not have a characteristic size scale. The magnified figure of the partial ice area coincides almost with its original figure; that is, it has a self-similar feature. If this characteristic is confirmed in the ice area, it may give a suggestion on the ice formation process [4]. To separate connected sea-ice floes into individual floes, the watershed transform have to use. Manually removed these over-segmented lines, while those in automatically removed the over segmented lines whose endpoints were both convex. However, over- and under segmentation still affected the ice floe detection results. This method is operated on the binary images and focused on the morphological characteristics of ice floes rather than on the real boundaries [5]. To solve this problem, Topology adaptive snake algorithm was proposed on GVF to avoid manual interaction and reduce

IJARCCE
ISSN (Online) 2278-1021
ISSN (Print) 2319 5940
International Journal of Advanced Research in Computer and Communication Engineering
ISO 3297:2007 Certified
Vol. 6, Issue 2, February 2017

the time required to run the algorithm and managed ice resulting from offshore operations in sea ice using K-Means clustering algorithm. Once individual ice floes have been identified, the floe boundaries are obtained, and the floe size distribution can be calculated from the resulting data.

II. LITERATURE REVIEW

T. Toyota and H. Enomoto [6] Using ADEOS/AVNIR images in the 1997 winter, the size distribution of sea ice floes in the southern Sea of Okhotsk is analyzed. These images have the high horizontal resolution of 16 m and enable us to recognize ice floes of the diameter from tens of meters to several kilometers. The area and perimeter of each floe are measured by means of image processing, and their statistical features are examined for four ice areas, including the interior ice pack regions, the marginal ice region, and the coastal region. As a result, it is shown that the floe size distribution has self-similarity characteristics within the range of 100 m to 1 km in individual areas and the fractal dimension is estimated to be 2.1 to 2.5, and that the perimeter is highly correlated with the diameter. These results may suggest the ice floe formation process in this size range.

Devyani Patil et al [7], An unmanned aerial vehicle was used as a mobile sensor platform to collect sea-ice features and several image processing algorithms have been applied to samples of Sea-Ice images to extract useful information about sea-ice. The sea-ice statistics given by the floe size distribution, being an important parameter for climate and wave and structure ice-analysis, is challenging to calculate due to difficulties in ice floe detection, particularly the separation of seemingly connected ice floes. Gray scale and OTSU algorithm will be applied to solve this problem. To evolve the Gray Scale and OTSU algorithm automatically, an initialization based on the distance transform is proposed to detect individual ice floes, and the morphological cleaning is afterward applied to smoothen the shape of each identified ice floe. Based on the identification result, the image is separated into four different layers: ice floes, brash pieces, slush, and water. This makes it further possible to present a color map of the ice floes and brash pieces based on sizes, and the corresponding ice floe size distribution histogram.

Vaibhav A. Desale [8] study the ice which was situated on the sea on the poles or at low temperature places an unmanned aerial vehicle was used for capturing images. The vehicle was able to capture the images of sea ice floes and by using the such images and by applying several image processing algorithm important information was collected. The information extracted is very useful statics for the climate and wave. But difficult problems are challenge of the identification of ice floe, mainly the separation of the ice floes. For this paper GVF algorithm is used mainly to solve the above difficulties. Given GVF algorithm is based on the distance transform propose for detecting the separate and individual ice-floe on the sea and after that morphological cleaning is applied to that detected individual ice-floe along with the GVF also OTSU algorithm is used for calculating results and canny edge detection for detecting boundaries. This result was being helpful for classifying the image into the four classifications like ice floes, brash pieces, slush and water. By using this algorithm it was made possible to make the color maps for the given ice floe, brash pieces. Study made acceptable information and results and also the effectiveness.

G.Ram Kumar and T.Sheik Yousuf [9] The sea ice, which is defined as any form of ice that forms as result of seawater freezing when broken into small pieces called as ice floes. Ice floes are the large pack of floating ice. Many Image Processing techniques have applied on the sea-ice to extract the useful information. Here there is a challenge that to calculate the structural analysis, due to the difficulties in ice floe identification , such as separation of seemingly connected ice floes, this sea statistics is given by the floe size distribution, is an important parameter for the climate and wave and structural ice analysis. To solve these problems, propose a gradient vector flow (GVF) snake algorithm which evolves automatically by using initialization based on the distance transform which detects individual ice floes and applying morphological cleaning for the smoothen the shape of every identified ice floes. Based on these results, the image is separated into four layers such as Ice floes, brash, pieces, slush, and water. This method yields an acceptable identification result, and its effectiveness is demonstrated.

T.Ravichandra Babu and Eman Bhattacharjee [10], An unmanned aerial vehicle was used as a mobile sensor platform to collect sea-ice features at NyÅlesund in early May 2011, and several image processing algorithms have been applied to samples of sea-ice images to extract useful information about sea ice. The sea-ice statistics given by the floe size distribution, being an important parameter for climate and wave- and structure-ice analysis, is challenging to calculate due to difficulties in ice floe identification, particularly the separation of seemingly connected ice floes. In this paper, the gradient vector flow (GVF) snake algorithm is applied to solve this problem. To evolve the GVF snake algorithm automatically, an initialization based on the distance transform is proposed to detect individual ice floes, and the morphological cleaning is afterward applied to smoothen the shape of each identified ice floe. The proposed algorithm yields an acceptable identification result, and its effectiveness is demonstrated in a case study.

III. PROBLEM DEFINITION

Automatic identification of individual floe edges is a key tool for extracting information of floe size distribution from satellite images. In an actual ice covered environment, ice floes typically touch each other, and the junctions may be difficult to identify in satellite images. This issue challenges the boundary detection of individual

IJARCCE
ISSN (Online) 2278-1021
ISSN (Print) 2319 5940
International Journal of Advanced Research in Computer and Communication Engineering
ISO 3297:2007 Certified
Vol. 6, Issue 2, February 2017

ice floes and significantly affects ice floe size analysis. Several researchers have tried to mitigate this issue like separated closely distributed ice floes by setting a threshold higher than the ice-water segmentation threshold and separated the connected ice floes manually when the threshold did not work well. When compared derivative and morphology boundary detection algorithms in both model ice and sea-ice images will not work in proper manner. The boundaries are too weak to be detected directly, which significantly affects the ice floe statistical result [11]. However, non-closed boundaries are often produced by traditional derivative boundary detection, while some boundary information is often lost by morphology boundary detection.

IV. PROPOSED WORK TO SOLVE WEAK BOUNDARY ON ICE FLOE

A. Ice Pixel Detection

Pixel detection is one of the important factors for sea ice image. With the capture of object from the satellite detection of pixel is an essential factor. Here ice and water have same molecules as ice is formed from the water itself. But in fact Ice is much whiter than the water. So it clearly shows the pixel difference between them pixels of ice have higher intensity. Intensity for an ice can be calculated from the given threshold method. Now we can also compare among the various pixels between different ices [12]. From the observations only light ice have the large intensity than threshold. Dark ice is having the double threshold between ice and water. Here K-means algorithm is used, which is a statistical data analysis technique that minimizes the within-cluster sum of distance to partition a set of data into groups and image is converted into three or more clusters. The cluster with the lowest average intensity value is considered to be water, while the other clusters are considered ice. So the classification is done and pixels are detected.

B. Ice Edge Detection:

Detection of the edge is very important and most difficult issue in the study. It might happen that some of ice floes have very less distance between them means they are very close from each other which means separating distance between them is close at that time edge detection becomes more difficult. It is most challenging task. So here in the edge detection we use the sequential analysis algorithm [13]. sequential analysis operates on the grayscale image in which real boundary information, particularly "weak" boundaries. The snake algorithm is based on the external and internal forces influence. Algorithm comes to conclusion when the both external and internal forces become in equilibrium. External forces define the boundary. This can be used in the case of the weak boundary condition. Sequential analysis is faster and less restricted by the initial contour.

This algorithm is able to detect the weak connections between floes and ensures that detected boundary area is

```
Sequential analysis (node n = (s1, ...., sk), Sn , In)
Begin
(1)  Stemp = φ.
(2)  Itemp = φ.
(3)  For each (i Sn)
(4)  if ((s1, ....., sk , {i}) is frequent)
(5)  Stemp = Stemp {i}
(6)  For each (i Stemp)
(7)  DFS-Pruning((s1,……..,sk,{i}),Stemp,
          all elements in Stemp greater than i )
(8)  For each (i In)
(9)  if ((s1, ..... , sk » {i}) is frequent)
(10) Itemp = Itemp {i}
(11) For each (i Itemp)
(12) DFS-Pruning ((s1, ....., sk {i}), Stemp,
          all elements in Itemp greater than i)
End
```

Algorithm 1: Sequential Analysis

closed to the initial contour does not need to be as close to the true boundary as for in the traditional snake algorithm. The distance transform of a binary image is the minimum distance from every pixel in an object to the background.

C. Ice Type Classification and Floe Size Distribution

To distinguish brash ice from ice floes in our algorithm, we define a brash-ice threshold parameter (pixel number or are) that can be tuned for each application. The ice pieces with size larger than the threshold are considered to be ice floes, while smaller pieces are considered to be brash ice. The remaining ice pixels were labeled as slush. The result is four layers of a sea-ice image: ice floe, brash ice, slush, and water .The ice floe (brash) size can be determined by the number of pixels in the identified floe (brash) [14]. If the focal length f and camera height are available, the actual size in SI unit of the ice floes and floe size distribution can be also calculated by converting the image pixel size to its SI unit size. The ice floe size (calculated by counting the pixel number of the floe) distribution. The residue ice, which is the detected boundary pixels between the connected floes, was previously considered as slush. However, the residue ice, as shown in can be also handled specifically according to the applied subsequent processing by the user.

D. Identifying Individual Ice Floes

To identify individual ice floes in the sea-ice image, in particular separating the floes that are very close or connected to each other. The boundaries between apparently connected floes have a similar brightness to the floes themselves. The boundaries are too weak to be detected directly, which significantly affects the ice floe statistical result. Therefore, the T-Snake on GVF snake algorithm is proposed to solve this problem. T-snakes model as a closed 2D contour consisting of a set of nodes connected in series. A T-snake is a discrete approximation to a conventional parametric snake's model and retains

IJARCCE
ISSN (Online) 2278-1021
ISSN (Print) 2319 5940
International Journal of Advanced Research in Computer and Communication Engineering
ISO 3297:2007 Certified
Vol. 6, Issue 2, February 2017

many of its properties [15]. The internal forces act as a smoothness constraint on sea ice and users can interact with the model using spring forces and other Ice floes. An 'inflation' force is used to push the model towards image edges until it is opposed by external image forces. The deformation of the model is governed by K-Means cluster and groups the object and finds the individual ice floe. It also keep track of the interior region of the model by 'turning on' any grid vertices passed over by the T-snake during its motion. By re- parameterzing the model at user-specified iterations of the evolutionary process, we create a simple, elegant and

For each deformation step (M time steps):
1. For M time steps: (a) compute the external and internal forces acting on T-snake nodes and elements; and (b) update the node positions using (8).
2. Perform reparameterization phase I.
3. Perform reparameterization phase II.
4. For all current T-snake elements, determine if the T-snake element is still valid. A T-snake element is valid if its corresponding grid cell is still a boundary cell. Discard invalid T-snake elements and unused nodes.
5. Use the grid vertices turned on in phase II above (if any) to determine new boundary cells and hence new T-snake nodes and elements.

Algorithm 2: T-Snake

The T-snake is considered to have reached its equilibrium state when all of its elements have been inactive for a user-specified number of deformation steps. T-snake element activity or movement is measured via the grid, again using a flame propagation analogy. A weak connection will also be detected if the initial contour is located on it. However, when the initial contour is located near the floe boundary inside the floe, the snake may only find a part of the floe boundary near the initial contour. It should be noted that the curve is always closed, regardless of how it deforms. Which appear to be non closed curves.

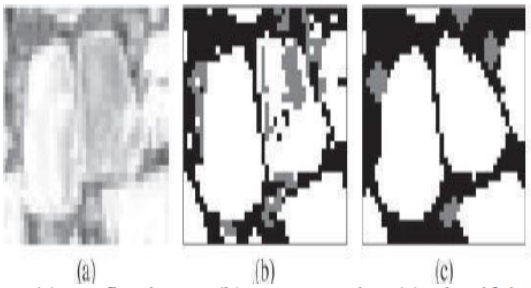

Fig: (a) Ice floe image (b) Segmentation (c) Identifying individual ice floe

This behavior occurs because the area bounded by the closed curve tends toward zero. This fact is beneficial for connected floe segmentation and the initial contours should be located inside the floes and centered as close to the ice floe center as possible.

V. EXPERIMENTAL RESULTS

In the experimental analysis is used to analyze the sequential pattern extraction in the sea ice image. The proposed method where implemented in the field of image processing to analyze the weak boundaries detection. Our proposed system is very helpful to find out the individual identification of ice floe and result shows the better one when compared to existing work in the case of accuracy, edge detection and boundaries.

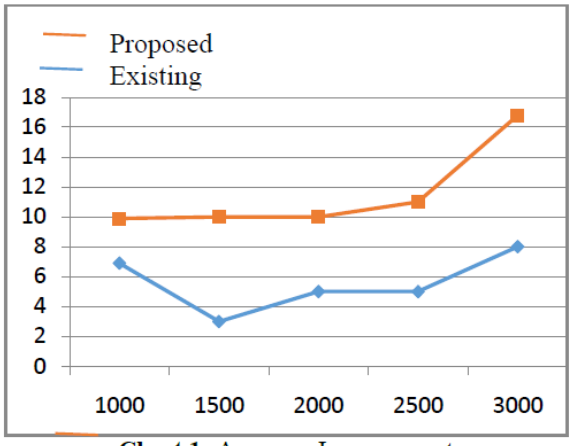

Chart 1: Accuracy Improvement

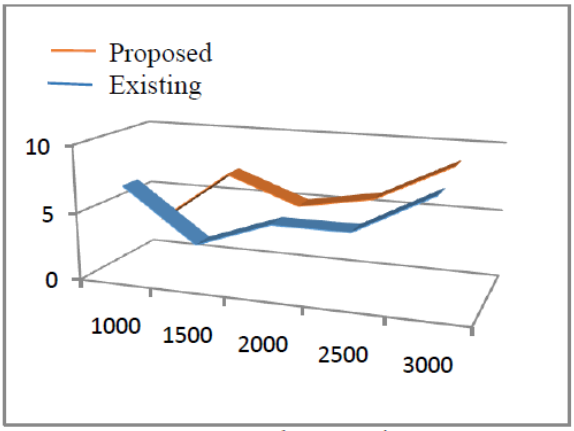

Chart 2: Edge Detection

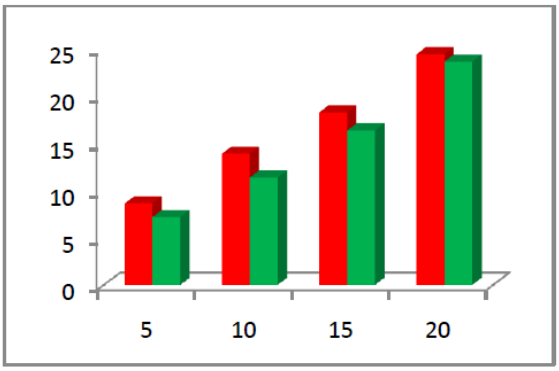

Chart 3: Boundary Detection

IJARCCE

ISSN (Online) 2278-1021
ISSN (Print) 2319 5940

International Journal of Advanced Research in Computer and Communication Engineering
ISO 3297:2007 Certified
Vol. 6, Issue 2, February 2017

Our proposed methodology improved the accuracy, edge detection, boundaries, etc and is used to create the experimental setup.

The performance of the proposed method is evaluated in terms of,

- Accuracy
- Edge detection and
- Boundaries

VI. CONCLUSION

The most challenging task is to identify individual ice floes in the sea-ice image, in particular separating the floes that are very close or connected to each other. The boundaries between apparently connected to ice floes. The boundaries are too weak to be detected directly, which significantly affects the ice floe statistical result. Therefore, with the help of the MATLAB we propose a T-Snake algorithm to solve the problem based on the GVF algorithm. Hence our result shows a better way to find the boundaries of the ice floe and provide an accurate identification of related pattern and structural boundaries for ice floe.

REFERENCES

[1] Gonzalez RC, Woods RE: Digital Image Processing, 2nd edition.Prentice Hall, Upper Saddle River, 2002
[2] Steele, M. Sea Ice melting and floe geometry in a simple ice-ocean model. Journal of Geophysical Research 97(C11): 17,729–17,738 (1992).
[3] Steele, M., Morison, J.H. and Untersteiner, N. The partition of air-ice-ocean momentum exchange as a function of ice concentration, floe sizes, and draft. Journal of Geophysical Research 94(C9): 12,739–12,750 (1989).
[4] G. Vachon, M. Sayed, and I. Kubat, "Methodology for determination of ice management efficiency," in Proc. Int. Conf. ICETECH Exhib. Perform. Ships Struct., Banff, AB, Canada, 2012,
[5] Keinonen, "Ice management for ice offshore operations," in Proc. Offshore Technol. Conf., Houston, TX, USA, 2008, pp. 690–704.
[6] [6] T. Toyota and H. Enomoto, "ANALYSIS OF SEA ICE FLOES IN THE SEA OF OKHOTSK USING ADEOS/AVNIR IMAGES"
[7] Devyani Patil et al, "Image Processing for Detecting Sea Ice Floes", IJIRT Volume 3 Issue 1 ISSN: 2349-6002.
[8] Vaibhav A. Desale, "Reorganization of the Sea- Ice Floes and Floe Size Distributions".
[9] G.Ram Kumar and T.Sheik Yousuf, "Identification of sea-ice floes and the floe size distributions based on probabilistic distribution function"
[10] T.Ravichandra Babu and Eman Bhattacharjee, "Sea-Ice Floes Identification and Detection using Matlab"
[11] Anjana Lakshmi K G, Nissa Surling, "Image Processing for Analyzing Ice Floes and the Floe Size Distributions".
[12] G. Vachon, M. Sayed, and I. Kubat, "Methodology for determination of ice management efficiency," in Proc. Int. Conf.
[13] R. Srikant and R. Agrawal, "Mining sequential patterns: Generalizations and performance improvements," in Proc. 5th Int. Conf. EDBT,
[14] J. Banfield, "Automated tracking of ice floes: A stochastic approach,"IEEE Trans. Geosci. Remote Sens., vol. 29, no. 6, pp. 905–911, Nov. 1991.
[15] Tim McInerney*, Demetri Terzopoulos, "T-snakes: Topology adaptive snakes"

BIOGRAPHY

Miss. Sindhuja completed MSc, and Msc in psychology and currently pursuing M.phil in Sakthi College of Arts and Science for Women Dindigul. Her teaching experience is 2 years. Her area of interest is computer network and digital image processing.

Medical Image Segmentation of Pancreas using D-Sift Algorithm	S.Kavitha	Computer Science	International Journal of Advanced Research in Computer and Communication Engineering	2017	ISSN (Online) 2278-1021 ISSN (Print) 2319 5940	h-indexed https://ijarcce.com/upload/2017/february-17/IJARCCE%20112.pdf

IJARCCE
ISSN (Online) 2278-1021
ISSN (Print) 2319 5940
International Journal of Advanced Research in Computer and Communication Engineering
ISO 3297:2007 Certified
Vol. 6, Issue 2, February 2017

Medical Image Segmentation of Pancreas using D-Sift Algorithm

S. Kavitha, M.Sc., M. Phil., (Ph.D)[1], P. Anusha MCA, M. Phil[2]
Assistant Professor & HOD, Sakthi College of Arts & Science for Women, Dindigul[1]
Research Scholar, Sakthi College of Arts & Science for Women, Dindigul[2]

Abstract: Analyzing the medical image in image processing is the most important research area. Capturing the image are analyzed to identify different medical imaging problems is the common factor in this field. Robust organ segmentation is a prerequisite for computer-aided diagnosis (CAD), quantitative imaging analysis, pathology detection and surgical assistance. Some of the organs in the human body have high anatomical variability, so segmentation of such organs is very complex. The proposed system segments the pancreas with the considerations of spatial relationships of splenic, portal and superior mesenteric veins with the pancreas. The proposed system uses macro super-pixels for fast and deep labeling and segmentation process. The proposed system is an automated bottom-up approach for pancreas segmentation with the consideration of spatial relationships with the veins in abdominal computed tomography (CT) scans. The method generates dynamic cascaded and macro super-pixel segmentation information's by classifying image patches at different resolutions. Fast organ analysis using Dense-SIFT algorithm.

Keyword: Image processing, medical image, pancreas segmentation, CT and Dense-SIFT algorithm.

I. INTRODUCTION

Image processing is any form of signal processing for which the input is an image, such as a photograph or video frame; the output of image processing may be moreover an image or a set of uniqueness or parameters linked to the image. The majority image-processing system involves treating the image as a two-dimensional signal and be appropriate standard signal-processing modus operandi to it. Image processing usually refers to digital image processing, but optical and analog image processing also are possible. This critique is about general modus operandi that apply to all of them. The acquisition of images (fabricate the input image in the first place) is referred to as imaging [1]. In every research area they analyze the problem, mostly image analysis involves maneuver the image data to conclude exactly the information compulsory to help to answer a computer imaging problem. This examination is typically part of a larger process which involves preprocessing, characteristic extraction, segmentation, remove noise data, etc, Image dispensation in medical image is a great critical task to find out the problems in the real world medical image. Image processing are done with the help of the digital image, which is captured from the digital format, capturing the image are used to identify the problem in the medical image. It is one of the common factor in this factual world they were many problems occurred to the people. Capturing their difference and analyzing the problem is the most critical task for these fields, most common factor in this field is to find out the problem in different areas such as brain, eye, abdomen, etc. In real world people were affected by many diseases, the most problematic area is the eye disease; without sight of people they cannot do anything in their lonely time [2]. Segmentation of image is an important factor in image processing. This paper uses the pancreas analysis of medical image.

Segmentation of the pancreas is an important step in the development of computer aided diagnosis (CAD) systems that can provide quantitative examination for diabetic patients and a required input for subsequent methodologies for pancreatic cancer detection. Mechanical segmentation of plentiful organs in CT scans with high understanding such as the liver, heart and kidneys [3]. Segmentation of the pancreas, high precision in repeated segmentation remains a confront. The pancreas shows high anatomical deviation in shape, size and setting that change from patient to patient. The amount of visceral fat tissue in the closeness can drastically vary the boundary distinction as well. All these factors make pancreas limb segmentation very challenging [4]. It prevents many segmentation method from achieve high accuracies when evaluate to other segmentation of organs like the liver, heart or kidneys. freshly, the availability of large annotated schooling sets and the accessibility of reasonable parallel computing property via GPUs have made it feasible for "deep learning" methods such as convolutional networks (ConvNets) to be successful in image organization tasks. These methods have the gain that used classification features are trained straight from the imaging data. The pancreas segmentation in computed tomography (CT) images of the abdomen. The process is based on hierarchical coarse-to-fine organization of local image regions (superpixels). Superpixels are removed from the abdominal region by means of Simple Linear Iterative

IJARCCE
ISSN (Online) 2278-1021
ISSN (Print) 2319 5940
International Journal of Advanced Research in Computer and Communication Engineering
ISO 3297:2007 Certified
Vol. 6, Issue 2, February 2017

Clustering (SLIC). An initial probability answer map is produce using patch-level assurance and a two-level cascade of haphazard forest classifiers, from which superpixel regions with prospect larger 0.5 are retained [5, 6]. These retained superpixels serve as a highly susceptible initial input of the pancreas and its environment to a ConvNet that samples a bounding box around each superpixel at poles apart scales (and unsystematic non-rigid deformations at preparation time) in order to dispense a more distinct probability of each superpixel province being pancreas or not. The method generates energetic cascaded and macro super-pixel segmentation information's by classifying image patches at different declaration Fast organ examination using Dense-SIFT algorithm was proposed to solve this question.

II. LITERATURE REVIEW

Holger R. Roth, Amal Farag et al [7], find the routine organ segmentation is an very important prerequisite for many computer-aided judgment systems. The high anatomical unpredictability of organs in the abdomen, such as the pancreas, avert many segmentation processes from achieving high accuracies when compared to other segmentation of organs like the liver, heart or kidneys. Recently, the simplicity of use of large annotated training sets and the accessibility of surrounded by your means parallel computing chattels via GPUs have made it feasible for "deep education" technique such as convolutional network (ConvNets) to do well in demonstration classification tasks. These methods have the advantage that used classification features are skilled directly from the imaging data. We present a fully-automated bottom-up scheme for pancreas segmentation in computed tomography (CT) images of the abdomen. The method is based on hierarchical coarse-to-fine classification of local image regions (superpixels). These retained superpixels serve as a highly susceptible initial input of the pancreas and its surroundings to a ConvNet that samples a bounding box approximately each superpixel at diverse scales (and random non-rigid deformations at training time) in organize to assign a more distinct likelihood of each superpixel region being pancreas or not. We appraise our method on CT images of 82 patients (60 for training, 2 for legalization, and 20 for testing). Using ConvNets we achieve regular Dice scores of 68%+-10% (range, 43-80%) in testing. This shows promise for precise pancreas segmentation, using a deep learning come up to and measure up to favorably to state-of-the-art methods.

Amal Farag, Le Lu et al [8], Organ segmentation is a requirement for a computer-aided diagnosis (CAD) system to perceive pathologies and carry out quantitative analysis. For anatomically high-variability abdominal organs such as the pancreas, previous segmentation works report low accuracies when measure up to to organs like the heart or liver. In this paper, a fully-automated bottom-up process is presented for pancreas segmentation, with abdominal of the computed tomography (CT) scans. The method is based on hierarchical two-tiered information promulgation by categorize image patches. It labels super pixels as pancreas or not via puddle patch-level self-confidence on 2D CT slices over-segmented by the Simple Linear Iterative Clustering approach. A supervised random forest (RF) classifier is qualified on the patch point and a two-level drop of RFs is applied at the superpixel level, coupled with multi-channel quality extraction, correspondingly. On six-fold cross-validation using 80 uncomplaining CT volume, we accomplish 68.8% Dice coefficient and 57.2% Jaccard Index, comparable to or somewhat better than available state-of-the-art methods.

Shimizu et. al [9] utilize three-phase contrast-enhanced CT data which are first inventory together for a particular patient and then registered to a mention patient by landmark-based deformable registration. Patient-specific probabilistic atlas conduct segmentation is conducted; go behind by an intensity-based organization and post-processing. Make available the best overall pancreas organ-level frontier recall by dividing wall each 2D CT axial slice into over-segmentation label maps of all patients. Their concluding binary labeling masks can be uncomplicatedly mound and project-ed back into the 3D CT scan space, to form the pancreas segmentation mask. Random forest classifier and flow of RF classifiers were trained at the image scrap- and superpixel-level respectively, via remove multi-channel features. Based on a six-fold cross corroboration of the 80 CT datasets, our results are comparable and somewhat better than the state-of-the art effort.

Anders Lindbjerg Dahl [10], noteworthy results have been acquire using image models based on image patches, for case in point sparse generative models for image inpainting, noise lessening and superresolution, sparse texture segmentation or texton models. In this paper we propose a commanding and yet straightforward approach for segmentation using vocabulary of image patches with connected label data. The move toward is based on ideas from sparse generative image models and texton based texture modeling. The intensity and label dictionaries are learned from training images with allied label information of (a subset) of the pixels based on a customized vector quantization approach. For new images the intensity dictionary is used to program the image data and the label dictionary is used to build a segmentation of the image. We reveal the algorithm on compound and real texture images and show how victorious training is possible even for noisy image and low-quality label preparation data. In our investigational evaluation we accomplish state-of-the-art presentation for segmentation.

Holger R. Roth et al [11], Automatic organ segmentation is an imperative yet demanding problem for medical image examination. The pancreas is an abdominal organ with very high anatomical inconsistency. This inhibits earlier segmentation methods from accomplish high accuracies, specially measure up to to other organs such as the liver, heart or kidneys. In this paper, we present a

IJARCCE
ISSN (Online) 2278-1021
ISSN (Print) 2319 5940
International Journal of Advanced Research in Computer and Communication Engineering
ISO 3297:2007 Certified
Vol. 6, Issue 2, February 2017

probabilistic bottom-up come within reach of for pancreas segmentation in abdominal computed tomography (CT) scans, by means of multi-level deep involvedness networks (ConvNets). We recommend and estimate several variation of deep ConvNets in the circumstance of hierarchical, coarse-to-fine cataloging on image patches and regions, i.e. superpixels. We first in attendance a dense category of local image patches via P-ConvNet and nearest neighbor fusions. Then we portray a regional ConvNet (R1−ConvNet) that model a set of bounding boxes around each image superpixel at different scales of circumstance in a "zoom-out" fashion. Our ConvNets learn to assign class prospect for each superpixel region of being pancreas. Last, we revise a stacked R2−ConvNet leveraging the combined space of CT intensities and the P−ConvNet dense likelihood maps. Both 3D Gaussian horizontal and 2D restricted random fields are exploited as structured forecast for post-processing. We evaluate on CT images of 82 patients in 4-fold crossvalidation.

III. PROBLEM DEFINITION

The problem in the existing system is pancreas segmentation. Segmentation process of organ can be divided into two grouping top-down and bottom-up methods. In top-down process a-priori knowledge such as atlas (es) and/or shape replica of the organ are generated and included into the structure via learning based shape model fitting or volumetric image register. In bottom-up methods, segmentation is achieved by local image similarity consortium and mounting or pixel; super pixel/super-voxel based cataloging. In previous segmentation come near description low accuracies [12]. It is apposite for well on purpose organs such as liver and heart. It does not size up easily to large datasets. Existing algorithm generate over fitting problem and therefore not correct result of data.

IV. PROPOSED FOR SEGMENTATION PROBLEM

a. Data preprocessing

The data processing task is also one of the criteria which must be taken care in the process of images from the dataset. The image data input to extracting algorithm need not be in proper format and is hence not suitable for processing image efficiently. In such a case, we need to see the data is in appropriate format so that it is apposite for processing. This case in general arrives when we try to excavation the image using preprocessing algorithms. Dissimilar tools available to make preprocessing in the market and that have dissimilar formats for input which makes the user forced to convert the obtainable input dataset into the new arrangement. This itself is very time consuming, backbreaking and has a chance of data loss as the data is to be go through physically into a new format to be sustain by the tool. For this preprocessing the Apriori algorithms [13] were used to determine image of relations and then, to produce the rule about the exposed associations. However the this algorithm is used to scrutinize the unrelated data in a progression image dataset– it find out the result of same or similar data from the image dataset.

Algorithm *Apriori*(Database: $\mathcal{T}$, Support: s)
begin
  Generate frequent 1-patterns and 2-patterns
    using specialized counting methods and
    denote by $\mathcal{F}_1$ and $\mathcal{F}_2$;
  $k := 2$;
  while $\mathcal{F}_k$ is not empty **do**
  begin
    Generate $\mathcal{C}_{k+1}$ by using joins on $\mathcal{F}_k$;
    Prune $\mathcal{C}_{k+1}$ with *Apriori* subset pruning trick;
    Generate $\mathcal{F}_{k+1}$ by counting candidates in
      $\mathcal{C}_{k+1}$ with respect to $\mathcal{T}$ at support s;
    $k := k + 1$;
  end
  return $\cup_{i=1}^{k} \mathcal{F}_i$;
end

Algorithm 1: APriori

b. Feature extraction

Feature extraction helps to reduce the feature space which improves the prediction accurateness and minimizes the addition time. This is achieved by removing irrelevant, redundant and noisy features .i.e., it selects the split of features that can achieve the best performance in terms of correctness and computation time. It performs the Dimensionality reduction [14]. Features are normally selected by search measures. A number of search measures have been proposed. In this work Gaussian Mixture Model Algorithm is proposed to select the most favorable features. The selected optimal features are painstaking for classification. GMM classifiers have been making the most of in various applications of computer vision and medical imaging. They are widely used in purpose where data can be viewed as a grouping of different populations mixed in varying scope. Gaussian Mixture Model is supervised learning classification algorithm that can be used to classify a wide variety of N-dimensional signals. The GMM algorithm is a admirable algorithm to use for the tagging of static position and non-temporal pattern recognition.

c. Superpixel detection

Superpixel-based 3D graph cut algorithm is planned to attain the prostate surface. In its place of pixels, superpixels are measured as the basic dispensation units to make a 3D superpixel-based graph. The superpixels are marker as the prostate or environment by minimizing an energy occupation using graph cut based on the 3D superpixel-based graph. Superpixel illustration is adapted

IJARCCE
ISSN (Online) 2278-1021
ISSN (Print) 2319 5940
International Journal of Advanced Research in Computer and Communication Engineering
ISO 3297:2007 Certified
Vol. 6, Issue 2, February 2017

to the local configuration of the image where, small regions that consequences from unadventurous over segmentation, or —superpixels, to be the uncomplicated unit of any detection, cataloging or localization scheme [15]. Together on the exterior, the existence of superpixels as the basic units seems counterproductive, because aggregate pixels into groups require a decision that is distinct to the final task. But, superpixel aggregation captures the local idleness in the data, and the aim is to reduce the risk of merging unrelated pixels.

d. Pancreas Segmentation

Segmentation is the method of dividing images into component sub-regions. Manual segmentation is achievable but is a time-consuming task and question to operator unevenness. Replicate a manual segmentation product is difficult and the levels of self-confidence ascribed endure for that reason. Mechanical methods are, therefore, preferable; however, important problems must be conquer to achieve segmentation by automatic by using SIFT algorithm. Accurate segmentation of abdominal organs from medical images is an indispensable part of surgical development and computer-aided disease judgment. Many existing algorithms are focused for the segmentation of healthy organs. Cystic pancreas segmentation is more than ever challenging due to its low contrast boundaries, variability in shape, setting and the stage of the pancreatic detection. Decomposition of CT sliced images into a set of displace boundary-preserving superpixels; Computation of pancreas class prospect maps via dense patch category. Macro-Super pixel categorization by pooling both intensity and probability features to form experimental statistics in pour random forest frameworks and Simple connectivity based post-processing. Intense image patch cataloging is demeanor using three methods: Efficient gradient-boosted trees on image histogram, location and texture feature.

D-SIFT algorithm

Step 1: Initialize a new DSIFT filter object by vl_dsift_new (or the simplified vl_dsift_new_basic).
Step 2: Customize the descriptor parameters by vl_dsift_set_steps, vl_dsift_set_geometry, etc.
Step 3: Process an image by vl_dsift_process.
Step 4: Retrieve the number of keypoints (vl_dsift_get_keypoint_num), the keypoints (vl_dsift_get_keypoints), and their descriptors (vl_dsift_get_descriptors).
Step 5: Optionally repeat for more images.
Step 6: Delete the DSIFT filter by vl_dsift_delete.

Algorithm 2: D-SIFT

Dense ScaleInvariant Feature Transform (D-SIFT) algorithm were planned to solve this issue. GBM can offer a bigger edge. GBM is a boosting method, which builds on feeble classifiers [16]. The idea is to add a classifier at a time, so that the next classifier is trained to get better the already trained ensemble. Become aware of that for RF each iteration the classifier is taught independently from the rest.

V. EXPERIMENTAL RESULT

We conduct experimental of datasets on medical image and our experimental result make available better result for pancreas segmentation. For extraction method we use the DSIFT with the applicable feedback of the user. By using this come near for the pancreas we got a good performance, measure up to with many established features extraction technique. Our estimate result of existing and proposed system are shown here.

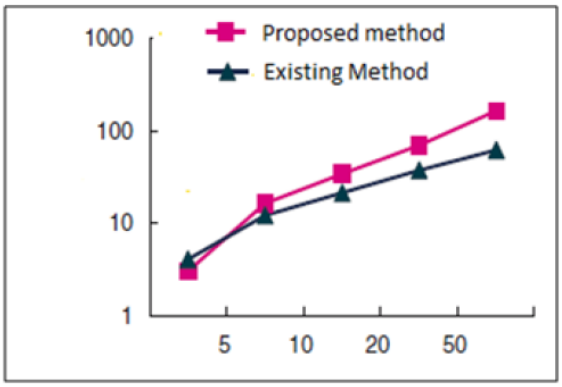

Chart 1: Feature extraction

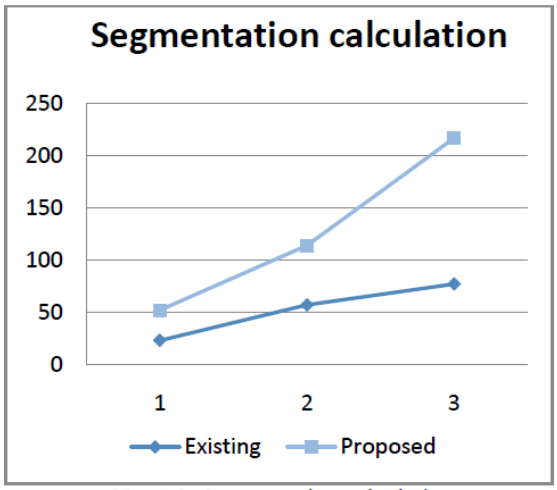

Chart 2: Segmentation calculation

Overall Evaluation Results: This system uses DSIFT to segment the retrieval performance of the algorithms. For every image in the data set, this obtains a ranking list of relevant images computed by each algorithm and compute the average precision based on the image segmentation. As per theoretical analysis the following chart describes the performance difference between existing and proposed systems.

IJARCCE
ISSN (Online) 2278-1021
ISSN (Print) 2319 5940
International Journal of Advanced Research in Computer and Communication Engineering
ISO 3297:2007 Certified
Vol. 6, Issue 2, February 2017

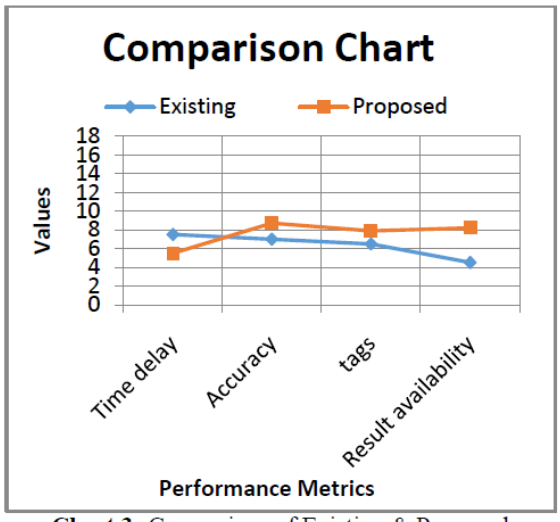

Chart 3: Comparison of Existing & Proposed

Our experimental results achieves the problem of pancreas segmentation is successfully solved, accurate results can be obtained, effective feedbacks provide better search suggestions, achieving fast convergence, reducing resource requirements, guaranteeing to find target images.

VI. CONCLUSION

From the analyses of the problem in medical data they were problem like image segmentation to solve the issue our proposed system segments the pancreas with the considerations of spatial relationships of splenic, portal and superior mesenteric veins with the pancreas. The proposed system uses macro super-pixels for fast and deep labeling and segmentation process. The proposed system is an automated bottom-up approach for pancreas segmentation with the consideration of spatial relationships with the veins in abdominal computed tomography (CT) scans. The method generates dynamic cascaded and macro super-pixel segmentation information's by classifying image patches at different resolutions. Fast organ analysis using Dense-SIFT algorithm.

REFERENCES

[1] Gonzalez RC, Woods RE: Digital Image Processing, 2nd edition.Prentice Hall, Upper Saddle River, 2002
[2] Causes and risk factors of diabetic retinopathy. United States National Library of Medicine. 15 September 2009.
[3] A. Lucchi, K. Smith, R. Achanta, G. Knott, and P. Fua, "Supervoxelbased segmentation of mitochondria in em image stacks with learned shape features," IEEE Trans. on Medical Imaging, vol. 31, no. 2, pp. 474–486, 2012.
[4] D. Mahapatra, P. Schuffler, J. Tielbeek, J. Makanyanga, J. Stoker, S. Taylor, F. Vos, and J. Buhmann, "Automatic detection and segmentation of crohn's disease tissues from abdominal mri,"
[5] J. Tighe and S. Lazebnik, "Superparsing: Scalable nonparametric image parsing with superpixels," International Journal of Computer Vision, vol. 101, no. 2, pp. 329–349, 2013.
[6] P. Neubert and P. Protzel, "Superpixel benchmark and comparison," in Proc. Forum Bildverarbeitung, 2012, pp. 1–12.
[7] Holger R. Roth, Amal Farag et al, "Deep convolutional networks for pancreas segmentation in CT imaging".
[8] Amal Farag, Le Lu et al, "A Bottom-Up Approach for Automatic Pancreas Segmentation in Abdominal CT Scans" .
[9] A. Shimizu, T. Kimoto, H. Kobatake, S. Nawano and K. Shinozaki. "Automated pancreas segmentation from three-dimensional contrast-enhanced computed tomography." Int. J. Comput. Assist. Radiol. Surg., 2010.
[10] Anders Lindbjerg Dahl, "Learning Dictionaries of Discriminative Image Patches".
[11] Holger R. Roth, "DeepOrgan: Multi-level Deep Convolutional Networks for Automated Pancreas Segmentation"
[12] Amal Farag, "A Bottom-up Approach for Pancreas Segmentation using Cascaded Superpixels and (Deep) Image Patch Labeling"
[13] Charu C. Aggarwal et al, "Frequent Pattern Mining Algorithms: A Survey".
[14] M.VASANTHA, "Medical Image Feature, Extraction, Selection And Classification"
[15] S. Ranjitham, "Superpixel Based Color Image Segmentation Techniques: A Review"
[16] Konstantin Dmitriev, "Pancreas and cyst segmentation"

BIOGRAPHIES

Mrs. S. Kavitha, M.Sc., Mphil., (Ph.D) She is working as Assistant Professor & Head of the Dept of Computer Science in Sakthi college of Arts & Science for women. Her teaching experience in 6 years and her area of interest is Digital image processing.

Miss. P. Anusha She completed MCA degree in Gandhigram rural institute-Deemed university and currently pursuing M.Phil in computer science in Sakthi college of Arts & Science for women, Dindigul. Her area of interest is software engineering and digital image processing.

The effect of incorporating carboxylic acid functionalities into 2,20-bipyridine on the biological activity of the complexes formed: synthesis, structure, DNA/protein interaction, antioxidant activity and cytotoxicity	Dr.T.Sathiya Kamatchi,	Chemistry	RSC advances	2017	ISSN: 2046-2069	Web of science https://sci-hub.mksa.top/10.1039/c7ra00425g

RSC Advances

PAPER

View Article Online
View Journal | View Issue

Cite this: *RSC Adv.*, 2017, **7**, 16428

The effect of incorporating carboxylic acid functionalities into 2,2′-bipyridine on the biological activity of the complexes formed: synthesis, structure, DNA/protein interaction, antioxidant activity and cytotoxicity†

Thangavel Sathiya Kamatchi,[af] Nataraj Chitrapriya,[b] Sarvana Loganthan Ashok Kumar,[c] Jang Yoon Jung,[c] Horst Puschmann,[d] Frank R. Fronczek[e] and Karuppannan Natarajan*[a]

In order to find out the influence of carboxylic acid functionalities (COOH) present at different positions in 2,2′-bipyridine on various biological activities such as DNA/protein binding, antioxidant activity and cytotoxicity, three new ruthenium(II) complexes $[RuCl_2(bpy)(S\text{-}DMSO)_2]$ (**1**) (bpy = 2,2′-bipyridine), $[RuCl_2(H_2L1)(S\text{-}DMSO)_2]$ (**2**) (H_2L1 = 2,2′-bipyridine-4,4′-dicarboxylic acid) and $[RuCl_2(H_2L2)(S\text{-}DMSO)_2]$ (**3**) (H_2L2 = 2,2′-bipyridine-5,5′-dicarboxylic acid) have been synthesized and structurally characterized by analytical and spectral methods. The structures of **1** and **3** have been determined by single crystal X-ray diffraction studies, which revealed that both are a roughly regular octahedron with bipyridine/bipyridine dicarboxylic acid as neutral bidentate donors with the involvement of both the nitrogen atoms of the bipyridine ring. *In vitro* DNA binding studies of the complexes were carried out employing absorption titrations, fluorescence spectra, thermal melting, viscosity and circular dichroic measurements, which disclosed that all the complexes bind to CT-DNA *via* groove binding. The interactions of the complexes with bovine serum albumin (BSA) were also investigated using UV-visible, fluorescence and synchronous fluorescence spectroscopic measurements. The results indicated that the new complexes quench the intrinsic fluorescence of BSA protein in a static quenching mode. The assessment of free radical scavenging ability involving the DPPH radical, hydroxyl radical, nitric oxide radical, superoxide anion radical, and hydrogen peroxide and a metal chelating assay showed that the new complexes **2** and **3** possess excellent radical scavenging properties over **1** and standard antioxidants vitamin C and BHT. The *in vitro* cytotoxic activity of the new ruthenium complexes has been validated against HCT-15, HeLa, SKOV3, MCF7 and SKMel2 human cancer cells by SRB assay and cytotoxic selectivity has been examined against NIH 3T3 and HEK 293 normal cells by MTT assay and compared with that of the ruthenium anticancer drug NAMI A and standard platinum drug, cisplatin. The results indicated that the new complexes **2** and **3** displayed substantial cytotoxic specificity towards cancer cells only. Incorporation of a carboxylic acid group in the bipyridine moiety has resulted in showing differences in DNA/protein binding affinity, efficiency in antioxidant activity and cytotoxicity.

Received 11th January 2017
Accepted 25th February 2017

DOI: 10.1039/c7ra00425g

rsc.li/rsc-advances

[a]*Department of Chemistry, Bharathiar University, Coimbatore 641046, India. E-mail: k_natraj6@yahoo.com; Fax: +91 422 242238; Tel: +91 422 2428319*
[b]*Department of Chemistry, Yeungnam University, Gyeongsan City, Gyeong-buk, 712-749, Republic of Korea*
[c]*Department of Chemistry, GRT Institute of Engineering Technology, Tiruttani 631209, India*
[d]*Department of Chemistry, Durham University, Durham, DH1 3KE, UK*
[e]*Department of Chemistry, Louisiana State University, Baton Rouge, LA 70803, USA*
[f]*Department of Chemistry, Sakthi College of Arts and Science for Women, Oddanchatram, Dindigul 624 619, India*

† Electronic supplementary information (ESI) available: Fig. S1–S9 and Tables S1–S7. CCDC 869937 and 843881. For ESI and crystallographic data in CIF or other electronic format see DOI: 10.1039/c7ra00425g

Introduction

Cancer is one of the diseases that has tormented human beings throughout history, for which a wide variety of treatments have been implemented over the years, like surgical removal of tumors, radiation treatment and chemotherapy.[1] Chemotherapy is done most effectively with platinum complexes and out of thousands of synthesized and evaluated Pt(II) complexes, only three of them, namely, cisplatin, carboplatin and oxaliplatin (Fig. 1) have only been approved for worldwide clinical practice and have enjoyed a huge clinical and commercial hit.[2–4] Despite the widespread clinical use, chemotherapy with

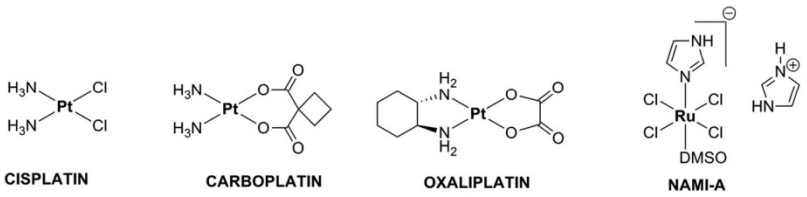

Fig. 1 Structures of some platinum and ruthenium chemotherapeutic complexes.

cisplatin and its analogues still has several drawbacks, in particular: (i) a relatively narrow spectrum of activity (ii) severe side-effects and (iii) acquired resistance.[5] To overcome these problems, a search for new pharmaceutical agents featuring alternative metals has been undertaken.[2,6] Among the several metals that are currently being investigated for their anticancer activity, ruthenium occupies a prominent position.[6a,7] However, many of the ruthenium complexes are barely soluble in aqueous solution[6a,7b,8] and the solubility of ruthenium compounds has been increased by incorporating dialkylsulfoxide derivatives in the complexes as in [*trans*-$RuCl_5$(DMSO)Im][ImH] (NAMI-A) (Fig. 1), which is now recognized as the most successful ruthenium-based anticancer complex that has entered clinical trials.[9] Hence, we attempted to synthesise new ruthenium complexes by incorporating the aforementioned key feature dimethylsulphoxide and also the DNA intercalating moiety bipyridine. Moreover, very little is known in the literature about the reactivity of Ru–chloride–DMSO complexes toward carboxylate or dicarboxylate ligands.[10] But, it is reported that an appropriate attachment of the carboxylic acid (COOH) group in coordination complexes could modulate the solubility of the complex, cell transport and biological activity.[11] This has inspired us to synthesize three new ruthenium complexes containing bipyridine and bipyridine dicarboxylic acids with DMSO as ancillary ligand.

It is a well known fact that DNA and protein are the major pharmacological targets of anticancer drugs,[12] and hence, the objective of the present work is to understand in detail the DNA binding mode of the new complexes with the aid of different techniques. It has been proved that free radicals such as superoxide anion ($O_2^{\bullet -}$), hydroxyl radical ($OH^{\bullet}$) and hydrogen peroxide (H_2O_2) can induce DNA damage in humans. This kind of damage to DNA has also been shown to contribute to aging and various diseases including cardiovascular, cancer and chronic inflammation.[13,14] This has prompted us to test the synthesized complexes as free radical scavengers against various free radicals. Further, the *in vitro* anticancer activities of the synthesized complexes were also evaluated on a panel of cancer and normal cell lines.

Experimental section

Materials and instrumentation

All chemicals were reagent grade and were used as received from commercial suppliers unless otherwise stated. Commercially available $RuCl_3 \cdot 3H_2O$ (Himedia) was used to prepare the starting complex. The starting complex *cis*-[$RuCl_2(DMSO)_4$] was prepared according to the method reported by Evans *et al.*[15] 2,2′-Bipyridine was purchased from Merck chemicals. 2,2′-Bipyridine-4,4′-dicarboxylic acid and 2,2′-bipyridine-5,5′-dicarboxylic acid were purchased from Sigma-Aldrich. Melting points were determined with Lab India instrument. Elemental analyses of carbon, hydrogen, nitrogen and sulphur were performed on Vario EL III Elementar elemental analyzer. Electronic absorption spectra of the complexes were recorded using JASCO 600 spectrophotometer and emission measurements were carried out by using a JASCO FP-6600 spectrofluorometer. Nicolet Avatar Model FT-IR spectrophotometer was used to record the IR spectra (4000–400 cm^{-1}) of the free ligands and complexes as KBr pellets. ^1H NMR spectra were recorded on Bruker AMX 500 at 500 MHz using tetramethylsilane as an internal standard. The chemical shifts are expressed in parts per million (ppm). Calf thymus DNA (CT-DNA) was purchased from Sigma and dissolved in 5 mM Tris–HCl buffer (pH 7.0) containing 100 mM NaCl and 1 mM EDTA. It was dialyzed several times against 5 mM Tris–HCl buffer. All experiments involving interactions of complexes with CT-DNA were carried out in Tris HCl buffer (pH 7.0). Bovine serum albumin (BSA) and ethidium bromide (EB) were obtained from Sigma-Aldrich and used as received. Antioxidant activity measurements were done using UV spectrophotometer (UV-1800, Shimadzu).

Synthesis of new ruthenium(II) complexes

Synthesis of [$RuCl_2$(bpy)(S-DMSO)$_2$] (1). *cis*-[$RuCl_2(DMSO)_4$] (0.100 g, 0.21 mmol) and the ligand 2,2′-bipyridine (0.032 g, 0.21 mmol) were suspended in ethanol (20 mL). 15 min at reflux was needed to solubilize both the metal and chelating partner. The resulting yellowish orange solution was maintained at reflux for five hours. Then the solution was allowed to stand for one week under air until orange crystals of the target complex was precipitated. Yield: 0.081 g, 80%. Melting point: 193 °C. Elemental analyses calculated for $C_{14}H_{20}N_2O_2S_2Cl_2Ru$: C, 34.71; H, 4.16; N, 5.78; S, 13.24%; found: C, 34.66; H, 4.16; N, 5.77; S, 13.25%. FT-IR (cm^{-1}) in KBr: 1473 ν(C=C), 1602 ν(C=N), 1085 $\nu(S{=}O)_{S\text{-bonded}}$. UV-visible (3% DMSO/$H_2O$), λ_{max}, nm (ε, dm^3 mol^{-1} cm^{-1}): 243 (38 941), 287 (58 800), 320 (34 858), 343 (9400), 400 (6325). ^1H NMR δ_H ($CDCl_3$, ppm): 3.58, 3.55, 3.24, 2.68 (4 s, $-CH_3$), 9.90 (1H, d, $J = 8.0$ Hz, $=CH_6$), 9.73 (1H, d, $J = 8.0$ Hz, $=CH_{6'}$), 8.04 (1H, t, $J = 5.5$, $J = 7.5$ Hz, $=CH_5$), 7.93 (1H, t, $J = 8$ Hz, $=CH_{5'}$), 7.63 (1H, t, $J = 7.0$ Hz, $=CH_4$), 7.48 (1H, dd, $J = 8.5$ Hz, $=CH_{4'}$), 8.19 (1H, d, $J = 7.0$ Hz, $=CH_3$), 8.14 (1H, d, $J = 7.5$ Hz, $=CH_{3'}$).

Synthesis of $[RuCl_2(H_2L1)(S\text{-}DMSO)_2]$ (2). *cis*-$[RuCl_2(DMSO)_4]$ (0.100 g, 0.21 mmol) and the ligand 2,2′-bipyridine-4,4′-dicarboxylic acid (0.050 g, 0.21 mmol) were heated under reflux in ethanol (25 mL) for 9 h whereby the solution turned from pale yellow to reddish brown. This solution was allowed to stand at room temperature for one week. The resulting orange red precipitate was filtered off, washed with ethanol, diethyl ether and dried under vacuum. The purity of the complex was checked by TLC ((99 : 5) chloroform–methanol) and attempts to isolate crystals suitable for single crystal XRD studies were unsuccessful. Yield: 0.085 g, 71%. Melting point: >300 °C. Elemental analyses calculated for $C_{16}H_{20}N_2O_6S_2Cl_2Ru$: C, 33.57; H, 3.52; N, 4.89; S, 11.20%; found: C, 33.51; H, 3.52; N, 4.89; S, 11.21%. FT-IR (cm^{-1}) in KBr: 3387 ν(COOH), 1711 ν(C=O), 1609 ν(C=N), 1075 $\nu(S{=}O)_{S\text{-bonded}}$. UV-visible (3% DMSO/$H_2O$), λ_{max}, nm (ε, $dm^3\ mol^{-1}\ cm^{-1}$): 246 (34 375), 300 (54 391), 331 (32 116), 405 (6775). ^1H NMR δ_H ($CDCl_3$, ppm): 3.51, 3.28, 3.09, 2.42 (4 s, $-CH_3$), 9.29 (1H, d, $J = 8.5$ Hz, $=CH_6$), 7.76 (1H, d, $J = 9.0$ Hz, $=CH_{6'}$), 7.98 (1H, dd, $J_o = 7.5$ Hz, $J_m = 1.5$ Hz, $=CH_5$), 7.07 (1H, dd, $J_o = 8$ Hz, $J_m = 2.0$ Hz, $=CH_{5'}$), 8.59 (1H, d, $J_m = 2.0$ Hz, $=CH_3$), 8.43 (1H, d, $J_m = 2.0$ Hz, $=CH_{3'}$), 12.74, 13.30 (2 s, –COOH).

Synthesis of $[RuCl_2(H_2L2)(S\text{-}DMSO)_2]$ (3). It was synthesized using the same procedure as described for **2** with the ligand 2,2′-bipyridine-5,5′-dicarboxylic acid (H_2L2) (0.050 g, 0.21 mmol) and the precursor complex (0.100 g, 0.21 mmol). Slow evaporation of the solvent after reduction to 50% gave orange crystals suitable for single crystal XRD studies. Yield: 0.092 g, 77%. Melting point: >300 °C. Elemental analyses calculated for $C_{16}H_{20}N_2O_6S_2Cl_2Ru$: C, 33.57; H, 3.52; N, 4.89; S, 11.20%; found: C, 33.49; H, 3.52; N, 4.89; S, 11.21%. FT-IR (cm^{-1}) in KBr: 3375 ν(COOH), 1711 ν(C=O), 1642 ν(C=N), 1075 $\nu(S{=}O)_{S\text{-bonded}}$. UV-visible (3% DMSO/$H_2O$), λ_{max}, nm (ε, $dm^3\ mol^{-1}\ cm^{-1}$): 254 (24 691), 301 (53 425), 330 (25 250), 407 (3983). ^1H NMR δ_H ($CDCl_3$, ppm): 3.42, 3.36, 3.02, 2.38 (4 s, $-CH_3$), 10.27 (1H, d, $J_m = 2.0$ Hz, $=CH_6$), 10.07 (1H, d, $J_m = 2.0$ Hz, $=CH_{6'}$), 8.86 (1H, d, $J = 8.0$ Hz, $=CH_4$), 8.81 (1H, d, $J = 8.5$ Hz, $=CH_{4'}$), 8.63 (1H, dd, $J_o = 8.0$ Hz, $J_m = 2.0$ Hz, $=CH_3$), 8.50 (1H, dd, $J_o = 8.0$ Hz, $J_m = 1.5$ Hz, $=CH_{3'}$), 13.49, 13.91 (2 s, –COOH).

X-ray crystallography

X-ray diffraction measurements of complex **1** were performed on a Xcalibur, Sapphire3, Gemini ultra diffractometer. The crystal was kept at 120 K during data collection. Using Olex2,[16] the structure was solved with the Olex2.solve[17] structure solution program using charge flipping and refined with the SHELXL[18] refinement package using least squares minimization. X-ray diffraction measurements of complex **3** were performed at 95 K on a Nonius Kappa CCD diffractometer equipped with graphite monochromated Mo Kα radiation and an Oxford Cryostream cryostat at temperature. The structures of the complexes were solved by direct methods and refinements were carried out by using full matrix least-squares techniques. The hydrogen atoms were generally visible in difference maps and were placed in idealized positions and treated as riding in the refinements, except for those on one water molecule, for which coordinates were refined. For the other two water molecules, H atoms were not located. The following computer programs were used: structure solution SIR-97,[19] refinement SHELXL-97,[18] molecular diagrams and ORTEP-3 (ref. 20) for Windows.

DNA binding experiments

The concentrations of DNA and the new complexes **1–3** were determined spectrophotometrically using their extinction coefficients $\varepsilon_{258\ nm} = 6700\ M^{-1}\ cm^{-1}$, $\varepsilon_{287\ nm} = 58\ 800\ M^{-1}\ cm^{-1}$, $\varepsilon_{300\ nm} = 54\ 391\ M^{-1}\ cm^{-1}$ and $\varepsilon_{301\ nm} = 53\ 425\ M^{-1}\ cm^{-1}$ respectively. The experiments were carried out in 5 mM Tris–HCl buffer (pH 7.0) at ambient temperature and the complexes were dissolved in 5 mM Tris–HCl buffer containing 3% DMSO. Changes in the fluorescence emission spectrum of the ethidium bromide–DNA complex were recorded under various complex concentrations. The fluorescence spectra in the fluorimeter were obtained at an excitation wavelength of 522 nm and an emission wavelength of 584 nm. Melting profiles were measured at 260 nm by a Cary 300 spectrophotometer. Readings were recorded for every 2 °C raise in temperature per minute. The viscosity measurement was carried out using an Ubbelohde viscometer immersed in a thermostatic water bath maintained at 25 ± 0.1 °C. DNA samples with approximately 200 base pairs in length were prepared by sonication in order to minimize complexities arising from DNA flexibility. Flow times were measured with a digital stopwatch; each sample was measured three times, and an average flow time was calculated. Relative viscosities for CT-DNA in the presence and absence of the complex were calculated from the relation $\eta = (t - t_0)/t_0$, where t is the observed flow time of DNA-containing solution and t_0 is the flow time of Tris–HCl buffer alone. Data are presented as $(\eta/\eta_0)^{1/3}$ *versus* binding ratio, where η is the viscosity of CT-DNA in the presence of complex and η_0 is the viscosity of CT-DNA alone.

Protein binding studies

Binding of the complexes with bovine serum albumin (BSA) was studied from the fluorescence spectra recorded with an excitation wavelength of at 280 nm and the corresponding emission at 345 nm assignable to that of BSA. The excitation and emission slit widths and scan rates were maintained constant for all of the experiments. A stock solution of BSA was prepared in 50 mM phosphate buffer (pH = 7.2) and stored in the dark at 4 °C for further use. A concentrated stock solution of the complexes was prepared as mentioned for the DNA binding experiments, except that the phosphate buffer was used instead of a Tris–HCl buffer for all of the experiments. In all the experiments the concentration of BSA was kept constant at 1 μM and complexes **1–3** were varied from 0–30 μM. Titrations were manually done by using a micropipette for the addition of the complexes. For synchronous fluorescence spectra also, the same concentrations of BSA and the complexes were used and the spectra were measured at two different $\Delta\lambda$ values (difference between the excitation and emission wavelengths of BSA), such as 15 and 60 nm.

Antioxidant assays

The ability of ruthenium complexes to act as hydrogen donors or free radical scavengers was tested by conducting a series of *in vitro* antioxidant assays involving DPPH radical, hydroxyl radical, nitric oxide radical, hydrogen peroxide, superoxide anion radical, metal chelating assay and the results were compared with that of standard antioxidants including natural antioxidant vitamin C and synthetic antioxidant BHT (Butylated Hydroxy Toluene).

The DPPH radical scavenging activity of the complexes was measured according to the method of Blois.[21] The DPPH radical is a stable free radical and due to the presence of an odd electron, it shows a strong absorption band at 517 nm in visible spectrum. If this electron becomes paired off in the presence of a free radical scavenger, this absorption vanishes resulting in decolorization stoichiometrically with respect to the number of electrons taken up. Various concentrations of the experimental complexes were taken and the volumes were adjusted to 100 μL with methanol. About 5 mL of 0.1 mM methanolic solution of DPPH was added to the aliquots of samples and standards (BHT and vitamin C) and shaken vigorously. Negative control was prepared by adding 100 μL of methanol in 5 mL of 0.1 mM methanolic solution DPPH. The tubes were allowed to stand for 20 min at 27 °C. The absorbance of the sample was measured at 517 nm against the blank (methanol).

The hydroxyl radical scavenging activity of the complex has been investigated by using the Nash method.[22] *In vitro* hydroxyl radicals were generated by Fe^{3+}/ascorbic acid system. The detection of hydroxyl radicals was carried out by measuring the amount of formaldehyde formed from the oxidation reaction with DMSO. The formaldehyde produced was detected spectrophotometrically at 412 nm. In a typical experiment, a mixture of 1.0 mL of iron–EDTA solution (0.13% ferrous ammonium sulfate and 0.26% EDTA), 0.5 mL of EDTA solution (0.018%), and 1.0 mL of DMSO (0.85% DMSO (v/v) in 0.1 M phosphate buffer, pH 7.4) were sequentially added in the test tubes which contains fixed concentration of the test compounds. The reaction was initiated by adding 0.5 mL of ascorbic acid (0.22%) and was incubated at 80–90 °C for 15 min in a water bath. After incubation, the reaction was terminated by the addition of 1.0 mL of ice-cold trichloroacetic acid (17.5% w/v). Subsequently, 3.0 mL of Nash reagent was added to each tube and left at room temperature for 15 min. The intensity of the colour formed was measured spectrophotometrically at 412 nm against the reagent blank.

Assay of nitric oxide ($NO^{\bullet}$) scavenging activity is based on the method,[23] where sodium nitroprusside in aqueous solution at physiological pH spontaneously generates nitric oxide, which interacts with oxygen to produce nitrite ions. This can be estimated using Griess reagent. Scavengers of nitric oxide compete with oxygen leading to reduced production of nitrite ions. For the experiment, sodium nitroprusside (10 mM) in phosphate buffered saline was mixed with a fixed concentration of the complex, standards and incubated at room temperature for 150 min. After the incubation period, 0.5 mL of Griess reagent containing 1% sulfanilamide, 2% H_3PO_4 and 0.1% *N*-(1-naphthyl) ethylenediamine dihydrochloride was added. The absorbance of the chromophore formed was measured at 546 nm.

The ability of the complexes to scavenge hydrogen peroxide was determined using the method of Ruch *et al.*[24] In a typical experiment, a solution of hydrogen peroxide (2.0 mM) was prepared in phosphate buffer (0.2 M, pH 7.4) and its concentration was determined spectrophotometrically from absorption at 230 nm with molar absorptivity 81 M^{-1} cm^{-1}. The complexes (100 μg mL^{-1}), BHT and vitamin C (100 μg mL^{-1}) were added to 3.4 mL of phosphate buffer prepared above together with hydrogen peroxide solution (0.6 mL). An identical reaction mixture without the sample was taken as negative control. Absorbance of hydrogen peroxide at 230 nm was determined after 10 min against the blank (phosphate buffer).

The superoxide anion radical ($O_2^{-\bullet}$) scavenging assay is based on the capacity of the complexes to inhibit formazan formation by scavenging the superoxide radicals generated in riboflavin-light-NBT system.[25] In a typical experiment, a 3 mL reaction mixture contained 50 mM sodium phosphate buffer (pH 7.6), 20 μg riboflavin, 12 mM EDTA, 0.1 mg NBT and 1 mL complex solution (20–100 μg mL^{-1}). Reaction was started by illuminating the reaction mixture with different concentrations of complex for 90 s. Immediately after illumination, the absorbance was measured at 590 nm. The entire reaction assembly was enclosed in a box lined with aluminium foil. Identical tubes with reaction mixture kept in dark served as blanks.

The chelation with ferrous ions by the experimental complexes was estimated by the method of Dinis *et al.*[26] Initially, about 100 μL of the samples and the standards were added to 50 μL solution of 2 mM $FeCl_2$. The reaction was initiated by the addition of 200 μL of 5 mM ferrozine and the mixture was shaken vigorously and left standing at room temperature for 10 min. Absorbance of the solution was then measured spectrophotometrically at 562 nm against the blank (deionized water).

For the above six assays, all the tests were run in triplicate and the percentage activity was calculated with the help of the following equation

$$\text{Scavenging activity } (\%) = [(A_0 - A_1)/A_0] \times 100$$

where, A_0 is the absorbance of the control and A_1 is the absorbance of the complex/standard.

When the inhibition of the tested compounds is 50%, the tested compound concentration is IC_{50}.

In vitro anticancer activity evaluation

SRB assay. The cell lines were grown in RPMI-1640 medium containing 10% fetal bovine serum and 2 mM L-glutamine. For the screening experiment, cells were inoculated into 96 well microtiter plates in 90 μL at plating densities, depending on the doubling time of individual cell lines. After cell inoculation, the microtiter plates were incubated at 37 °C, 5% CO_2, 95% air and 100% relative humidity for 24 h prior to addition of experimental compounds. After 24 h, one plate of each cell line was fixed *in situ* with TCA, to represent a measurement of the cell population for each cell line at the time of compound addition. NAMI A, cisplatin and the complexes to be tested were dissolved in dimethylsulphoxide and stored frozen prior to use. The

cytotoxicity assay was done against HeLa (human cervix cancer), HCT-15 (human colon tumor), SKOV3 (human ovarian adenocarcinoma), MCF7 (human breast cancer), SKMel2 (human skin melanoma) cell lines which were obtained from National Centre for Cell Science (NCCS), Pune, India. Cell viability was carried out using colorimetric SRB assay method. Solutions of different concentration of the test compounds under test were added to the cell monolayer. Triplicate wells were prepared for each individual concentration. After compound addition, plates were incubated at standard conditions for 48 h and assay was terminated by the addition of cold trichloroacetic acid (TCA). Cells were fixed *in situ* by the gentle addition of 50 μL of cold 30% (w/v) TCA (final concentration, 10% TCA) and incubated for 60 min at 4 °C. Sulforhodamine B (SRB) solution (50 μL) at 0.4% (w/v) in 1% acetic acid was added to each of the wells, and plates were incubated for 20 min at room temperature. After staining, unbound dye was recovered and the residual dye was removed by washing five times with 1% acetic acid. Bound stain was subsequently eluted with 10 mM tris base (pH 10.5) for 5 min. The absorbance was read on an Elisa plate reader at a wavelength of 540 nm with 690 nm as reference wavelength. The results were expressed as the concentration at which there was 50% inhibition (IC_{50}).

MTT assay. The cytotoxicity assay was done against NIH 3T3 (mouse embryonic fibroblasts) and HEK 293 (Human Embryonic Kidney 293 cells), which were obtained from National Centre for Cell Science (NCCS), Pune, India. Cell viability was carried out using the MTT assay. The cells were grown in Dulbeccos modified Eagles medium (DMEM) containing 10% FBS. For screening experiments, the cells were seeded into 96-well plates in 100 μL of respective medium containing 10% FBS, at plating density of 10 000 cells per well and incubated at 37 °C, 5% CO_2, 95% air and 100% relative humidity for 24 h prior to addition of complexes and the standard drugs NAMI A and cisplatin. The test compounds were dissolved in DMSO and diluted in respective medium containing 1% FBS. After 24 h, the medium was replaced with respective medium with 1% FBS containing the test compounds at various concentration and incubated at 37 °C, 5% CO_2, 95% air and 100% relative humidity for 48 h. Triplicate was maintained and the medium without the test compounds was served as control. After 48 h, 10 μL of MTT (5 mg mL^{-1}) in phosphate buffered saline (PBS) was added to each well and incubated at 37 °C for 4 h. The medium with MTT was then flicked off and the formed formazan crystals were dissolved in 100 μL of DMSO and then measured the absorbance at 570 nm using micro plate reader. The % cell inhibition was determined using the following formula, and a graph was plotted between % of cell inhibition and concentration. From this plot, the IC_{50} value was calculated.

$$\% \text{ inhibition} = [\text{mean OD of untreated cells (control)/mean OD of treated cells (control)}] \times 100.$$

Results and discussion

Synthesis and characterization of the complexes

The straightforward reactions of the bipyridine (bpy) and bipyridine dicarboxylic acids (H_2LI/H_2L2) with *cis*-[$RuCl_2$(-DMSO)$_4$] gave new complexes of the types [$RuCl_2$(bpy)(S-DMSO)$_2$] and [$RuCl_2(H_2L)$(S-DMSO)$_2$] where $H_2L = H_2L1/H_2L2$ as sketched out in Scheme 1. The complexes are diamagnetic corresponding to bivalent state of ruthenium (low-spin d^6, $S = 0$). The complexes were stable to air and light, non-hygroscopic in nature and were remarkably soluble in $CHCl_3$, CH_2Cl_2, CH_3CN, DMF and DMSO. These complexes were synthesized in good yields and characterized by elemental analysis, IR and ^1H NMR spectroscopic techniques. The retention of the IR band around 3375–3387 cm^{-1} in **2** and **3** confirms the non participation of COOH group of bipyridine dicarboxylic acid in coordination, which is consistent with the results of NMR and X-ray analysis. ^1H NMR spectrum of the complex **1** is given in Fig. S1 (ESI†). It has been observed that a molecule of the ligands (bpy,

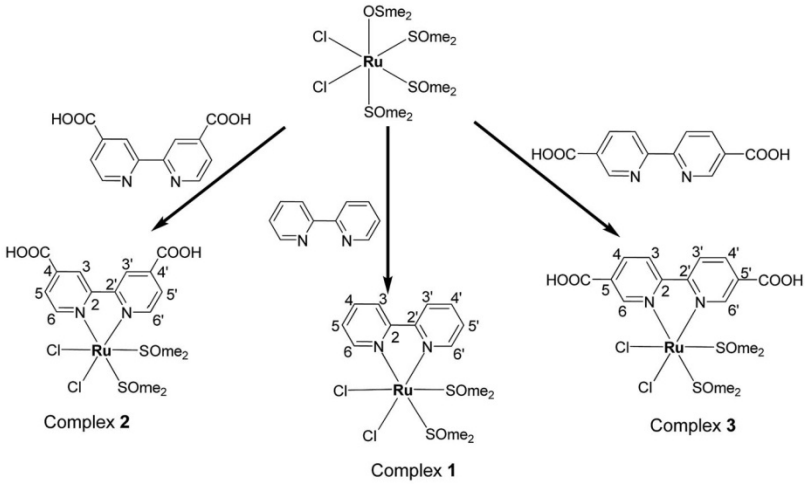

Scheme 1 General scheme for the synthesis of new ruthenium(II) complexes.

H_2L1 and H_2L2) replaced an S-bonded DMSO and an O-bonded DMSO from the precursor complex *cis*-[$RuCl_2$(O-DMSO)(S-DMSO)$_3$]. The solid state structure of the complexes **1** and **3** were determined by single crystal X-ray crystallographic studies. It revealed that bipyridine and bipyridine dicarboxylic acid were coordinated to the metal ion as neutral bidentate NN donors.

X-ray crystallography

The molecular structures of complexes **1** and **3** were established by single crystal X-ray analysis. The ORTEP diagrams with the atom numbering scheme of **1** and **3** are displayed in Fig. 2 and 3 respectively. The relevant details concerning the data collection and structure refinement of the complexes were summarized in Table 1 and selected geometrical parameters (inter atomic distances and angles) are given Table S1 (ESI†). Numerous ruthenium complexes with two or three N–N ligands are known, but examples of mono (N–N) complexes remain scarce, because it is difficult to prevent ligand redistribution during synthesis. The precursor contains three S-bonded DMSO's and one O-bonded DMSO and the structural formula can be written as *cis*,*fac*-[$RuCl_2$(DMSO)$_3$(-DMSO)]. The O-bonded DMSO is the most labile ligand in *cis*,*fac*-[$RuCl_2$(DMSO)$_3$(DMSO)] and is selectively replaced by stronger σ- and π-donors (L) leaving the geometry of the resulting complex unchanged forming *cis*,*fac*-[$RuCl_2$(-DMSO)$_3$(L)]. With the chelating ligands (LL′), displacement of the more weakly held O-bonded DMSO occurs first followed by the displacement of a DMSO ligand *cis* to it.

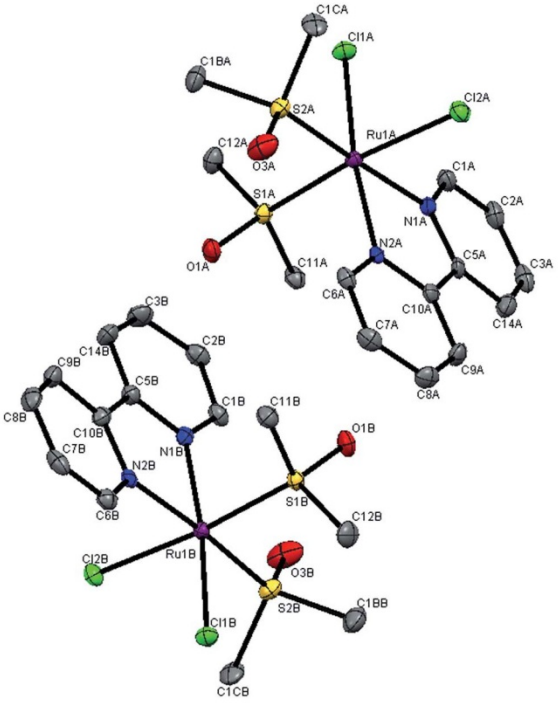

Fig. 2 X-ray crystal structure with atom numbering scheme for complex **1** as thermal ellipsoids at 50% probability level. The hydrogen atoms have been omitted for clarity.

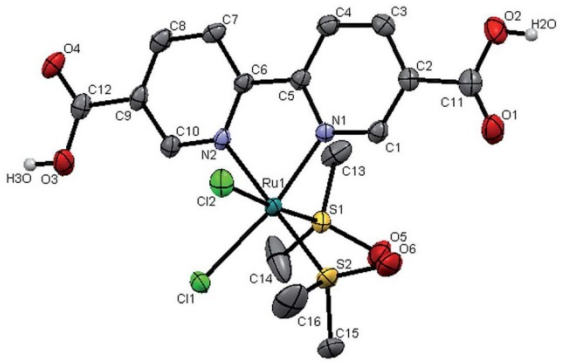

Fig. 3 X-ray crystal structure with atom numbering scheme for complex **3** as thermal ellipsoids at 50% probability level. The hydrogen atoms have been (except carboxylic acid protons) omitted for clarity.

Crystal structure of the complexes 1 and 3

The crystal structures of the complexes **1** and **3** were obtained by examining the nice crystals obtained in the course of slow evaporation. From unit cell dimensions, it is clear that the crystal system of complex **1** is orthorhombic belonging to the space group $Pca2_1$ whereas complex **3** is crystallized in monoclinic space group $P2_1/c$. In complex **1**, there are two independent complex molecules in the asymmetric unit, related by an approximate inversion center near 1/8, 3/4, *z*, as shown in the ORTEP diagram 2. This is the most common location for local centers in this space group.[27] For the new complexes, the coordination sphere around ruthenium centre constitutes distorted octahedron with coordination of bipyridine N–N atoms with bite angles N(1A)–Ru(1A)–N(2A) = 78.17(19)°, N(1B)–Ru(1B)–N(2B) = 78.84(19)° for complex **1** and N(1)–Ru(1)–N(2) = 78.7(1)° for complex **3**. The two S-coordinated DMSO molecules and the two chloride ions in the coordination sphere were found to be *cis* pairs. The basal plane is constructed of two nitrogen atoms of the bipyridine ligand, a chloride and an S-bonded DMSO. The remaining apical coordination sites are filled up by a chloride and an S-bonded DMSO. The distortion in the complex from ideal octahedral geometry is due to the customary small bite angle of the NN chelate and the bending of somewhat bulky chloride and a DMSO ligands towards the chelate, which is evident from the angles N(1A)–Ru(1A)–N(2A) = 78.17(19)°, N(1B)–Ru(1B)–N(2B) = 78.84(19)° [smaller than S(1A)–Ru(1A)–S(2A) = 92.68(6)°; S(1B)–Ru(1B)–S(2B) = 93.80(6)° and Cl(1A)–Ru(1A)–Cl(2A) = 89.31(5)°; Cl(1B)–Ru(1B)–Cl(2B) = 90.39(5)°] and S(1A)–Ru(1A)–Cl(2A) = 174.17(6)°, S(1B)–Ru(1B)–Cl(2B) = 174.58(6)° in complex **1**, where as N(1)–Ru(1)–N(2) = 78.70(1)° [smaller than S1–Ru(1)–S(2) = 92.94(4)° and Cl(1)–Ru(1)–Cl(2) = 89.55(4)°] and S(1)–Ru(1)–Cl(2) = 175.96(4)° in complex **3**. The average Ru–Cl bond lengths in complex **1**, Ru(1)–Cl(1) = 2.427 Å; Ru(1)–Cl(2) = 2.426 Å [Ru(1A)–Cl(1A) = 2.4229(14), Ru(1A)–Cl(2A) = 2.4310(15), Ru(1B)–Cl(1B) = 2.4209(15), Ru(1B)–Cl(2B) = 2.43091(16)] and in

Table 1 Crystallographic data for complexes **1** and **3**

	Complex **1**	Complex **3**
CCDC deposit number	869937	843881
Empirical formula	$C_{14}H_{20}Cl_2N_2O_2RuS_2$	$C_{16}H_{26}Cl_2N_2O_9RuS_2$
Formula weight	484.41	626.48
Temperature/K	120.0 (2)	95.0 (5)
Crystal system	Orthorhombic	Monoclinic
Space group	$Pca2_1$	$P2_1/c$
a/Å	27.7264(7)	13.794(2)
b/Å	7.7631(3)	12.924(2)
c/Å	16.5025(7)	14.1348(15)
α/°	90	90
β/°	90	114.513(7)
γ/°	90	90
Volume/Å^3	3552.1(2)	2292.7(5)
Z	8	4
ρ_{calc} mg mm^{-3}	1.812	1.815
m/mm^{-1}	1.427	1.150
F(000)	1952	1272
Crystal size/mm^3	0.47 × 0.36 × 0.26	0.25 × 0.10 × 0.10
2θ range for data collection	5.25 to 52°	6.24 to 61°
Index ranges	$-34 \le h \le 34$	$-18 \le h \le 19$
	$-9 \le k \le 9$	$-11 \le k \le 18$
	$-20 \le l \le 20$	$-19 \le l \le 18$
Reflections collected	46 162	24 867
Independent reflections	6978 [R(int) = 0.0526]	6251 [R(int) = 0.0208]
Data/restraints/parameters	6978/1/423	6251/0/302
Goodness-of-fit on F^2	1.128	1.013
Final R indexes [$I \ge 2\sigma(I)$]	R_1 = 0.0292	R_1 = 0.0479
	wR_2 = 0.0703	wR_2 = 0.1064
Final R indexes [all data]	R_1 = 0.0301	R_1 = 0.0633
	wR_2 = 0.0709	wR_2 = 0.1151
Largest diff. peak/hole/e Å^{-3}	2.31/−0.72	1.79/−1.32

complex **3**, Ru(1)–Cl(1) = 2.414 (1) Å; Ru(1)–Cl(2) = 2.4289 (9) Å is comparable with that of *cis*,*fac*-[$RuCl_2(DMSO)_3$(DMSO)] (average Ru–Cl = 2.42 Å)[28] and other Ru(II)–DMSO–Cl complexes.[29,30] The geometry of the coordinated DMSO is approximately tetrahedral with angles ranging from 111 to 119° in the two complexes. The Ru–S bond lengths [for **1**, Ru(1A)–S(1A) = 2.2322(15); Ru(1A)–S(2A) = 2.2888(16); Ru(1B)–S(1B) = 2.2366(15); Ru(1B)–S(2B) = 2.2885(15) Å; for **3**, Ru(1)–S(1) = 2.2258(9); Ru(1)–S(2) = 2.291(1) Å] are in the same range as observed in other Ru(II)–DMSO–Cl complexes.[31–33] The S–O bond distance [for **1**, S(1A)–O(1A) = 1.484(4), S(2A)–O(3A) = 1.489(5); S(1B)–O(1B) = 1.478(4), S(2B)–O(3B) = 1.477(5) Å; for **3**, S(1)–O(5) = 1.493(3), S(2)–O(6) = 1.487(4) Å] and the S–C bond distance [1.784–1.790 Å in **1**, 1.7745–1.797 Å in **3**] are consistent with the values reported in the literature.[31,34,35] The deviation of the bond angles in complex **1**, S(1A)–Ru(1A)–S(2A) = 92.68(6)°; S(1B)–Ru1B–S2B = 93.80(6)° and in complex **3**, S(1)–Ru(1)–S(2) = 92.68(4) from 90° is most probably due to steric repulsion between the DMSO molecules. The average Ru–N bond distance fall in the range of Ru–N = 2.082–2.086 Å in **1**, and Ru–N = 2.083 Å in **3** and are consistent with the values reported in the literature.[33,36,37]

DNA binding studies

UV-visible measurements. Electronic absorption spectroscopy is one of the most useful and important techniques for DNA-binding studies of metal complexes. Absorption spectra were recorded for the solutions of the complexes in the absence and in the presence of increasing concentrations of CT-DNA to evaluate the binding affinity. In the UV-visible spectra of the complexes, transition bands were observed around 250, 300 and 400 nm. These are assigned to the predominant π–π*, L-delocalized (L = bpy, H_2L1, and H_2L2) n–π* transition with shoulder and (Ru → L) metal-to-ligand charge transfer (MLCT) based transitions respectively. The electronic spectra of the complexes are slightly different from each other in their visible region. The complexes (12 μM) were titrated with varying concentrations of CT-DNA and the change in the absorption spectral profile of all the complexes at different DNA concentrations is shown in Fig. 4. The absorbance intensity of all the complexes around 300 nm was seen to steadily decrease with increasing DNA concentration. These DNA induced spectral changes reveal interesting interaction of the complexes with the DNA helix. The absorption spectrum of the DNA was subtracted from that of the mixtures for the ease of comparison. The addition of DNA resulted in hypochromism of about 8%, 15% and 6% with insignificant bathochromic shift of the complexes **1–3** respectively in the π–π* absorption around 300 nm. The

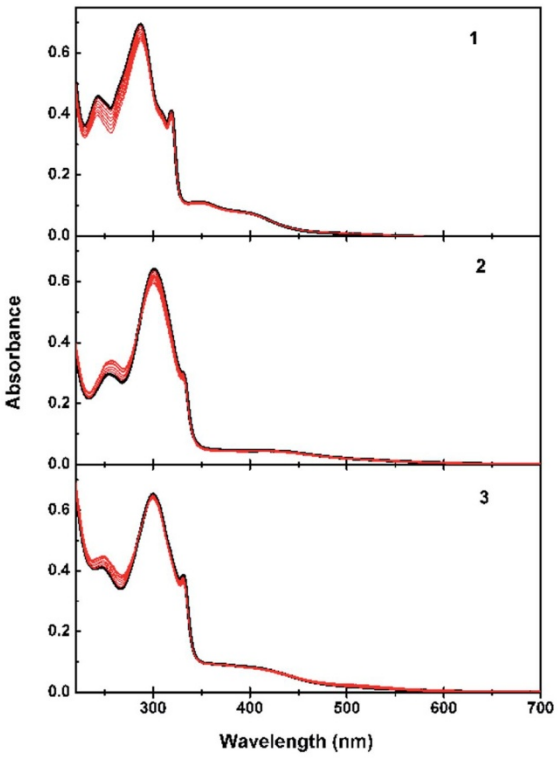

Fig. 4 UV-visible spectra for the titration of complexes (12 μM, black) with CT-DNA (0–110 μM).

peaks can be seen to shift progressively toward a limit which represents a spectrum of the complex in a fully complexed form. Addition of DNA results in a moderate hypochromism of the absorption peaks accompanied by a minor bathochromic shift indicating that the complexes do not strongly bind to DNA with bipyridine and bipyridine dicarboxylic acid moieties and hence, intercalative binding mode may be ruled out. However, these spectral characteristics demonstrated that the complexes may bind to one of the grooves of the double helix structure of DNA *via* the intermolecular interactions of carboxylic acid substituents on bipyridine moiety or by ancillary ligand. The complex **2** showed significantly higher DNA binding propensity possibly due to the position of the substituent on the chelating part of bipyridine favouring considerable interaction into the DNA than complex **1** and **3**. This trend suggests that the binding strength of the complex to DNA is being effectively controlled by the position of substituent.

From the observed spectral data, the intrinsic binding constants for the complexes **1–3** were calculated using the eqn (1) at the π–π^* absorption band and the values obtained are smaller than those that observed for intercalators.

$$[\mathrm{DNA}]/(\varepsilon_a - \varepsilon_f) = [\mathrm{DNA}]/(\varepsilon_b - \varepsilon_f) + 1/(K_b(\varepsilon_b - \varepsilon_f)) \quad (1)$$

where [DNA] is the concentration of DNA in base pairs, ε_a, ε_f, and ε_b are the apparent-, free- and bound-metal-complex extinction coefficients respectively. K_b is the equilibrium binding constant of complex binding to DNA. Each set of data, when fitted to the above equation, gave a straight line with a slope of $1/(\varepsilon_b - \varepsilon_f)$ and a y-intercept of $1/K_b(\varepsilon_b - \varepsilon_f)$ and K_b was determined from the ratio of the slope to intercept (Fig. S2 and Table S2, ESI†). The binding constants K_b obtained for **1**, **2** and **3** are 3.74×10^3 M^{-1}, 1.34×10^4 M^{-1} and 3.53×10^3 M^{-1} respectively, which support appreciable groove binding of the complexes to the CT-DNA. However, further investigation is absolutely necessary to establish the exact nature of the binding of complexes to DNA.

Fluorescence competition experiment. In order to further confirm the interaction between the test compounds and CT-DNA, steady-state competitive binding experiments using **1**, **2** and **3** as quenchers were undertaken. Ethidium bromide (EB), a planar cationic dye has been widely used as a sensitive fluorescence probe for native DNA. Usually, EB intercalates strongly between adjacent DNA base pairs which results in emitting intense fluorescent light. As and when a quencher is added, it displaces the EB and a decrease of fluorescence results and the quenching is due to the reduction of the number of binding sites on the DNA that are available to EB. EB–DNA experiments were performed by adding increasing amounts of test solutions to the EB bound CT-DNA solution in Tris–HCl buffer. In our experiment, the EB–DNA system exhibited a strong emission band around 592 nm. The fluorescence quenching spectra of DNA-bound EB by complexes **1**, **2** and **3** shown in Fig. 5 which illustrates that, as the concentrations of the complexes increases, the emission intensity at 592 nm of EB–DNA system decreased in different amounts. Correlation equation and R^2 value for EB–DNA fluorescence quenching by complexes **1–3** are given in Table S3 (ESI†). Upon addition of **1** and **3** to the EB–DNA system, meagre reduction in

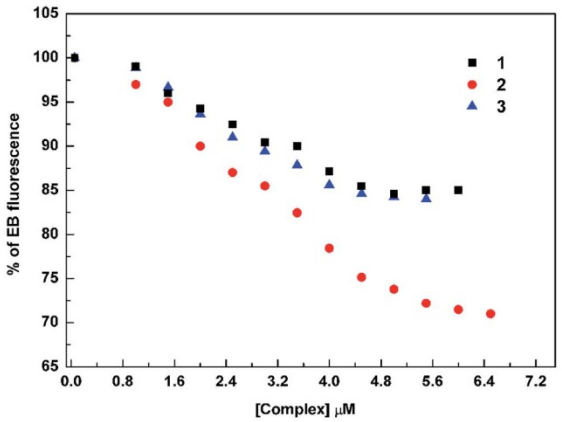

Fig. 5 Plot of EB relative fluorescence intensity (%) *vs.* [complex].

emission intensities of EB by 16% and 15% respectively was observed, relative to that observed in the absence of complexes. On the other hand, addition of **2** to the EB–DNA mixture produced a remarkable reduction in fluorescence intensity, but the value of fluorescence intensity decreased by no more than 50%. The apparent binding constant (k_{app}) values for the complexes could not be calculated, due to the lack of 50% of EB emission in the concentration range used in the present study. The changes observed here are characteristic of groove binding mode which is consistent with that reported earlier.[38]

Mechanism for the fluorescence quenching. From the fluorescence spectroscopic studies, we found that the fluorescence intensity of the EB–DNA system decreased regularly with the addition of increasing concentration of the complexes. In order to determine the type of fluorescence quenching, the fluorescence intensity of EB–DNA complex with various concentrations of ruthenium complexes **1–3** was measured at different temperatures. There are two types of quenching and they are classified as either dynamic quenching or static quenching. Dynamic and static quenching can be distinguished by their different dependencies on temperature. Dynamic quenching depends upon diffusion and it increases with increase in temperature. On the other hand there will be decrease in diffusion in case of static quenching.[39]

In order to confirm the quenching mechanism in our cases, the fluorescence quenching was analyzed according to Stern–Volmer eqn (2) at different temperatures (Fig. S3 and Table S4, ESI†) and the quenching constants are given in Table 2.

$$F_0/F = 1 + K_{sv}[\mathrm{Q}] \quad (2)$$

where F_0 and F are the fluorescence intensities in the absence and presence of the quencher, respectively, [Q] is the concentration of the quencher and K_{sv} is the Stern–Volmer quenching constant.

The results in Table 2 indicate that the probable quenching mechanism of fluorescence of EB–DNA by complexes **1–3** is by static quenching since in all cases K_{sv} has been seen to be inversely proportional to temperature.[40]

Table 2 Stern–Volmer quenching constants of complexes–DNA system at various temperatures

Complexes	27 °C	45 °C
1	3.15×10^4	2.51×10^4
2	5.52×10^4	1.68×10^4
3	3.02×10^4	2.56×10^4

DNA melting studies. The thermal behaviours of DNA in the presence of complexes can give insight into DNA conformational changes when temperature is raised. The melting temperature T_m of DNA solution, which is defined as the temperature when half of the total base pairs are unbonded or at which the double helix denatures into single stranded DNA through the breaking of hydrogen bonding between the bases, is usually introduced to study the interaction of transition metal complexes with nucleic acid. Generally, the melting temperature of DNA increases when metal complexes bind to DNA by intercalation, as intercalation of the complexes between DNA base pairs causes stabilization of base stacking and hence raises the melting temperature of double-stranded DNA. Therefore, the thermal denaturation experiment of DNA provides a convenient tool for detecting binding and also assessing relative binding strengths and hence DNA melting experiments were performed. In the present work, the thermal denaturation temperature (T_m) of unbound CT-DNA in the absence of complexes is 61.2 °C under our experimental conditions. But, a moderate positive shift in the DNA melting temperature (ΔT_m) is observed on the addition of the complexes to DNA (Fig. 6) and the ΔT_m value of DNA was found to increase by 2 °C, 4 °C and 2 °C upon binding to **1**, **2** and **3** respectively. The results primarily suggest the groove binding or electrostatic binding nature of the complexes to DNA in preference to intercalative mode of binding DNA that normally gives significantly high positive ΔT_m values.[41]

Viscometric studies. As a means for further clarifying the binding of ruthenium complexes with DNA, the viscosity of DNA solutions containing varying amounts of complexes was measured. The electrostatic binding generally has no obvious effect on the viscosity of DNA, while a classical intercalation will result in lengthening of the DNA helix as base pairs are separated to accommodate the foreign molecules, leading to the increase of DNA viscosity.[42,43] The effects upon the addition of increasing concentrations of the complexes to DNA and a typical intercalator, namely EB on viscosity of DNA are shown in Fig. 7. Correlation equation and R^2 value of EB and complexes on viscosity of DNA are given in Table S5 (ESI†). It is known that the drug molecules normally bind exclusively in the DNA groove (*e.g.*, netropsin and distmycine, Hoechst 33258) typically causing a less pronounced (positive or negative) or no change in the viscosity of DNA solution.[44–46] From our viscosity measurements, it is seen that our complexes increase the viscosity of DNA but only to lesser extent as compared to EB, indicating primarily either a groove binding or surface binding nature of the complexes. Based on the change in the degree of viscosity, the binding of our complexes to DNA is in the order **2** > **1** ∼ **3**, which is consistent with our foregoing hypothesis.

Circular dichroism. CT-DNA in the B conformation exhibits two conservative circular dichroic (CD) bands, a positive band around 275 nm due to base stacking and a negative band around 240 nm due to right handed helicity. These bands are sensitive towards binding of any small molecule or drug and hence, can be exploited to investigate the binding of small molecules to DNA.[47] Simple groove binding and electrostatic interactions of small molecules lead to no perturbation or marginal perturbations in these two CD bands of B-DNA. On the other hand, intercalative interaction of small molecules with DNA leads to enhancement in the intensity of 275 nm band and decrease in the intensity of 245 nm band.[48] CD spectra of CT-DNA in the absence as well as in the presence of increasing amounts of the test complexes were recorded and they are shown in Fig. 8. It is seen from the spectra that upon the addition of complexes to DNA, the intensity of the positive peak increased while the intensity of the negative peak decreased without any shift in the peak positions. Further, it is also noticed that the CD spectral changes for **2** are larger than

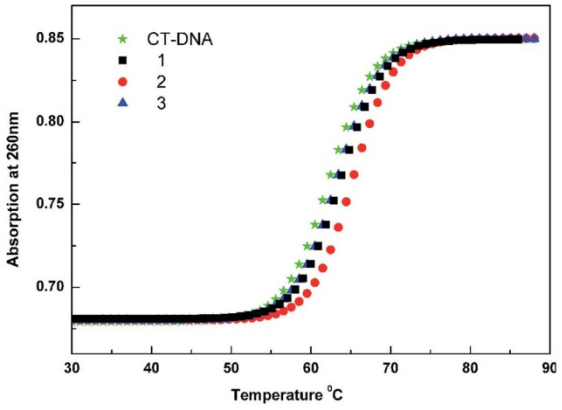

Fig. 6 Melting curves of CT-DNA in absence and presence of complexes, [DNA] = 100 μM and [Ru(II) complex] = 12 μM.

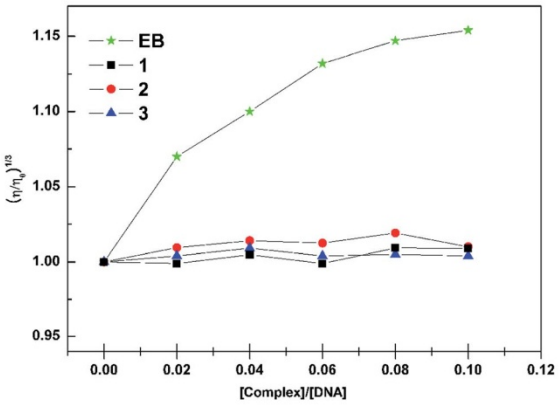

Fig. 7 Effect of the increasing amount of the complexes on the relative viscosity of CT-DNA.

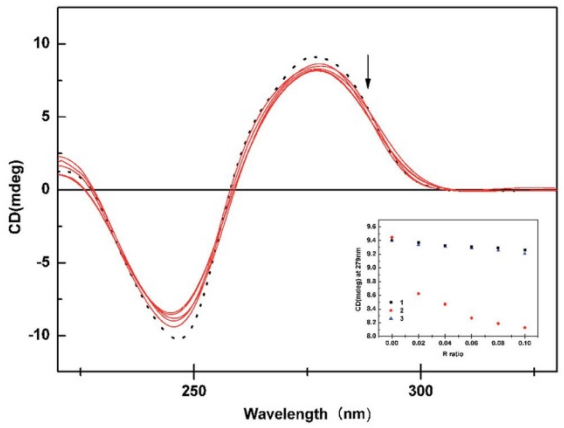

Fig. 8 CD spectrum of CT-DNA in the absence (dotted) and presence (solid) of complex **2**. Inset: changes in CD intensity at 278 nm with respect to *R* ratio.

those that observed for **1** and **3** indicating a better interaction of **2** with DNA, a finding which has been seen already in the absorption titrations, fluorescence quenching, DNA melting and viscosity measurements.

Protein binding studies

Since the interaction of biologically active compounds with proteins leads to either enhancement or loss of the biological properties of such compounds, it is important to study the interaction of any test compound with proteins. Hence, we have studied the interactions of our new complexes with BSA by means of UV-visible and fluorescence spectroscopy since BSA is one of the most extensively studied proteins, particularly because of its structural homology with human serum albumin (HSA). UV-visible spectra of BSA in the absence and presence of the complexes is shown in Fig. S4 (ESI†). It is seen from the Fig. S4† that the absorption intensity of BSA was enhanced as the complexes were added, and there was a small red shift of about 2, 7 and 2 nm for the compounds **1**, **2** and **3** respectively. This result suggested not only the complex formation between BSA and the test compounds but also confirms a static quenching process.[49]

Fluorescence quenching studies of BSA

In order to get more information on the binding of the compounds with BSA, fluorescence spectrum of BSA was studied upon the addition of the test compounds. Even though three fluorophores, namely, tryptophan, tyrosine and phenylalanine are present in BSA, the intrinsic fluorescence of BSA is mainly due to tryptophan alone[50] and changes in the emission spectra of tryptophan can give information about protein conformational transitions, subunit associations, substrate binding, or denaturation. Therefore, the intrinsic fluorescence of BSA can provide considerable information on their structure and dynamics and is often employed in the study of protein folding and association reactions. Hence, the interaction of BSA with our complexes (**1–3**) was studied by fluorescence measurement at room temperature and from which the binding constants of the complexes were calculated. In a typical experiment, a solution of BSA (1 μM) was titrated with various concentrations of the complexes (0–35 μM). Fluorescence spectra were recorded in the range of 290–500 nm upon excitation at 280 nm. The changes observed on the fluorescence emission spectra of a solution of BSA on the addition of increasing amounts of complexes **1–3** are shown in Fig. 9. Addition of complexes to BSA produced a dramatic modification on the emission profile. The fluorescence of BSA was quenched effectively with the red shift of 5 nm in the case of complex **1** and blue and red shift of 8 and 2 nm in the emission maximum of the complexes **2** and **3** respectively. The observed difference in the initial fluorescence of BSA is mainly due to the fact that the active site in protein is buried in a hydrophobic environment. This result indicated a definite interaction of all of the test compounds with the BSA protein.

To study the quenching process further, fluorescence quenching data were analyzed with the Stern–Volmer eqn (3) and Scatchard eqn (4). The ratio of the fluorescence intensity in the absence of (I_0) and in the presence of (I) the quencher is related to the concentration of the quencher [Q] by a coefficient K_{sv}.

$$I_0/I = 1 + K_{sv}[Q] \quad (3)$$

K_{sv} value obtained from the plot of I_0/I *vs.* [Q] was found to be 3.18×10^4 M^{-1}, 1.36×10^5 M^{-1} and 1.17×10^5 M^{-1} corresponding to the complexes **1–3** respectively. The observed linearity in the plots (Fig. S5 and Table S6, ESI†) indicated the ability of the complexes to quench the emission intensity of BSA. From K_{sv} values (Table 3), it can be seen that the complexes **2** and **3** exhibited strong protein-binding ability than that of **1**.

For the static quenching, when molecules bind independently to a set of equivalent sites on a macromolecule, the binding constant (K) and the number of binding sites (n) can be determined by the Scatchard eqn (4).

$$\log\left[\frac{F_0 - F}{F}\right] = \log K + n \log[Q] \quad (4)$$

where K is the binding constant of quencher with BSA, n is the number of binding sites, F_0 and F are the fluorescence intensity in the absence and presence of the quencher. The value of K can be calculated from the slope of $\log[(F_0 - F)/F]$ *versus* $\log[Q]$. (Fig. S6 and Table S7, ESI†). The calculated value of binding constant (K) and the number of binding sites (n) were listed in Table 3. The values of n at room temperature are approximately equal to 1, which indicates that there is just one single binding site in BSA for the complexes **1–3**.

Synchronous fluorescence spectra

After having obtained the binding constant and binding number of the compounds with BSA, it is important to know about the conformational change of protein molecular environment in a vicinity of the fluorophore functional groups.[51] The different

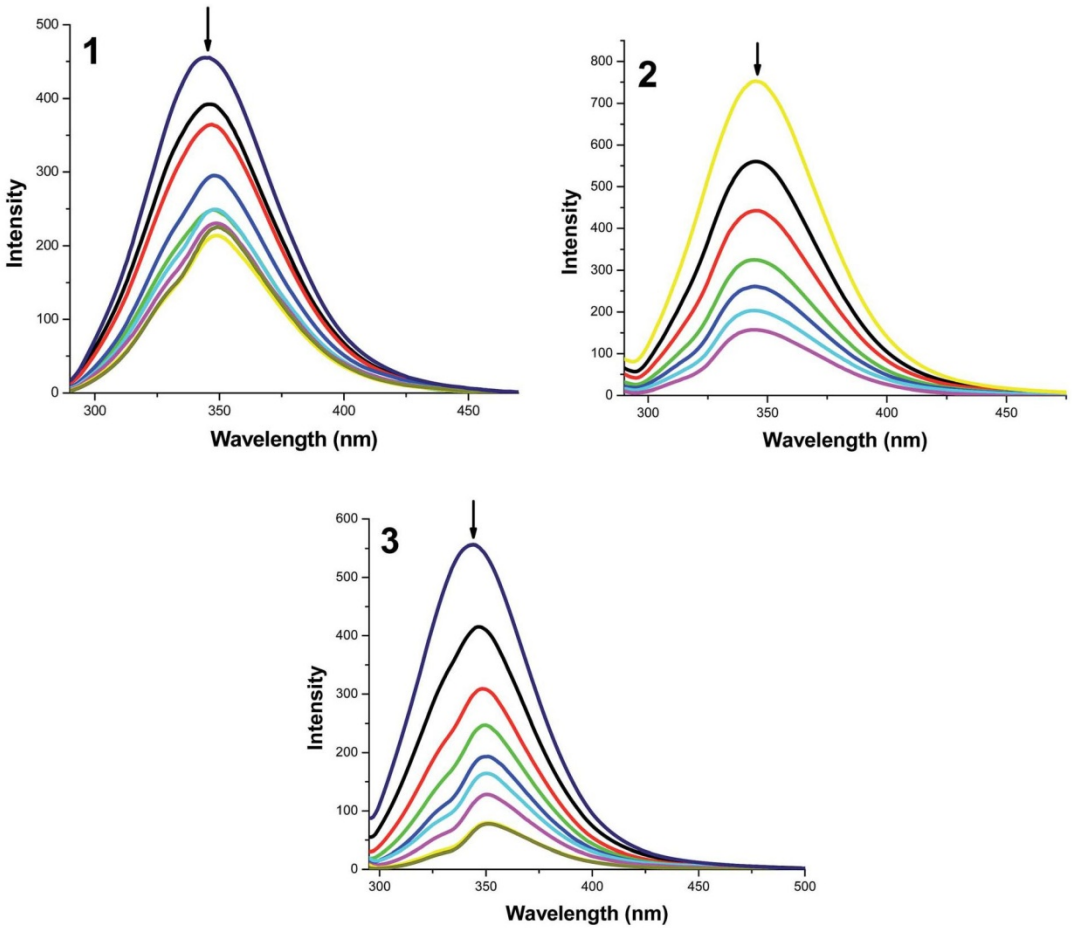

Fig. 9 The emission spectrum of BSA (1 μM; $\lambda_{exc} = 280$ nm; $\lambda_{emi} = 345$ nm) in the presence of increasing amounts of the complexes **1–3** (0–35 μM). The arrow shows the fluorescence quenching upon increasing complex concentration.

Table 3 Binding constant and number of binding sites for interaction of complexes with BSA

Complexes	$K_{sv} \times M^{-1}$	$K \times M^{-1}$	n
BSA + **1**	3.18×10^4	5.79×10^4	1.05
BSA + **2**	1.36×10^5	3.77×10^6	1.34
BSA + **3**	1.17×10^5	1.33×10^6	1.25

nature of chromophores can be found from synchronous fluorescence spectroscopy by looking at the difference between excitation and emission wavelength ($\Delta\lambda = \lambda_{emi} - \lambda_{exc}$).[52] A value of 15 nm for $\Delta\lambda$ is characteristic of tyrosine residue, whereas a value of 60 nm is characteristic of tryptophan.[53] This kind of variation in the tryptophan emission occurs due to protein conformational changes. In order to explore the structural change of BSA, we measured synchronous fluorescence spectra at $\Delta\lambda = 15$ nm (Fig. S7, ESI†) and $\Delta\lambda = 60$ nm (Fig. S8, ESI†) of BSA with complexes **1–3**. The synchronous fluorescence spectral studies clearly suggested that the fluorescence intensities of both the tryptophan and tyrosine were affected with an increasing concentration of the complexes, which clearly indicated that the interaction of complexes with BSA affects the conformation of both the tryptophan and tyrosine micro regions. So, the strong interaction between the test compounds and BSA protein implied that these compounds can easily be stored in protein and can be released in desired targets.

Bipyridine ligand systems are extremely versatile in that small structural changes can be readily made that lead to very different chemical and physical properties. The spectroscopic results show that the carboxylic acid functionalities at different positions on the bipyridine ligand can cause some interesting differences in their DNA/protein binding properties. Since the chelating part of the ligand and ancillary ligands is same in all the three complexes the difference in binding affinity depends on the position of the –COOH groups at bipyridine moiety. The substitution on 5,5′-position of pyridine rings of bipyridine ligand may cause steric constraints, when the complex

approaches the DNA base pairs and protein, thus decreasing the binding affinity of complex with DNA/protein. In complex **2**, the two –COOH substituents present at 4,4′-position of bipyridine ligand may bring some flexibility to the complex or furnish slightly tapered shape to chelating ligand which would help to approach the DNA/protein easily. This will lead to the formation of favourable H-bonding interactions with DNA groove/protein surface and two –COOH groups, thus resulting in the complex **2** bound to the grooves of DNA/protein more strongly. Surprisingly, the complexes **1** and **3** exhibit similar binding affinity although complex **1** does not have carboxylic acid functionality, which may be due to the less accessibility of the complex **3** towards DNA/protein and contribution of the ancillary ligands of bipyridine into the binding. It is remarkable that even seemingly minor changes in the ligand architecture and electronic structure can lead to profound effects on DNA/protein binding. These results have confirmed that the affinity magnitudes of the complexes toward DNA/protein may be controlled and tuned by playing with the position of the substituent on the chelating ligand and this strategy may be valuable in understanding the DNA/protein binding properties of the complexes containing bipyridine and bipyridine dicarboxylic acids as well as laying a foundation for the rational design of novel, powerful agents for probing and targeting nucleic acids.

Antioxidant activity studies

Since the experiments carried out so far revealed that the new ruthenium complexes exhibit reasonable DNA and protein binding affinity, it is considered worthwhile to test their ability to quench the free radicals and study their antioxidant properties. Usually free radicals are generated in many bioorganic redox processes and they induce oxidative damage in various components of the body (lipids, proteins and DNA) and they have been implicated in chronic diseases such as cancer, hypertension, Parkinson disease, Alzheimer, cardiac infarction, atherosclerosis, rheumatism, cataracts *etc.*[54,55] Efforts to counteract the damage caused by the free radicals are gaining acceptance as an origin for novel therapeutic approaches and the field of preventive medicine is experiencing an upsurge of interest in medically useful antioxidants.

The *in vitro* antioxidant properties of ruthenium complexes have attracted a lot of interest, but the radical scavenging activity is limited to hydroxyl radical.[56] Hence, we carried out experiments to investigate the free radical scavenging ability of the new ruthenium complexes against a panel of free radicals, with a hope to develop potential antioxidants and therapeutic reagents. The IC_{50} value of all the complexes (Table 4) obtained from different types of assay experiments strongly supports that the new complexes possess good antioxidant activities, which are much better than that of the standard antioxidants vitamin C and BHT.

Antioxidants exert their effect by different mechanisms such as scavenging or inhibiting free radicals by the donation of an electron or proton (H^+) or chelation of metal ions that otherwise may lead to free radical formation. From the radical scavenging data (Table 4), it can be seen that complexes **2** and **3** showed better radical scavenging activity than complex **1**. This might be due to the presence of free carboxylic acid groups in the bipyridine moiety of **2** and **3** thus making those complexes efficient hydrogen donors to stabilize the unpaired electrons and thereby scavenging the free radicals. Out of the five radical species chosen to examine, the DPPH radical scavenging power of the tested complexes was the most (9.44 ± 1.21 μM), and the hydrogen peroxide scavenging ability was the least (208.49 ± 5.19 μM). The antioxidant ability of any compound besides being related with the hydrogen atom transfer reaction could also be due to its capacity to chelate metal ions and/or inhibit oxidative enzymes. Earlier investigations have shown that the participation of perferryl complex ($ADP–Fe^{3+}–O_2^{-\bullet}$) in the initiation and propagation of lipid peroxidation, indicating the requirement of oxygen and free iron.[57] Hence, it is inferred that the presence of molecules with the ability to chelate metal ions could reduce the reactive species which will lead to the protection of lipid membranes against peroxidation. Hence, we studied the metal chelating capacity of our compounds with Fe^{2+} ion which showed that the complexes exhibited moderate to high metal chelating activity which might be due to the chelation of Fe^{2+} ion by the uncoordinated COOH group. A plausible mechanism for metal chelating and DPPH scavenging activity of the complexes is given in Fig. S9 (ESI†). The appropriate attachment of COOH group (H^+ donation and COO^- chelation) is only the responsible factor, which makes **2** and **3** superior to **1** in all the radical scavenging assays including metal chelating activity. Though the structural differences between the two compounds **2** and **3** are not very pronounced, the complex **3** displayed better antioxidant activity than **2** in of all assays, suggesting that the possible intramolecular hydrogen bonding formation

Table 4 Antioxidant activity of the new complexes, vitamin C and BHT against various radicals

	IC_{50}[a] (μM)					
Compounds	DPPH$^\bullet$	OH$^\bullet$	NO$^\bullet$	$O_2^{-\bullet}$	H_2O_2	Metal chelation
1	21.89 ± 0.92	59.24 ± 0.13	75.96 ± 0.30	57.06 ± 0.93	208.49 ± 5.19	117.80 ± 0.72
2	9.66 ± 0.82	44.42 ± 0.11	60.27 ± 0.21	35.86 ± 1.28	165.62 ± 0.69	7.11 ± 0.40
3	9.44 ± 1.21	43.56 ± 0.15	56.38 ± 0.20	26.36 ± 0.38	123.09 ± 0.72	6.65 ± 0.69
Vitamin C	147.6 ± 4.2	232.8 ± 1.9	215.8 ± 2.7	221.4 ± 1.2	238.5 ± 3.6	—
BHT	86.2 ± 1.8	163.4 ± 0.7	154.3 ± 2.4	131.6 ± 1.5	149.8 ± 4.3	—

[a] Fifty percent inhibitory concentration of the test compounds against free radicals.

in **2** may hinder the donation of H^+ in neutralizing the free radicals. The metal chelating and DPPH radical scavenging ability of the new complexes are better than those that were previously reported by us for other ruthenium(II) complexes comprising dicarboxylic acids.[58,11c]

Anticancer activity studies

Since the results of antioxidant activity experiments revealed that the new complexes exhibit good antioxidant activity, we switched over our study to anticancer activity evaluation because nowadays it has been strongly suspected that cancer may be one of those degenerative disease induced by free radicals. Further, substantial evidence supports the active involvement of free radicals in the development of several pathological conditions including neurodegenerative and cardiovascular diseases, diabetes, cancer or even normal aging. To study cytotoxic activity of the new complexes on cancer cells, the SRB test was used. Moreover, since the balance between the therapeutic potential and toxic side effects of a compound is very important when evaluating its usefulness as a pharmacological drug, experiments were also designed to investigate the *in vitro* cytotoxic selectivity of synthesized ruthenium complexes against normal cells by MTT assay. The cytotoxic activity study was carried with the complexes **1–3**, using five different cancer cell lines HeLa, HCT-15, SKOV3, MCF7, SKMel2 and two normal cell lines NIH 3T3, HEK 293. The effects of the test compounds on the viability of these cells were evaluated after an exposure period of 48 h. The cells were treated with different concentrations of the test compounds. The test compounds were dissolved in DMSO and the blank samples containing same volume of DMSO were taken as controls to identify the activity of the solvent in the cytotoxicity experiment. In parallel, the influence of ruthenium anticancer drug NAMI A and widely used platinum anticancer drug, cisplatin have also been assayed as a positive control. The IC_{50} values for three new ruthenium complexes **1–3**, NAMI A and cisplatin for selected cell lines are shown in Table 5. In the case of all the cancer cells tested, it is interesting to observe that while complex **1** is not active, complexes **2** and **3** show some cytotoxic activity against cell lines, although the activities are lower than those exhibited by cisplatin which is very common for ruthenium based anticancer agents.[40] However, while comparing the cytotoxicity of the new complexes with NAMI A, they displayed better activity corresponding to inhibition over NAMI A in almost all the cancer cells tested. The lack of cytotoxic activity of **1** was expected in view of its specific structure *i.e.* the absence of COOH; by contrast, the activity of **2** and **3** toward the cancer cell lines is quite striking in view of the presence of the carboxylic acid arm in the bipyridine ligand. As evaluated by their IC_{50} values, **2** and **3** displayed better cytotoxic activity against SKOV3 cells when compared to the other cancer cells screened. **1** did not show any significant activity even up to 500 μM concentration on HeLa and MCF7 cells. The results of MTT assay also indicated that the IC_{50} values of complexes **2** and **3** against NIH 3T3 and HEK 293 cells are found to be above 1000 μM, which confirmed that the complexes are very specific on cancer cells and even less toxic compared to NAMI A ($IC_{50(NIH\ 3T3)} = 570$ μM; $IC_{50(HEK\ 293)} = 533$ μM) and cisplatin ($IC_{50(NIH\ 3T3)} = 175$ μM; $IC_{50(HEK\ 293)} = 115$ μM). Considering the specific structures of **1** and **2**, **3**, it appears that the carboxyl moiety of **2** and **3** may play a critical role for the observed cytotoxic activity and selectivity on the tested cell lines. The COOH group could not easily penetrate the hydrophobic cellular membrane of noncancerous cells but could readily bind to certain biomolecules over expressed on surfaces of the rapidly growing cancer cells. The activity results suggest a variation of cell sensitivity in the cell lines studied and was in the sequence of **2** ∼ **3** > **1**, which is consistent with the trends of their radical scavenging abilities. Another generalization is that there is no substantial variation in the cytotoxic activities when the position of COOH in the bipyridine moiety of the complexes was changed. Though the new ruthenium complexes did not show significant *in vitro* cytotoxicity, further studies are needed to assess their antiproliferative activity *in vivo* and to elucidate the actual mechanism of the anti-tumor activity. But the cytotoxicity and selectivity of the synthesized complexes may be improved by introducing more carboxylic acid functionalities, other functional groups like sulphonic acid, ester, methoxy, amine, DNA intercalating terpyridine, phenanthroline moieties and one or more ruthenium ions in the form of bi or polynuclear ruthenium complexes.

Conclusion

The present contribution describes the synthesis and characterization of two types of three new ruthenium(II) complexes. One is composed by bipyridine moiety with COOH and the

Table 5 IC_{50} (μM) ruthenium complexes, NAMI A and cisplatin against various cancer and normal cells

	IC_{50}[a] (μM)						
	SRB assay					MTT assay	
Complexes	HCT-15	HeLa	SKOV3	MCF7	SKMel2	NIH 3T3	HEK 293
1	376.23 ± 2.20	>500	241.76 ± 1.22	>500	357.22 ± 3.50	235 ± 1	197 ± 2
2	227.74 ± 0.08	380.34 ± 0.58	192.98 ± 1.47	258.00 ± 0.55	279.42 ± 0.39	>1000	>1000
3	208.12 ± 0.59	291 ± 0.11	189.47 ± 0.14	227.74 ± 1.47	235.76 ± 1.60	>1000	>1000
NAMI A	>500	>500	>500	>500	>500	570 ± 4	533 ± 3
Cisplatin	45.49 ± 0.40	54.00 ± 0.7	32.56 ± 1.36	18.73 ± 0.28	25.53 ± 0.3	175 ± 2	115 ± 5

[a] Fifty percent inhibitory concentration after exposure for 48 h.

other is only with the bipyridine moiety and two chlorides and dimethylsulphoxides are common to both. In both the cases, ruthenium is bonded to the nitrogen atoms of the bipyridine ring, which is confirmed by single crystal X-ray crystallographic studies. The groove binding of the mentioned complexes with DNA was deduced by taking account of relevant UV-visible absorption spectra, fluorescence spectra, DNA melting, viscosity measurements and circular dichroism. The protein binding properties of the complexes were examined by the fluorescence spectra and a greater binding affinity was observed for the complexes **2** and **3** over **1**. The incorporation and position of COOH group in the bipyridine ring played a significant role in modulating the DNA/protein binding behaviours of the complexes. Moreover, the results obtained from various antioxidant assays and cytotoxic studies showed that the complexes **2** and **3** showed good radical scavenging ability, moderate cytotoxic activity and greater cytotoxic selectivity over **1**. It is seen from the results that the introduction of COOH group in the bipyridine ring markedly increased the antitumor and antioxidant efficiency of the new complexes. We can envision this to open up new avenues for the designing and screening of the suitable ruthenium complexes containing free COOH group for anticancer activity studies.

Electronic supplementary information

^{1}H NMR spectrum of complex **1** (Fig. S1†); selected geometrical parameters for complexes **1** and **3** (Table S1†); plot of [DNA]/($\varepsilon_a - \varepsilon_f$) *vs.* [DNA] for the titration of CT-DNA with complexes **1–3** (Fig. S2†); correlation equation and R^2 value of the complexes **1–3** for plot of [DNA]/($\varepsilon_a - \varepsilon_f$) *vs.* [DNA] (Table S2†); correlation equation and R^2 value for EB–DNA fluorescence quenching by complexes **1–3** (Table S3†); Stern–Volmer plots for EB–DNA quenching by the ruthenium complexes at different temperatures (Fig. S3†); correlation equation and R^2 value of **1–3** for Stern–Volmer plots for EB–DNA quenching by the ruthenium complexes at different temperatures (Table S4†); correlation equation and R^2 value of EB and complexes on viscosity of DNA (Table S5†); UV-visible absorption spectra of BSA in the absence and presence of the complexes **1–3** (Fig. S4†); plot of I_0/I *vs.* log [Q] (Fig. S5†); correlation equation and R^2 value of complexes **1–3** for plot of I_0/I *vs.* log[Q] (Table S6†); plot of log[($F_0 - F$)/F] *vs.* log[Q] (Fig. S6†); correlation equation and R^2 value of the complexes **1–3** for plot of log[($F_0 - F$)/F] *vs.* log[Q] (Table S7†); synchronous spectra of BSA in the presence of increasing amounts of the complexes **1–3** for a wavelength difference of $\Delta\lambda$ = 15 nm (Fig. S7†); synchronous spectra of BSA in the presence of increasing amounts of the complexes **1–3** for a wavelength difference of $\Delta\lambda$ = 60 nm (Fig. S8†); plausible mechanisms for DPPH radical scavenging and metal chelating activity for complex **3** (Fig. S9†); CCDC reference numbers 869937 and 843881.

Acknowledgements

Council of Scientific and Industrial Research, New Delhi, India, for the award of Senior Research Fellowship to T. Sathiya Kamatchi is gratefully acknowledged. We would like to thank Dr P. Kalaivani for her help in carrying out the protein binding studies. Acknowledgment is also made to Mr S. Saravanan and Dr T. Parimelazhagan, Department of Botany, Bharathiar University, India for their help in radical scavenging assays.

References

1 (*a*) B. A. Chabner and T. G. Roberts, *Nat. Rev. Cancer*, 2005, **5**, 65–72; (*b*) J. Bernier, E. J. Hall and A. Giaccia, *Nat. Rev. Cancer*, 2004, **4**, 737–747.
2 M. Galanski, V. B. Arion, M. A. Jakupec and B. K. Keppler, *Curr. Pharm. Des.*, 2003, **9**, 2078–2089.
3 M. A. Jakupec, M. Galanski and B. K. Keppler, *Rev. Physiol., Biochem. Pharmacol.*, 2003, **146**, 1–53.
4 M. Galanski, M. A. Jakupec and B. K. Keppler, *Curr. Med. Chem.*, 2005, **12**, 2075–2094.
5 (*a*) G. Daugaard and U. Abildgaard, *Cancer Chemother. Pharmacol.*, 1989, **25**, 1–9; (*b*) V. Pinzani, F. Bressolle, I. J. Haug, M. Galtier, J. P. Blayac and P. Balmes, *Cancer Chemother. Pharmacol.*, 1994, **35**, 1–9; (*c*) D. Screnci and M. J. McKeage, *J. Inorg. Biochem.*, 1999, **77**, 105–110; (*d*) L. Troy, K. McFarland, S. Littman-Power, B. J. Kelly, E. T. Walpole, D. Wyld and D. Thomson, *Psycho Oncol.*, 2000, **9**, 29–39; (*e*) M. Markman, *Expert Opin. Drug Saf.*, 2003, **2**, 597–607; (*f*) P. C. Bruijnincx and P. J. Sadler, *Curr. Opin. Chem. Biol.*, 2008, **12**, 197–206; (*g*) K. Barabas, R. Milner, D. Lurie and C. Adin, *Vet. Comp. Oncol.*, 2008, **6**, 1–18; (*h*) P. Borst, S. Rottenberg and J. Jonkers, *Cell Cycle*, 2008, **7**, 1353–1359.
6 (*a*) M. J. Clarke, F. C. Zhu and D. R. Frasca, *Chem. Rev.*, 1999, **99**, 2511–2533; (*b*) R. H. Fish and G. Jaouen, *Organometallics*, 2003, **22**, 2166–2177.
7 (*a*) C. S. Allardyce and P. J. Dyson, *Platinum Met. Rev.*, 2001, **45**, 62–69; (*b*) M. J. Clarke, *Coord. Chem. Rev.*, 2003, **236**, 209–233; (*c*) Y. K. Yan, M. Melchart, A. Habtemariam and P. J. Sadler, *Chem. Commun.*, 2005, **38**, 4764–4776; (*d*) P. J. Dyson and G. Sava, *Dalton Trans.*, 2006, **16**, 1929–1933; (*e*) M. Melchart and P. J. Sadler, in *Bioorganometallics: Biomolecules, Labeling, Medicine*, ed. G. Jaouen, Wiley-VCH, New York, 2006, pp. 39–62; (*f*) A. Levina, A. Mitra and P. A. Lay, *Metallomics*, 2009, **1**, 458–470; (*g*) I. Bratsos, T. Gianferrara, E. Alessio, C. G. Hartinger, M. A. Jakupec and B. K. Keppler, in *Bioinorganic Medicinal Chemistry*, ed. E. Alessio, Wiley-VCH, Weinheim, 2011, pp. 151–174; (*h*) S. B. Fricker, *Dalton Trans.*, 2007, 4903–4917.
8 I. Bratsos, S. Jedner, T. Gianferrara and E. Alessio, *Chimia*, 2007, **61**, 692–697.
9 (*a*) F. Frausin, V. Scarcia, M. Cocchietto and G. Sava, *J. Pharmacol. Exp. Ther.*, 2005, **313**, 227–233; (*b*) B. Serli, E. Zangrando, T. Gianferrara, L. Yellowlees and E. Alessio, *Coord. Chem. Rev.*, 2003, **245**, 73–83; (*c*) G. Sava, R. Gagliardi, A. Bergamo, E. Alessio and G. Mestroni, *Anticancer Res.*, 1999, **19**, 969–972.
10 E. Alessio, *Chem. Rev.*, 2004, **104**, 4203–4242.
11 (*a*) C. M. Giandomenico, M. J. Abrams, B. A. Murrer, J. F. Vollano, M. I. Rheinheimer, S. B. Wyer, G. E. Bossard

and J. D. Higgins, *Inorg. Chem.*, 1995, **34**, 1015–1021; (*b*) M. Galanski and B. K. Keppler, *Inorg. Chem.*, 1996, **35**, 1709–1711; (*c*) T. Sathiya Kamatchi, N. Chitrapriya, H. Lee, F. R. Fronczek and K. Natarajan, *Eur. J. Med. Chem.*, 2013, **59**, 253–264.

12 (*a*) H. Y. Mei and J. K. Barton, *Proc. Natl. Acad. Sci. U. S. A.*, 1988, **85**(5), 1339–1343; (*b*) V. Brabec, *Prog. Nucleic Acid Res. Mol. Biol.*, 2002, **71**, 1–68; (*c*) B. M. Zeglis, V. C. Pierre and J. K. Barton, *Chem. Commun.*, 2007, **44**, 4565–4579; (*d*) C. Gaiddon, P. Jeannequin, P. Bischoff, M. Pfeffer, C. Sirlin and J. P. Loeffler, *J. Pharmacol. Exp. Ther.*, 2005, **315**(3), 1403–1411; (*e*) R. L. Hayward, Q. C. Schornagel, R. Tente, J. S. Macpherson, R. E. Aird and S. Guichard, *Cancer Chemother. Pharmacol.*, 2005, **55**(6), 577–583; (*f*) S. Chatterjee, S. Kundu, A. Bhattacharyya, C. G. Hartinger and P. J. Dyson, *J. Biol. Inorg Chem.*, 2008, **13**(7), 1149–1155; (*g*) B. Wu, M. S. Ong, M. Groessl, Z. Adhireksan, C. G. Hartinger, P. J. Dyson and C. A. Davey, *Chem.–Eur. J.*, 2011, **17**, 3562–3566.

13 K. B. Beckman and B. N. Ames, *Phys. Rev.*, 1998, **78**, 447–453.

14 B. Halliwel and J. M. C. Gutteridge, *Free Radicals in Biology and Medicine*, Clarendon Press, Oxford, 2nd edn, 1989, pp. 416–494.

15 I. P. Evans, A. Spencer and G. Wilkinson, *J. Chem. Soc., Dalton Trans.*, 1973, **2**, 204–209.

16 O. V. Dolomanov, L. J. Bourhis, R. J. Gildea, J. A. K. Howard and H. Puschmann, OLEX2: a complete structure solution, refinement and analysis program, *J. Appl. Crystallogr.*, 2009, **42**, 339–341.

17 L. J. Bourhis, O. V. Dolomanov, R. J. Gildea, J. A. K. Howard and H. Puschmann, *olex2.solve*, 2011.

18 G. M. Sheldrick, *Acta Crystallogr., Sect. A: Found. Crystallogr.*, 2008, **64**, 112–122.

19 M. C. Altomare, M. Burla, G. L. Camalli, C. Cascarano, A. Giacovazzo, A. G. G. Guagliardi, G. Moliterni and R. Polidori, *J. Appl. Crystallogr.*, 1999, **32**, 115–119.

20 L. J. Farrugia, *J. Appl. Crystallogr.*, 1997, **30**, 565–566.

21 M. S. Blois, *Nature*, 1958, **29**, 1199–1200.

22 T. Nash, *J. Biochem.*, 1953, **55**, 416–421.

23 L. C. Green, D. A. Wagner, J. Glogowski, P. L. Skipper, J. S. Wishnok and S. R. Tannenbaum, *Anal. Biochem.*, 1982, **126**, 131–138.

24 R. J. Ruch, S. J. Cheng and J. E. Klaunig, *Carcinogenesis*, 1989, **10**, 1003–1008.

25 C. Beauchamp and I. Fridovich, *Anal. Biochem.*, 1971, **44**, 276–287.

26 T. C. P. Dinis, V. M. C. Madeira and L. M. Almeida, *Arch. Biochem. Biophys.*, 1994, **315**, 161–169.

27 R. E. Marsh, V. Schomaker and F. H. Herbstein, *Acta Crystallogr., Sect. B: Struct. Sci.*, 1998, **54**, 921–924.

28 E. Alessio, G. Mestroni, G. Nardin, W. M. Attia, M. Calligaris, G. Sava and S. Zorzet, *Inorg. Chem.*, 1988, **27**, 4106–4113.

29 M. Trivedi, Y. K. Sharma, R. Nagarajan and N. P. Rath, *J. Mol. Struct.*, 2010, **975**, 335–342.

30 J. Mola, I. Romero, M. Rodriguez, F. Bozoglian, A. Poater, M. Sola, T. Parella, J. Benet-Buchholz, X. Fontrodona and A. Llobet, *Inorg. Chem.*, 2007, **46**(25), 10707–10716.

31 E. Reisner, V. B. Arion, A. Rufinska, I. Chiorescu, W. F. Schmid and B. K. Keppler, *Dalton Trans.*, 2005, **21**(14), 2355–2364.

32 M. B. Cingi, M. Lanfranchi, M. A. Pellinghelli and M. Tegoni, *Eur. J. Inorg. Chem.*, 2000, 703–711.

33 C. Tan, S. Hu, J. Liu and L. Ji, *Eur. J. Med. Chem.*, 2011, **46**, 1555–1563.

34 I. Bratsos, B. Serli, E. Zangrando, N. Katsaros and E. Alessio, *Inorg. Chem.*, 2007, **46**, 975–992.

35 M. Calligaris, *Coord. Chem. Rev.*, 2004, **248**, 351–375.

36 I. Bratsos, D. Urankar, E. Zangrando, P. Genova-Kalou, J. Kosmrlj, E. Alessio and I. Turel, *Dalton Trans.*, 2011, **40**, 5188–5199.

37 C. Sens, M. Rodriguez, I. Romero, A. Llobet, T. Parella, B. P. Sullivan and J. Benet-Buchholz, *Inorg. Chem.*, 2003, **42**, 2040–2048.

38 D. J. Patel, *Acc. Chem. Res.*, 1979, **12**, 118–125.

39 (*a*) G. Z. Chen, X. Z. Haong, J. C. Xu, Z. Z. Zhang and Z. B. Wang, *The methods of Fluorescence Analysis*, Beijing Science Press, 2nd edn, 1990, pp. 2–112; (*b*) Y. Lu, Y. L. Wang, S. H. Gao, G. K. Wang, C. L. Yan and D. J. Chen, *J. Lumin.*, 2009, **129**, 1048–1054; (*c*) S. Ashoka, J. Seetharamappa, P. B. Kandagal and S. M. T. Shaikh, *J. Lumin.*, 2006, **121**, 179–186.

40 J. Chen, X. Y. Jiang, X. Q. Chen and Y. Chen, *J. Mol. Struct.*, 2008, **876**, 121–126.

41 (*a*) M. J. Han, L. H. Gao and K. Z. Wang, *New J. Chem.*, 2006, **30**, 208–214; (*b*) Y. Z. Ma, H. J. Yin and K. Z. Wang, *J. Phys. Chem. B*, 2009, **113**, 111039–111047.

42 S. Satyanarayana, J. C. Dabrowiak and J. B. Chaires, *Biochemistry*, 1993, **32**, 2573–2584.

43 Y. Wang, G. Lin, J. Hong, T. Lu, L. Li, N. Okabe and M. Odoko, *Inorg. Chim. Acta*, 2009, **362**, 377–384.

44 E. C. Long and J. K. Barton, *Acc. Chem. Res.*, 1990, **23**, 271–273.

45 D. Suh and J. B. Chaires, *Bioorg. Med. Chem.*, 1995, **3**(6), 723–728.

46 L. Lerman, *J. Mol. Biol.*, 1961, **3**, 18–30.

47 B. Norden and F. Tjerneld, *Biopolymers*, 1982, **21**, 1713–1734.

48 P. T. Selvi and M. Palaniandavar, *Inorg. Chim. Acta*, 2002, **337**, 420–428.

49 H. Y. Liu, Z. H. Xu, X. H. Liu, P. X. XI and Z. Z. Zeng, *Chem. Pharm. Bull.*, 2009, **57**, 1237–1242.

50 A. Sulkowska, *J. Mol. Struct.*, 2002, **614**, 227–232.

51 G. Z. Chen, X. Z. Huang, J. G. Xu, Z. B. Wang and Z. Z. Zhang, *Method of Fluorescent Analysis*, Science Press, Beijing, 2nd edn, 1990, vol. 126, ch. 4, p. 123.

52 J. N. Miller, Recent advances in molecular luminescence analysis, *Proc. Anal. Div. Chem. Soc.*, 1979, **16**, 203–208.

53 J. H. Tang, F. Luan and X. G. Chen, *Bioorg. Med. Chem.*, 2006, **49**, 3210–3217.

54 K. Tsai, T. G. Hsu, K. M. Hsu, H. Cheng, T. Y. Liu, C. F. Hsu and C. W. Kong, *Free Radical Biol. Med.*, 2001, **31**, 1465–1472.

55 C. S. Rivas, J. C. Espin and H. Wichers, *Phytochem. Anal.*, 2000, **11**, 330–338.

56 (*a*) H. L. Huang, Y. J. Liu, C. H. Zeng, J. H. Yao, Z. H. Liang, Z. Z. Li and F. H. Wu, *J. Mol. Struct.*, 2010, **966**, 136–143; (*b*) Y. J. Liu, C. H. Zeng, Z. H. Liang, J. H. Yao, H. L. Huang, Z. Z. Li and F. H. Wu, *Eur. J. Med. Chem.*, 2010, **45**, 3087–3095; (*c*) X. L. Hong, H. Li and C. H. Peng, *J. Mol. Struct.*, 2011, **990**, 197–203; (*d*) Z. Z. Li, Z. H. Liang, H. L. Huang and Y. J. Liu, *J. Mol. Struct.*, 2011, **1001**, 36–42; (*e*) Y. J. Liu, Z. H. Liang, Z. Z. Li, J. H. Yao and H. L. Huang, *J. Organomet. Chem.*, 2011, **696**, 2728–2735.

57 K. Kogure, H. Sassa, K. Abe, K. Kitahara, Y. Sano, H. Kawano, Y. Nakagawa and H. Terada, *Biol. Pharm. Bull.*, 1998, **21**, 180–183.

58 T. Sathiya Kamatchi, N. Chitrapriya, S. K. Kim, F. R. Fronczek and K. Natarajan, *Dalton Trans.*, 2012, **41**, 2066–2077.

A Review on Relation between Dominating and Total Dominating Color Transversal Number of Graph and Monotonicity	R.Jeyamani Assistant Professor of Mathematics	Maths	International Journal of Mathematics Trends and Technology (IJMTT)	April 2017	ISSN: 2231-5373 (P:23-27)	**UGC Approved Journal in 2017** https://www.ijmttjournal.org/2017/Volume-44/number-1/IJMTT-V44P503.pdf

A Review on Relation between Dominating and Total Dominating Color Transversal Number of Graph and Monotonicity

[1] J.Sangeetha [2] R.Jeyamani
[1]*Research Scholar, Sakthi College of Arts and Science for Women, Oddanchatram.*
[2]*Associate Professor, Department of Mathematics, Sakthi College of Arts and Science for Women, Oddanchatram.*

ABSTRACT – *Domination is a very fast developing area in Graph Theory. This paper deals with combination of domination, total domination, proper colouring and transversal sets. Also demonstrate the domination transversal number for different types of graphs. We also extend some relation between domination and total domination colour transversal number of graphs. We also provide some examples to justify our results. We also obtain an upper bound of this number which increases monotonically.*

Keywords: *Domination, Total domination, Transversal sets, Proper colouring.*

1. INTRODUCTION

Graphs are mathematical structures used to model pair-wise relations between objects from a certain collection. Graph can be defined a set V of vertices and set of edges. Where, V is collection of |V| = n abstract data types. Vertices can be any abstract data types and can be presented with the points in the plane. These abstract data types are also called nodes. A line (line segment) connecting these nodes is called an edge. Again, more abstractly saying, edge can be an abstract data type that shows relation between the nodes (which again can be an abstract data types).

Euler proposed that any given graph can be traversed with each edge traversed exactly once if and only if it had, zero or exactly two nodes with odd degrees. The graph following this condition is called, Eulerian circuit or path. We can easily infer this theorem. Exactly two nodes are, (and must be) starting and end of your trip. If it has even nodes than we can easily come and leave the node without repeating the edge twice or more. In actual case of seven bridges of Konigsberg, once the situation was presented in terms of graph, the case was simplified as the graph had just 4 nodes, with each node having odd degree. So, Euler concluded that these bridges cannot be traversed exactly once.

2. DOMINATING COLOUR TRANSVERSAL NUMBER

An std-set D is minimal if and only if for every $u \in D$ any one of the following holds:
(i) u is an isolate of D
(ii) There exists a vertex $v \in V-D$ such that $N(v) \cap D = \{u\}$
(iii) For every χ-partition, $\Pi = \{V_1, V_2, ..., V_\chi\}$, there exists one V_i such that $V_i \cap D = \{u\}$ or $\emptyset$.

Proof
Let D be an std-set. If D is minimal, then $D-\{u\}$ is not an std-set for every $u \in D$.
This implies that either $D-\{u\}$ is not a dominating set or not a transversal of every χ-partition of G.

Case 1:
Suppose $D-\{u\}$ is not a dominating set. Then there exists a vertex $v \in (V-D) \cup \{u\}$ that is not adjacent to any vertex of $D-\{u\}$.
If u = v, then u is an isolate of D. If $u \neq v$, then v is adjacent to u but not to any other vertex of D.
Hence $N(v) \cap D = \{u\}$.

Case 2:
Suppose $D-\{u\}$ is not a transversal for every χ-partition $\{V_1, V_2, ..., V_\chi\}$. This implies that $D - \{u\} \cap V_i = \emptyset$ for some i. That is $V_i \cap D = \{u\}$ or $\emptyset$ for some i.
Hence (iii) is satisfied.

Conversely assume any one of the three conditions. We prove that D is a minimal std-set. Suppose not. Then D is an std-set but not minimal. This implies that D and $D-\{u\}$ are std-sets for some $u \in D$.

Let $\{V_1,V_2,...,V_\chi\}$ be a χ-partition of V for which D $-\{u\}$and D are transversals. Then D $-\{u\}\cap V_i \neq \emptyset$ and D $\cap V_i \neq \emptyset$ for every i.

This implies that D $\cap$ $V_i \neq \{u\}$ or $\emptyset$ contradicting condition (iii).

Theorem: For any graph G, $\gamma \leq \gamma_g \leq \gamma_{st}$.

Proof :

Let D be any std-set of G. So there exists a χ-partition $\Pi=\{V_1,V_2,...,V_\chi\}$ such that D $\cap$ $V_i \neq \emptyset$ for every i. Each V_i is an independent set and so is a clique in G. Since $D\cap V_i \neq \emptyset$ for every i, D is a dominating set for G. Hence D is a global dominating set and $\gamma_g \leq \gamma_{st}$.

Result : If G has k-components say $G_1,G_2,...,G_k$ such that $\chi(G_1) \geq \chi(G_i)$ for i = 2, 3, ..., k, then $\gamma_{st}(G) \leq \gamma_{st}(G_1) + \sum_{i=2}^{k} \gamma(G_i)$.

Proof: It is given that $G = \sum_{i=1}^{k} G_i$. As $\chi(G_1) \geq \chi(G_i)$, for every i, any γ_{st}-set of G_1 is a transversal of every χ-partition of G. Hence the union of a γ_{st}-set of G_1 and γ-sets of G_i, i = 2,3, ..., k is an std-set of G. So $\gamma_{st}(G) \leq \gamma_{st}(G_1) + \sum_{i=2}^{k} \gamma(G_i)$.

3. TOTAL DOMINATING COLOR TRANSVERSALS IN GRAPH

Let G = (V, E) be a graph with chromatic number χ and minimum total dominating set S. If < S > contains a complete sub graph of order χ, then $\gamma_{tstd}(G) = \gamma_t(G)$.

Proof: Suppose S is a minimum total dominating set of G and < S > contains complete sub graph H of order χ. All the vertices of H must be assigned distinct χ colors and hence S is a transversal of every χ –partition of G. Hence S is a total dominating color transversal set of G.

Therefore $\gamma_{tstd}(G) \leq \gamma_t(G)$. As $\gamma_t(G) \leq \gamma_{tstd}(G)$, Hence $\gamma_{tstd}(G) = \gamma_t(G)$.

Theorem: If $\chi(G) = 2$ then $\gamma_{tstd}(G) = \gamma_t(G)$.

Proof : Given that $\gamma(G) = 2$. We know that if S is a minimum total dominating set of G then < S > contains complete sub graph of order 2. Hence by the above theorem, $\gamma_{tstd}(G) = \gamma_t(G)$.

Corollary:

For $n \geq 2$, $\gamma_{tstd}(P_n) = \gamma_t(P_n)$ and $\gamma_{tstd}(T) = \gamma_t(T)$

Proof : Let P_n and T are bipartite graph. We know that if S is a minimum total dominating set of G then < S > contains complete sub graph of order 2. Hence $\gamma_{tstd}(P_n) = \gamma_t(P_n)$ and $\gamma_{tstd}(T) = \gamma_t(T)$.

Result: For $n \geq 2$, $\gamma_t(P_n) = \frac{n}{2}$, if $n \equiv 0 \bmod(4)$

$= \frac{n+2}{2}$, if $n \equiv 2 \bmod(4)$

$= \frac{n+1}{2}$, otherwise.

Result: For $n \geq 3$, $\gamma_t(C_n) = \gamma_t(P_n)$.

Theorem:

For $n \geq 4$, $\gamma_{tstd}(C_n) = \gamma_t(C_n) = \frac{n}{2}$, if $n \equiv 0 \bmod(4)$

$= \frac{n+2}{2}$, if $n \equiv 2 \bmod(4)$

$= \frac{n+1}{2}$, otherwise.

Proof: We first note that cycle with even vertices is bipartite and otherwise it is tripartite. Divide vertices of C_n into groups of four like $\{v_1,v_2,v_3,v_4\}$, $\{v_5,v_6,v_7,v_8\}$,…..where the last group may contain one, two, three or four vertices.

Case 1: n≡ 0 mod(4) or n≡ 2 mod(4)

In such case Last group has four vertices or two vertices. So cycle C_n will have even number of vertices and hence C_n will be bipartite. Hence by theorem 4.2 and by $\gamma_t(C_n) = \gamma_t(P_n)$, we have $n \geq 4$, $\gamma_{tstd}(C_n) = \gamma_t(C_n) = \frac{n}{2}$, if $n \equiv 0 \bmod(4)$

$= \frac{n+2}{2}$, if $n \equiv 2 \bmod(4)$.

Case 2: n≡ 1mod(4)

Here we first note that $\gamma_{tstd}(C_n) \geq \gamma_t(C_n) = \frac{n+2}{2}$ .In this case last group has one vertex. So cycle C_n will have odd number of vertices and hence C_n will be tripartite. Select middle two vertices from each group of four vertices except second last group and from second last group select three vertices. The resultant set S, will be a total dominating set with cardinality is $\frac{n-5}{2} + 3 = \frac{n+1}{2}$.

Consider the χ- coloring of vertices of each group by using 1,2, and 3 colors as $\{1,2,1,3\},\{2,1,2,3\},\{2,1,2,3\},\{2,1,2,3\}$. Note that the set S will be a transversal of χ-partition of G formed by such χ-coloring of G is a minimum total dominating color transversal set of G with cardinality $\frac{n+1}{2}$. Hence $\gamma_{tstd}(C_n) = \frac{n+1}{2}$, if n≡1mod(4).

Case3: n≡ 3 mod(4)

Here we first that $\gamma_{tstd}(C_n) \geq \gamma_t(C_n) = \frac{n+1}{2}$.

In this case cycle C_n will be tripartite. Select middle two vertices from each group except from last group and from last

group select last two vertices. The resultant set S, will be a total dominating set with cardinality $\frac{n-3}{2}+2=\frac{n+1}{2}$.

Consider the χ-coloring of vertices of each group by using 1,2 and 3 colors as {1,2,1,3},{2,1,2,3},{2,1,2,3},……,{1,2,3}. Note that the S will be a transversal of χ-partition of G formed by such χ-coloring of G and this set S is a minimum total dominating color transversal set of G with cardinality $\frac{n+1}{2}$. Hence $\gamma_{tstd}(C_n) = \frac{n+1}{2}$, if n≡3mod(4). Hence the theorem.

4. RELATION BETWEEN DOMINATING AND TOTAL DOMINATING COLOR TRANSVERSAL NUMBER OF GRAPH.

Theorem: For any graph G, $\gamma_{std}(G) \leq \gamma_{tstd}(G) \leq 2\gamma_{std}(G)$

Proof: $\gamma_{std}(G) \leq \gamma_{tstd}(G)$ as total dominating set is always a dominating set. If dominating color transversal set S is not a total dominating color transversal set then there exists isolates in S.

At most |S| number of vertices in S can be isolates. As G is a graph without isolated vertices, each vertex in S has adjacent vertex in G and hence by adding at most |S| vertices to S from V\S, we obtain a total dominating color transversal set. Hence $\gamma_{tstd}(G) \leq 2\gamma_{std}(G)$.

Example: Consider a disconnected graph G

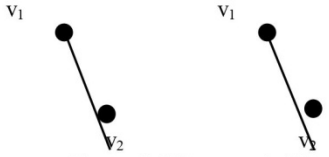

Figure-1: Disconnected Graph G

$\gamma_{tstd}(G) = 4$ and $\gamma_{std}(G) = 2$.

Example: Consider a graph G

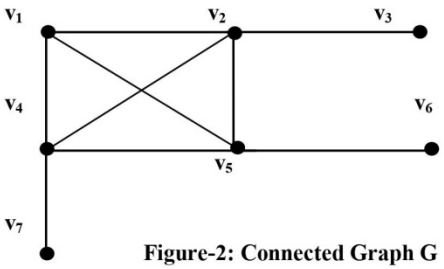

Figure-2: Connected Graph G

$\gamma = \{v_2, v_4, v_5\}$, $\gamma(G) = 3$

$\gamma_t = \{v_2, v_4, v_5\}$, $\gamma_t(G) = 3$

$\chi(G) = 4$, $\gamma_{std} = \gamma_{tstd} = 3$

Example: Consider a graph G

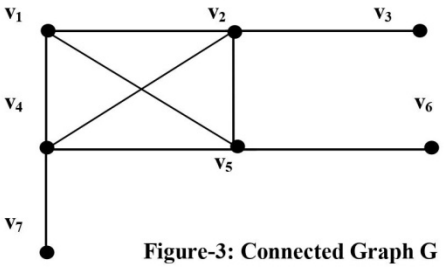

Figure-3: Connected Graph G

$\gamma_{tstd}(G) = \gamma_{std}(G) = \chi(G) = 4$ but $\gamma(G) = \gamma_t(G) = 3$.

Example: Consider a graph G ($\neq K_n$) for which $\gamma_{tstd}(G) = \gamma_{std}(G) \neq \chi(G)$ and $\gamma(G) \neq \gamma_t(G)$.

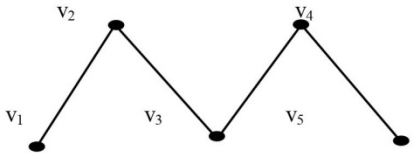

Figure-4: Bipartite Graph G

$\gamma_{tstd}(G) = \gamma_{std}(G) = 2 \neq \chi(G) = 3$ and $\gamma(G) = 2 \neq \gamma_t(G) = 3$.

Example:

Consider a graph G is connected.

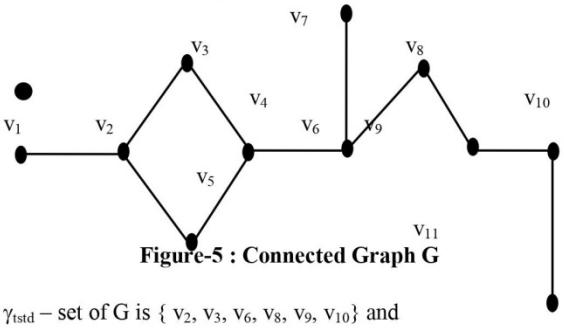

Figure-5 : Connected Graph G

γ_{tstd} – set of G is { v_2, v_3, v_6, v_8, v_9, v_{10}} and

γ_{std} – set of G is { v_2, v_6, v_{10}}

So, $\gamma_{tstd}(G) = 6$ and $\gamma_{std}(G) = 3$.

Hence $\gamma_{tstd}(G) = 2\gamma_{std}(G)$.

5. TOTAL DOMINATING COLOR TRANSVERSAL NUMBER OF GRAPHS AND MONOTONICITY

Theorem: Let G = (V, E) be a graph with k – components say $G_1, G_2, ..., G_k$ and each component is without isolated vertex. If $\chi(G) \leq 2k$ then $\gamma_{tstd}(G) = \gamma_t(G)$.

Proof : Let $\chi(G) = 2k$. Let $\gamma_t(G_i)$ denote the Total Domination number of G_i (i =1, 2, 3,...., k). Each γ_t - set has at least two adjacent vertices. So assign two distinct colors to two adjacent vertices in γ_t - set of component G_1. Again, assign two arbitrary colors, not used early, to two different vertices in γ_t - set of component G_2.

Likewise continue assigning two arbitrary distinct colors, not used early, to two distinct vertices of γ_t - set of components of G till we reach upto γ_t - set to of component $G_{\frac{x}{2}}$ (= G_k) of G. Hence $\bigcup_{i=1}^{k} \gamma_t(G_i) = \gamma_t(G)$ is a transversal of such χ – Partition of G. Therefore $\gamma_{tstd}(G) = \gamma_t(G)$. For $\chi(G) < 2k$, the result is obvious by applying the above method of coloring the γ_t – set of components of G.

Theorem: Let G = (V, E) be a graph with k – components, say $G_1, G_2,...., G_k$, such that $\chi(G_1) \geq \chi(G_i), \forall\ i \in \{2,....., k\}$. Then $\gamma_{tstd}(G) \leq \gamma_{tstd}(G_1) + \sum_{i=2}^{k} \gamma_t(G_i)$.

Proof : Trivially as $\chi(G_1) \geq \chi(G_i), \forall\ i \in \{2,....., k\}$ we have $\chi(G) = \chi(G_1)$. Then any γ_{tstd} -set of G_1 is a transversal of every χ– Partition of G. So union of γ_{tstd} -set of G_1 and γ_t -Sets of each G_i (i = 2, 3,....., k) yields Total Dominating Color Transversal set of G. Hence $\gamma_{tstd}(G) \leq \gamma_{tstd}(G_1) + \sum_{i=2}^{k} \gamma_t(G_i)$.

6. DOMINATION GRAPH WITH APPLICATION

Domination in graphs has been an extensively researched branch of graph theory. Graph theory is one of the most flourishing branches of modern mathematics and computer applications. The last 30 years have witnessed spectacular growth of Graph theory due to its wide applications to discrete optimization problems, combinatorial problems and classical algebraic problems. It has a very wide range of applications to many fields like engineering, physical, social and biological sciences; linguistics etc., the theory of domination has been the nucleus of research activity in graph theory in recent times. This is largely due to a variety of new parameters that can be developed from the basic definition of domination. The NP-completeness other basic domination problems and its close relationship to other NP-completeness problems have contributed to the enormous growth of research activity in domination theory.

Applications of Domination in Graph

Domination in graphs has applications to several fields. Domination arises in facility location problems, where the number of facilities (e.g., hospitals, fire stations) is fixed and one attempts to minimize the distance that a person needs to travel to get to the closest facility. A similar problem occurs when the maximum distance to a fality is fixed and one attempts to minimize the number of facilities necessary so that everyone is serviced. Concepts from domination also appear in problems involving finding sets of representatives, in monitoring communication or electrical networks, and in land surveying (e.g., minimizing the number of places a surveyor must stand in order to take height measurements for an entire region).

6.1 School Bus Routing

Most school in the country provide school buses for transporting children to and from school Most also operate under certain rules, one of which usually states that no child shall have to walk farther than, say one quarter km to a bus pickup point. Thus, they must construct a route for each bus that gets within one quarter km of every child in its assigned area. No bus ride can take more than some specified number of minutes, and Limits on the number of children that a bus can carry at any one time. Let us say that the following figure represents a street map of part of a city, where each edge represents one pick up block. The school is located at the large vertex. Let us assume that the school has decided that no child shall have to walk more than two blocks in order to be picked up by a school bus. Construct a route for a school bus that leaves the school, gets within two blocks of every child and returns to the school.

6.2 Computer Communication Networks

Consider a computer network modeled by a graph G = (V,E) for which vertices represents computers and edges represent direct links between pairs of computers. Let the vertices in following figure represent an array, or network, of 16 computers, or processors. Each processor to which it is directly connected. Assume that from time to time we need to collect information from all processors. We do this by having each processor route its information to one of a small set of collecting processors (a dominating set). Since this must be done relatively fast, we cannot route this information over too long a path. Thus we identify a small set of processors which are close to all other processors. Let us say that we will tolerate at most a two unit delay between the time a processor sends its information and the time it arrives at a nearby collector. In this case we seek a distance-2 dominating set among the set of all processors.

6.3 Radio Stations

Suppose that we have a collection of small villages in a remote part of the world. We would like to locate radio stations in some of these villages so that messages can be broadcast to all of the villages in the region. Since each radio station has a limited broadcasting range, we must use several stations to reach all villages. But since radio stations are costly, we want to locate as few as possible which can reach all other villages. Let each village be represented by a vertex. An edge between two villages is labeled with the distance, say in kilometers, between the two villages.

6.4 Locating Radar Stations Problem

The problem was discussed by Berge. A number of strategic locations are to be kept under surveillance. The goal is to locate a radar for the surveillance at as few of these locations as possible. How a set of locations in which the radar stations are to be placed can be determined.

7. CONCLUSION

This paper "A Review on relation between dominating and total dominating color transversal number of graph and monotonicity" is discussed about new domination parameters and characterize the graphs that attain some bounds. Every total dominating set is dominating set. A graph G is bipartite graph then total dominating color transversal number and total dominating number of graph are equal.

REFERENCES

[1]. T. W. Haynes, S. T. Hedetniemi, and P. J. Slater, Domination in graphs: Advanced topics, Mercel Dekker, New York, 1998.

[2]. S. Thomasse and A. Yeo, Total domination of graphs and small transversals of hyper graphs, Combinatorica 27 (2007), 473-487.

[3]. M. Chellali and T. W. Haynes, A note oSSSSn the total domination number of a tree, J. Combin. Math. Combin. Computer 58 (2006), 189-193.

[4] D. B. West. Introduction to Graph Theory. Prentice Hall,1996.

[5] D. K. Thakkar and A. B. Kothiya, Total Dominating Color Transversal number of Graphs, Annals of Pure and Applied Mathematics, Vol. 11(2), 2016, 39 – 44.

[6] R. L. J. Manoharan, Dominating colour transversals in graphs, Bharathidasan University, September, 2009.

[7] D.K.Thakkar and A.B.Kothiya, Relation between Total Dominating Color Transversal number and Chromatic number of a Graph, Communicated for publication in AKCE International Journal of Graphs and Combinatorics.

[8] Michael A. Henning and Andres Yeo, Total Domination in Graphs, Springer, 2013.

[9] D.K.Thakkar and K.N.Kalariya, Strong vertex covering in hypergraph, Annals of Pure and Applied Mathematics, 11(1) (2016) 123- 131.

[10] V.R.Kulli and B.Janakiram, Total global domination number of a graph, Indian Journal of Pure and Applied Math., 27(6) (1996) 537-542.

[11] Sandi Klavzar, Coloring Graph Products-A survey, Elsevier Discrete Mathematics, 155(1996), 135-145.

[12] David Amos, On total domination in graphs, University of Houston Downton, December 2012.

[13] Goksen BACAK, "Vertex Color of a Graph", Master of Science Thesis, ˙IZM˙IR, December, 2004.

[14] Dr. S. Sudha and R. Alphonse Santhanam, "Total Domination on Generalised Petersen Graphs", International Journal of Scientific and Innovative Mathematical Research (IJSIMR) Volume 2, Issue 2, February 2014, PP 149-155.

A Review on Domination Block subdivision Graphs	V.Revathi Assistant Professor of Mathematics	Maths	International Journal of Mathematics Trends and Technology (IJMTT)	April 2017	ISSN: 2231-5373 (P:28-31)	**UGC Approved Journal in 2017** https://www.ijmttjournal.org/2017/Volume-44/number-1/IJMTT-V44P504.pdf

A Review on Domination Block Subdivision Graphs

[1] M.Karthiga [2] V.Revathi

[1]*Research Scholar, Sakthi College of Arts and Science For Women, Oddanchatram.*
[2]*Assistant Professor, Department of Mathematics, Sakthi College of Arts and Science For Women, Oddanchatram.*

ABSTRACT –*This paper, some result Y[BS(G)] were obtained in terms of vertices, edges and other different parameters of G. But not in terms of the numbers of BS(G). In addition, we establish the relationship of Y"[BS(G)] with other domination parameters of G. Also its relationship with other domination parameters were established.*

Keywords: *Domination sets, Block Subdivision, Edge Domination number, Connected Domination number.*

1. INTRODUCTION

Graph theory is study of points and lines. In particular, it involves the ways in which sets of points, called vertices, can be connected by lines or arcs, called edges. Graphs in this context differ from the more familier coordinate plots that potray mathematical relations and functions. Graph theory concerns the relationship among lines and points and some lines between them. No attention is paid to the position of points and the length of the lines. Dominating set other related subjects and the corresponding graph parameters form an important research area of graph theory, which is rich in history, application, interesting results and unsolved research questions. This is one of the fastest growing areas in Graph Theory.

2. DOMINATION SUBDIVISION NUMBERS OF GRAPHS

Theorem: For any connected graph G and edge uv, where deg(u) ≥ 2 and deg(v) ≥ 2, $sd_\gamma(G) \leq deg(u) + deg(v) - 1$.

Proof: $sd_\gamma(G)$ is defined for every connected graph G of order $n \geq 3$. Every such graph G either has an edge uv, where deg(u) ≥ 2 and deg(v) ≥ 2, or it does not. If G has such an edge uv, To shows that the domination number of G must increase if every edge incident to either u or v is subdivided. If G does not have such an edge, then for every edge uv, either deg(u) = 1 or deg(v) = 1. But this implies that G is a star $K_{1,n}$. But for $G = K_{1,n}$, since n≥3, it is easy to see that the domination number is increased by subdividing any edge, that is, $sd_\gamma(G) = 1$.

Therefore, $sd_\gamma(G)$ is defined for every connected graph of order n≥3. Although the upper bound in this theorem for the subdivision number of an arbitrary graph is not a constant, it can be used to obtain a constant upper bound for the domination subdivision number of all graphs in some classes of graphs.

Results : 1. For any r x s grid graph $G_{r,s}$, $1 \leq sd_\gamma(G_{r,s}) \leq 4$.
2.For any k-regular graph G, where k ≥ 2, $1 \leq sd_\gamma(G) \leq 2k-1$.

Theorem: For any cubic graph G, $1 \leq sd_\gamma(G) \leq 5$.
Proof: A vertex which is adjacent to only one other vertex is called a leaf, and its neighbor is called a support vertex. A vertex which is adjacent to two or more leaves is called a strong support vertex.

Theorem: If G has a strong support vertex, then $sd_\gamma(G) = 1$.
Proof : Let w be adjacent to leaves u and v. Subdividing either edge wu or wv will increase the domination number. Thus, $sd_\gamma(G) = 1$.

Theorem: If G has adjacent support vertices, then $sd_\gamma(G) \leq 3$.
Proof : Let w and x be adjacent support vertices, and let u and y be leaves adjacent to w and x, respectively. Subdividing edges wu, wx, and xy will increase the domination number. Thus, $sd_\gamma(G) \leq 3$.
We show that $sd_\gamma(G) = 1$ for any graph G having $\gamma(G) = 1$.

Theorem: If G is a graph of order n ≥ 3 and $\gamma(G) = 1$, then $sd_\gamma(G) = 1$.
Proof : If you subdivide any edge in a graph of order n whose domination number equals one, the resulting graph cannot have domination number equal to one. We are able to

determine an upper bound on $sd_\gamma(G)$ in terms of $\gamma(G)$ for graphs G with no isolated vertices. For this purpose we need the following result which establishes a connection between the matching number of a graph and its domination subdivision number. A matching in a graph G is a set M of edges having the property that no two edges in M have a vertex in common. The maximum cardinality of a matching in G is called the matching number of G and is denoted $\beta_1(G)$.

3. EDGE DOMINATION IN BLOCK SUBDIVISION GRAPHS

Theorem: For any connected graph G, $\Upsilon'[BS(G)] \leq n(G)$ where n(G) is the number of blocks of G. Equality holds if G is isomorphic to K_2.

Proof : The result can be proved by induction on number of blocks n of G. If n(G) = 2, then $\Upsilon'[BS(G)] = 1 < n(G)$. Assume the result is true for all connected graphs G with n -1 blocks. hat is, $\Upsilon'[BS(G)] \leq n(G) - 1$

Let G_1 be a connected graph with n block With this n^{th} block of G only one edge will be added in $BS(G_1)$. Then by the definition of edge dominating set, $\Upsilon'[BS(G)] \leq (n(G) - 1) + 1$ $\Upsilon'[BS(G)] \leq n(G)$. Hence, by induction on n(G), $\Upsilon'[BS(G)] \leq n(G)$ For an equality, if G is isomorphic to K_2, then $\Upsilon'[BS(G)] = 1 = n(G)$. …….($\because$ for K_2, n(G) = 1)

Theorem: For any separable connected (p, q) graph $\Upsilon'[BS(G)] \leq q(G)$. Equality holds if G is isomorphic to K_2.

Proof : Let G be a graph with n blocks. For any connected graph G, $n(G) \leq p(G)$ - and $p(G)-1 \leq q(G)$ This implies $n(G) \leq q(G)$. For any connected graph G, $\Upsilon'[BS(G)] \leq n(G)$. $\Upsilon'[BS(G)] \leq q(G)$. Hence, $\Upsilon'[BS(G)] \leq q(G)$. If G is isomorphic to K_2, then $\Upsilon'[BS(G)] = 1 = q(G)$ ($\because$ for K_2, q(G) = 1)

Theorem : For any connected graph G, $\Upsilon'(G) + \Upsilon'[BS(G)] \leq 2q(G)$. Equality holds if $G \cong K_2$.

Proof : For any separable connected (p,q) graph G, $\Upsilon'[BS(G)] \leq q(G)$. For any nontrivial connected graph G, $\Upsilon'(G) \leq q(G)$. Hence , $\Upsilon'(G) + \Upsilon'BS(G) \leq 2q(G)$. For an equality if G is isomorphic to K_2, then $\Upsilon'[BS(G)] = 1$, $\Upsilon'(G) = 1$ and q(G) = 1. Hence, $\Upsilon'(G) + \Upsilon'[BS(G)] = 2$. Therefore, $\Upsilon'(G) + \Upsilon'[BS(G)] = 2\,q(G)$ ($\because$ q(G) = 1)

Theorem : For any connected graph G, $\Upsilon'[BS(G)] < p(G)$.

Proof : Suppose $H = \{ v_1 , v_2 , v_3, \ldots v_s \}$, $D \subseteq V[BS(G)]$ be the set of vertices in BS(G) corresponding to the blocks $\{ B_1 , B_2 , B_3 \ldots . B_S \}$ in S(G). Then $D \subseteq E[BS(G)]$ forms an edge dominating set of BS(G) with $\Upsilon'[BS(G)] = |D|$. Suppose P′ be the number of vertices in BS(G). Since for any connected graph G, $\Upsilon'[BS(G)] = |D| \leq \frac{P}{2} < p(G)$. Therefore, $\Upsilon'[BS(G)] < p(G)$.

4. CONNECTED DOMINATION IN BLOCK SUBDIVISION GRAPHS

Theorem: For any connected (p,q) graph G, $\Upsilon_c[BS(G)] < 2p - 2$

Proof :Case (i)

Suppose G is a tree, then q = p - 1 and $|[E(G)]| = q$ Therefore, $|E[S(G)]| = 2q$

That is, $V[BS(G)] = 2q$

$V[BS(G)] = 2(p-1)$

$V[BS(G)] = 2p - 2$

Let $D \subseteq V[BS(G)]$ is a connected dominating set in BS(G) such that , $\Upsilon_c[BS(G)] = |D|$. Since total number of vertices in BS(G) is 2p - 2, from the definition of connected dominating set in BS(G), $\Upsilon_c[BS(G)] = |D| < 2p - 2$. Hence the theorem is true in this case.

Case (ii): Suppose G is not a tree and at least one block contains maximum number of vertices. Let D denote the connected dominating set in BS(G) such that $\Upsilon_c[BS(G)] = |D|$ and $|D| < 2p - 2$ Hence, $\Upsilon_c[BS(G)] < 2p - 2$. Therefore, the theorem is true in this case.

Theorem: For any connected (p,q) graph G, $\Upsilon_c[BS(G)] < p(G) + s(G)$ where S(G) is number of cut vertices of G.

Proof : If G has no cut vertices, then G is non separable, $\Upsilon_c[BS(G)] = 1 < p(G) + s(G)$.

For any separable graph G consider the following two cases.

Case(i): Let the graph G be separable and c be the cut vertices of G. Let G be a tree.

Since S is number of cut vertices of G, $C \subseteq V(G)$ and $|C| = S(G)$. Suppose $C' \subseteq V[BS(G)]$ be the set of cut vertices of BS(G)

such that $\Upsilon[BS(G)] = |D|$. Now $F = \{u_i \in N(D)\} - \{v_j\}$ where $\{u_i\}$ is a set of elements in neighbourhood of D and $\{v_j\}$ is a set of end vertices of BS(G) such that $< D \cup F >$ forms a connected dominating set of BS(G). Hence, $\Upsilon_c[BS(G)] = |< D \cup F >| = |D| + |F| = \Upsilon[BS(G)] + |F|$ Since $\Upsilon[BS(G)] < P$, then $\Upsilon_c[BS(G)] < P(G) + S(G)$.

Case(ii) : Suppose G is not a tree and at least one block contains maximum number of vertices. Then, $\Upsilon_c[BS(G)] < P(G) + S(G)$ From the above two cases, $\Upsilon_c[BS(G)] < P(G) + S(G)$.

5. SPLIT BLOCK SUBDIVISION DOMINATION IN GRAPHS

All graphs considered here are simple, finite, nontrivial, undirected and connected. As usual p,q and n denote the number of vertices, edges and blocks of a graph G respectively. The minimum degree and maximum degree of a graph G are denoted by $\delta(G)$ and $\Delta(G)$ respectively. A vertex cover of a graph G is a set of vertices that covers all the edges of G .

The vertex covering number $\alpha_o(G)$is a minimum cardinality of a vertex cover in G. The vertex independence number $\beta_o(G)$ is the maximum cardinality of an independent set of vertices. A edge cover of G is a set of edges that covers all the vertices. The edge covering number $\alpha_1(G)$of G is minimum cardinality of a edge cover. The edge independence number $\beta_1(G)$ of a graph G is the minimum cardinality of an independent set of edges. A set of vertices $D \subseteq V(G)$ is a dominating set. If every vertex in V-D is adjacent to some vertex in D .The Domination number $\gamma(G)$ of G is the minimum cardinality of a dominating set in G. A dominating set D of a graph G is a split dominating set if the induced subgraph <V-D> is disconnected. The split domination number $\gamma_S(G)$ of G a graph is the minimum cardinality of a split dominating set.

Theorem: For any graph G n-blocks and $n \geq 2$, then $\gamma_{ssb}(G) \leq n-1$.

Proof : For any graph G with n=1 block, a split domination does not exists. Hence we required $n \geq 2$ blocks. Let $S=\{B_1,B_2,B_3,\ldots,B_n\}$ be the number of G and $M=\{b_1,b_2,b_3,\ldots,b_n\}$ be the vertices in B(G) with corresponding to the blocks of S. Also $V=\{v_1,v_2,v_3,\ldots,v_n\}$ be the set of vertices in[SB(G)].

Let, $V_1=\{v_1,v_2,v_3,\ldots,v_i\}$, $1\leq i\leq n$, $V_1 \subseteq V$ be a set of cut vertices. Again consider a subset $V_1^1$of V such that$\forall$ $v_i \in N(V) \cap N(V_1^1)$ and $V_1=V-V_1^1$. Let $V_1=\{v_1,v_2,v_3,\ldots,v_s\}$, $1 \leq s \leq n$, $\forall$ $v_s \in V$ which are not cut vertices such that $N(V_1) \cap N(V_2)=\phi$,then $\{V_1 \cup V_2\}$is a dominating set. Clearly $V[SB(G)-\{V_1 \cup V_2\}] =H$ is disconnected graph. Then $(V_1 \cup V_2)$ is a γ_{ssb}-set of G.

Hence $|V_1 \cup V_2| = \gamma_{ssb}(G)$ which gives $\gamma_{ssb}(G) \leq n-1$. In the following Theorem, we obtain an upper bound for in terms of vertices added to B(G).

Theorem: For any connected (p, q) graph with $n \geq 2$ blocks, then $\gamma_{ssb}(G) \leq$ R where R is the number of vertices added to B(G).

Proof: For any nontrivial connected graph G. If the graph G has n=1 block .Then by the definition, split domination set does not exists. Hence $n \geq 2$ blocks.

Let $S=\{B_1,B_2,B_3,\ldots,B_n\}$ be the blocks of G and $M=\{b_1,b_2,b_3,\ldots,b_n\}$ be the vertices in B(G) which corresponds to the blocks of S. Now we consider the following cases.

Case 1: Suppose each block of B(G) is an edge. Then R=q=E[B(G)] . Let $V_1=\{v_1,v_2,v_3,\ldots,v_i\}$ be the set of vertices of [SB(G)]. Now consider, $V_1=\{v_1,v_2,v_3,\ldots,v_i\}$, $1 \leq i \leq n$ is a set of cut vertices in [SB(G)]. Let $V_1 \subseteq V_2$, $\forall$ $v_i \in V_2$ are adjacent to end vertices of [SB(G)]. Again there exists a subset $V_3$of V_1 with the property V [SB(G)]-$\{V_2 \cup V_3\}$=H. where $\forall$ $v_n \in H$ is adjacent to atleast one vertex of $(V_2 \cup V_3)$ and H is a disconnected graph. Hence $V_2 \cup V_3$ is as γ_{ssb} set of G.

$$|V_2 \cup V_3| \leq R.$$

Case 2 : Suppose each block of B(G) is a complete graph with $p \geq 3$ vertices. Again we consider the sub cases of case 2.

Subcase 2.1: Assume $B(G)=K_p$,$p \geq 3$. Then $V[SB(G)]= V[B(G)]+ q[B(G)]$ and $V[SB(G)]- V[B(G)]= q[B(G)]$ where is an isolates.

Hence $|q[B(G)] \geq V[B(G)]|$ which gives $\gamma_{ssb}(G) \leq R$.

Subcase 2.2: Assume every block of B(G) is K_p, $p \geq 3$. Let $B(G)=\{K_{p1},K_{p2},K_{p3},\ldots\ldots,K_{pm}\}$ then

$V\{S[B_1(G) \cup B_2(G) \cup B_3(G) \cup \ldots\ldots \cup B_m(G)]\} = V[B1, B_2, B_3, B_4 ,\ldots\ldots,B_m]+ q_1[B(G)] \cup q_2[B(G)] \cup q_3[B(G)]\ldots\ldots. \cup q_m[B(G)]$ and $V[S[B_1(G) \cup B_2(G) \cup B_3(G) \cup \ldots\ldots \cup B_n(G)] -V[B1, B_2, B_3, B_4 ,\ldots\ldots,B_n] = q_1[B(G)] \cup q_2[B(G)] \cup q_3[B(G)]\ldots\ldots.$

$\cup q_m[B(G)]$ where $v_i \in q_1[B(G)] \cup q_2[B(G)] \cup q_3[B(G)] \ldots\ldots \cup q_m[B(G)]$ is an isolate.
Hence $|q_1[B(G)] \cup q_2[B(G)] \cup q_3[B(G)] \ldots \cup q_m[B(G)]| \geq |V[B1, B_2, B_3, B_4, \ldots, B_m]|$ which gives $\gamma_{ssb}(G) \leq R$.

We establish an upper bound involving the Maximum degree $\Delta(G)$ and the vertices of G for split block sub division domination in graphs.

6. CONCLUSION

A non-trivial connected graph G with at least one cut vertex is called separable graph, otherwise a non-separable graph. This paper deals "The Review on Domination Block Subdivision Graph", can make an in-depth study in domination subdivision and its related works.

REFERENCES

[1] S.Arumugam and S.Ramachandran, Invitation of graph theory scitech publications(2001).

[2] S. Arumugam and S. Velammal, Edge domination in graphs, Taiwanese J. of
Mathematics, 2(2), 173 – 179, 1998.

[3] R.Balakrishnan and K.Ranganathan , A text book of Graph theory, Springer international edition (2000).

[4] G. Chartrand and Ping Zhang, "Introduction to graph Theory", Newyork (2006).

[5] Gary chartrand and Ping zhang, Introduction to graph theory, Tata McGraw – hill publishing company limited. New Delhi (2006).

[6] F.Harary, Graph Theory, Adison Wesley, Reading Mass (1972).

[7] T.W. Haynes, S.T. Hedetniemi and P.J. Slater, Fundamentals of Domination in Graphs (Marcel Dekker, Inc., New York, 1998).

[8] T.W. Haynes, S.T. Hedetniemi and P.J. Slater, eds, Domination in Graph (Advanced Topics, Marcel Dekker, Inc., New York, 1998).

[9] F.Harary ,Graph theory, Narosa publishing house (1969)

[10] S.T.Hedetniemi and R.C.Laskar, Conneced domination in graphs, in B.Bollobas, editor, Graph Theory and Combinatorics, Academic Press, London, 209-218, 1984.

A Review on Graphs with Unique Minimum Dominating Sets	V.Revathi Assistant Professor of Mathematics	Maths	International Journal of Mathematics Trends and Technology (IJMTT)	April 2017	ISSN: 2231-5373 (P:32-37)	**UGC Approved Journal in 2017** https://www.ijmttjournal.org/2017/Volume-44/number-1/IJMTT-V44P505.pdf

A Review on Graphs with Unique Minimum Dominating Sets

[1] D.Malarvizhi [2] V.Revathi

[1]Research Scholar, Sakthi College of Arts and Science For Women, Oddanchatram.

[2]Assistant Professor, Department of Mathematics, Sakthi College of Arts and Science For Women, Oddanchatram.

ABSTRACT – A dominating set for a graph G is a subset D of V such that every vertex not in D is adjacent to at least one member of D. This paper deals with some of the graphs having unique minimum dominating sets. We also find a unique minimum dominating sets for block graphs and maximum graphs.

Keywords: Domination sets, Block graphs, Unique Υ set, Unique minimum Domination sets.

1. INTRODUCTION

Graphs can be used to model many types of relations and processes in physical, biological, social and information systems. Many practical problems can be represented by graphs. Emphasizing their application to real-world systems, the term network is sometimes defined to mean a graph in which attributes (e.g. names) are associated with the nodes and/or edges. In computer science, graphs are used to represent networks of communication, data organization, computational devices, the flow of computation, etc. For instance, the link structure of a website can be represented by a directed graph, in which the vertices represent web pages and directed edges represent links from one page to another. A similar approach can be taken to problems in social media, travel, biology, computer chip design, and many other fields. The development of algorithms to handle graphs is therefore of major interest in computer science. The transformation of graphs is often formalized and represented by graph rewrite systems. Complementary to graph transformation systems focusing on rule-based in-memory manipulation of graphs are graph databases geared towards transaction-safe, persistent storing and querying of graph-structured data.

Graph theory is also used to study molecules in chemistry and physics. In condensed matter physics, the three-dimensional structure of complicated simulated atomic structures can be studied quantitatively by gathering statistics on graph-theoretic properties related to the topology of the atoms. In chemistry a graph makes a natural model for a molecule, where vertices represent atoms and edges bonds. This approach is especially used in computer processing of molecular structures, ranging from chemical editors to database searching.

In statistical physics, graphs can represent local connections between interacting parts of a system, as well as the dynamics of a physical process on such systems. Similarly, in computational neuroscience graphs can be used to represent functional connections between brain areas that interact to give rise to various cognitive processes, where the vertices represent different

areas of the brain and the edges represent the connections between those areas. Graphs are also used to represent the micro-scale channels of porous media, in which the vertices represent the pores and the edges represent the smaller channels connecting the pores.

2. GRAPHS WITH UNIQUE MINIMUM DOMINATING SETS

Lemma: Let D be a γ-set of a graph G. Suppose for every $x \in D$, $\gamma(\mathrm{D}-x) > \gamma(\mathrm{G})$. Then D is the unique γ-set of G.

Proof : Suppose there exists a second γ-set D' of G. If $\mathrm{D} \neq D'$, choose $\mathrm{a} \in D - D'$. Now D' dominates G, and hence D' certainly dominates $G - a$, so that $|D'| \geq \gamma(\mathrm{G}-a)$. However, $\gamma(\mathrm{G}-a) > \gamma(\mathrm{G}) = |D| = |D'| \geq \gamma(\mathrm{G}-a)$, which is a contradiction.

We see that there are three conditions of interest

(i) G has a unique γ-set D.

(ii) G has a γ-set D for which every vertex in D has at least two private neighbours other than itself.

(iii) G has a γ-set D for which every vertex $x \in D$ satisfies $\gamma(\mathrm{G}-x) > \gamma(\mathrm{G})$.

As Lemmas 3.2.2 and 3.2.3 show, for all graphs G we have (i) ⇒ (ii) and (iii) ⇒ (i), the converse of those, however, is false, as the following examples sh

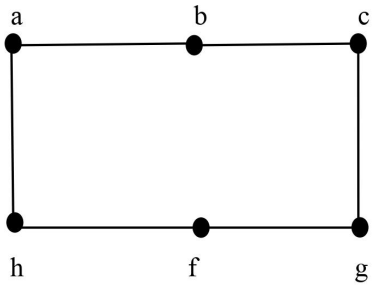

Figure – 1: Connected Graph

C_6 shown above in Figure-1 has a γ-set$D = \{a, d\}$ both vertices in D have two private neighbours; however, D is not a unique γ-set.

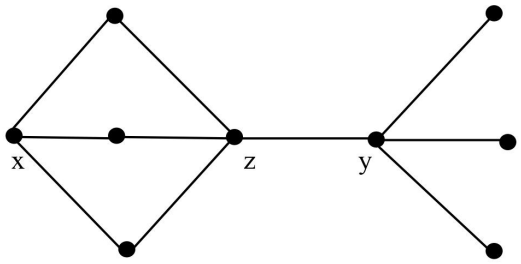

Figure-2: Connected Graph

The graph shown in Figure-2 has the unique γ-set $D = \{x, y\}$. If we delete x,the resultant graph still has domination number 2 as it is dominated by $\{x, y\}$.

Lemma : Let G be a graph which has a unique γ-set D.Then for any $x \in G - D$,$\gamma(\mathrm{G}-x) = \gamma(\mathrm{G})$.

Proof : Certainly D dominates $\mathrm{G}-x$ and so $\gamma(\mathrm{G}-x) \leq \gamma(\mathrm{G})$. If $\gamma(\mathrm{G}-x) < \gamma(\mathrm{G})$,then $\mathrm{G}-x$ is dominated by some set D' with $|D'| < |D|$. But then $D' \cup \{x\}$ would be a second γ-set for G, different from D, contradicting the uniqueness of D.

Lemma: Let G be a graph with unique γ-set D. Then $\gamma(\mathrm{G}-x) \geq \gamma(\mathrm{G})$for all $x \in D$.

Proof : Suppose $\gamma(\mathrm{G}-x) < \gamma(\mathrm{G})$for some $x \in D$. Let D' be a γ-set of $\mathrm{G}-x$.Then$|D'| < |D|$ and D' dominates all the private neighbours of x with respect to D, other than x. But now the set $D' \cup \{x\}$ is a γ-set of G in which x has only itself as a private neighbours, a contradiction to lemma 3.2.2.

3. MAXIMUM GRAPHS WITH A UNIQUE MINIMUM DOMINATING SET

Theorem: Let G = (V, E) be a graph without isolated vertices with a unique minimum dominating set of cardinality $\gamma \geq 2$ and order $n = 3\gamma$. Then

$$m = |E| \leq \binom{n}{2} - \gamma\left(n + \frac{\gamma - 5}{2}\right) = 2\gamma + 2\binom{\gamma}{2}.$$

Proof : Let $D = \{x_1, x_2, \cdots, x_\gamma\}$ be the unique minimum dominating set of G and let $P_i = epn(x_i, D, G)$ for $1 \leq i \leq \gamma$. Since $|P_i| \geq 2$ for $1 \leq i \leq \gamma$ and $n = 3\gamma$, we have $|P_i| = 2$ for $1 \leq i \leq \gamma$. Let $P_i = \{p_i', p_i''\}$ for $1 \leq i \leq \gamma$. If there is some $1 \leq i \leq \gamma$ such that $p_i', p_i'' \in E$, then $(D\backslash\{x_i\}) \cup \{p_i'\} \neq D$ is a minimum dominating set of G, which is a contradiction.

If there are some $1 \leq j < k \leq \gamma$ such that there are two independent edges between P_i and P_j, say $p_i'p_j', p_i''p_j'' \in E$, then $(D\backslash\{x_i, x_j\}) \cup \{p_i', p_j''\} \neq D$ is a minimum dominating set of G, which is a contradiction.

If there are some $1 \leq i < j \leq \gamma$ such that $x_ix_j, p_i'p_j'$ and $p_i'p_j'' \in E$, then $(D\backslash\{x_j\}) \cup \{p_i'\} \neq D$ is a minimum dominating set of G, which is a contradiction. This implies that for all $1 \leq i < j \leq \gamma$ there are at most two edges between P_i and P_j and if there are two such edges, then they are incident. Furthermore, if $x_ix_j \in E$, thenthere is at most one edge between P_i and P_j . Let v_l for $l \geq 0$ be the number of pairs $\{i, j\}$ with $1 \leq i < j \leq \gamma$ such that there are exactly $l$edges between P_i and P_j. By the above reasonings, we obtain that $v_l = 0$ for all $l \geq 3$ and $m(G[D]) \leq v_0 + v_1$.This implies that $m = |E| = 2\gamma + m(G[D]) + 0.v_0 + 1.v_1 + 2.v_2$

$$\leq 2\gamma + v_0 + v_1 + 0.v_0 + 1.v_1 + 2.v_2$$

$$\leq 2\gamma + 2(v_0 + v_1 + v_2)$$

$$= 2\gamma + 2\binom{\gamma}{2}$$

This completes the proof.

Theorem: If $\gamma \geq 2$,then $\tilde{m}(n, \gamma) = \binom{n}{2} - \gamma\left(n + \frac{\gamma-5}{2}\right)$.

Proof : We prove that $\tilde{m}(n, \gamma) \leq \binom{n}{2} - \gamma\left(n + \frac{\gamma-5}{2}\right)$. Therefore, let G be a graph of order n without isolated vertices that has domination number γ and property$(*)$.

Let $D = \{x_1, x_2, \cdots, x_\gamma\}$ be the unique minimum dominating set and for $1 \leq i \leq \gamma$ let $P_i = epn(x_i, D, G)$. As above $|P_i| \geq 2$ for $1 \leq i \leq \gamma$. Let $R = V\backslash(D \cup \cup_{i=1}^{\gamma} P_i)$. Let $n_0 = |R|$and $n_i = |P_i|$for $1 \leq i \leq \gamma$. We assume $n_1 \geq n_2 \geq n_3 \geq \cdots \geq n_\gamma$.

We will estimate the number of edges of G. There are exactly $\sum_{i=1}^{\gamma} n_i$ edges between D and $\cup_{i=1}^{\gamma} P_i$. There are at most $\binom{\gamma}{2} + \binom{n_0}{2} + \gamma n_0$ edges in G $[D \cup R]$. Let $1 \leq i \leq \gamma$. Since there is no vertex $p_i \in P_i$such that $P_i \subseteq$ N$[p_i,$ G], there are at most $\binom{n_i}{2} - \lceil n_i/2 \rceil$ edges in G$[P_i]$. Since there is no vertex $r_i \in R$ such that $P_i \subseteq$ N$[r_i,$ G] there are at most $n_0(n_i - 1)$edges between P_i and R. Now let $1 \leq i < j \leq \gamma$.

Since there is no vertex $p_i \in P_i$such that $P_j \subseteq$ N$[p_i,$ G],there are at most $n_i(n_j - 1)$ edges between P_i and P_j .

Furthermore, if $n_i = 2$, then also $n_j = 2$ and it is easy to see that there is at most one edge between P_i and P_j .

Altogether we obtain that $m = |E| \leq f(n_0, n_1, \cdots, n_\gamma)$ for a function f defined as follows

$$f(n_0, n_1, \cdots, n_\gamma) = \sum_{i=1}^{\gamma} n_i + \binom{\gamma}{2} + \binom{n_0}{2} + \gamma\, n_0 + \sum_{i=1}^{\gamma} \left(\binom{n_i}{2} - \left[\frac{n_i}{2}\right] \right) + \sum_{i=1}^{\gamma} (n_0\, n_i - n_0) + \sum_{1 \leq i < j \leq \gamma} (n_i\, n_j - max\{n_i, 3\})$$

$$= \binom{n}{2} - (\gamma - 1) \sum_{i=1}^{\gamma} n_i - \sum_{i=1}^{\gamma} \left[\frac{n_i}{2}\right] - \gamma\, n_0 - \sum_{i=1}^{\gamma} (\gamma - i)\, max\{n_i, 3\}.$$

Claim: Let $\gamma \geq 2$, $n_i \geq 2$ for $1 \leq i \leq \gamma$ and $n_0 \geq 0$ be integers.

Let $n = \gamma + \sum_{i=0}^{\gamma} n_i$ and let $n_1 \geq n_2 \geq n_3 \geq \cdots \geq n_\gamma$. If $\gamma = 2, n_1 = n_2 \geq 4, n_1$ and n_2 are even, then

$$f(n_0, n_1, \cdots, n_\gamma) \leq \binom{n}{2} - \gamma\left(n + \tfrac{\gamma - 5}{2}\right) + 1.$$

otherwise

$$f(n_0, n_1, \cdots, n_\gamma) \leq \binom{n}{2} - \gamma\left(n + \frac{\gamma - 5}{2}\right).$$

Proof :

We claim that, If there is some $1 \leq i \leq \gamma - 1$ such that $n_i \geq 4$ and $n_i > n_{i+1}$, then

$$f(n_0, n_1, \cdots, n_i \cdots, n_\gamma) \leq f(n_0 + 1, n_1, \cdots, n_i - 1, \cdots, n_\gamma) - (\gamma - 1) - \left[\tfrac{n_i}{2}\right] + \left[\tfrac{n_i - 1}{2}\right] + \gamma - (\gamma - i)$$

$$\leq f(n_0 + 1, n_1, \cdots, n_i - 1, \cdots, n_\gamma).$$

Similarly, if $\gamma = 2$ and $n_i \geq n_2 + 2$, then $f(n_0, n_1, n_2) < f(n_0 + 2, n_1 - 2, n_2)$ and if $\gamma = 2, n_1 = n_2 + 1$ and n_2 is even, then $f(n_0, n_1, n_2) < f(n_0 + 1, n_1 - 1, n_2)$.

We will consider two special cases.

First, let $n_1 = n_2 = \cdots = n_l = 3$ and $n_{l+1} = n_{l+2} = \cdots = n_\gamma = 2$ for some $0 \leq l \leq \gamma$. We obtain

$$f(n_0, n_1, \cdots, n_\gamma) = \binom{n}{2} - (\gamma - 1)(2\gamma + l) - (\gamma + l) - \gamma(n - (3\gamma + l)) - 3\left(\gamma^2 - \tfrac{1}{2}\gamma(\gamma + 1)\right) = \binom{n}{2} - \gamma\left(n + \frac{\gamma - 5}{2}\right).$$

Now let $n_1 = n_2 = \cdots = n_\gamma \geq 4$.

For $\in = \frac{1}{2}[n_1 (mod\ 2)]$ we obtain

$$f(n_0, n_1, \cdots, n_\gamma) = \binom{n}{2} - (\gamma - 1)\gamma\, n_1 - \gamma\left[\tfrac{n_1}{2}\right] - \gamma n_0 - \left(\gamma^2 - \tfrac{1}{2}\gamma(\gamma + 1)\right) n_1$$

$$= \binom{n}{2} - (\gamma - 1)\gamma\, n_1 - \gamma\frac{n_1}{2} - \gamma \in -\gamma n_0 - \left(\gamma^2 - \tfrac{1}{2}\gamma(\gamma + 1)\right) n_1$$

$$= \binom{n}{2} - \gamma\left(\frac{3}{2}\gamma - 1\right) n_1 - \gamma n_0 - \gamma \in$$

$$= \binom{n}{2} - \gamma\left(\frac{3}{2}\gamma - 1\right) n_1 - \gamma(n - (n_1 + 1)\gamma) - \gamma \in$$

$$= \binom{n}{2} - \gamma\left(\frac{1}{2}\gamma - 1\right) n_1 - \gamma(n - \gamma) - \gamma \in$$

$$\leq \binom{n}{2} - \gamma(2\gamma - 4) - \gamma(n - \gamma) - \gamma \in$$

$$f(n_0, n_1, \cdots, n_\gamma) = \binom{n}{2} - \gamma(n + \gamma - 4) - \gamma \in$$

If $\gamma = 2$ and $n_1 = n_2 \geq 5$ are odd or if $\gamma \geq 3$, then this implies

$$f(n_0, n_1, \cdots, n_\gamma) \leq \binom{n}{2} - \gamma\left(n + \left(\gamma - 5/2\right)\right).$$

If $\gamma = 2$ and $n_1 = n_2$ are even, then this implies $f(n_0, n_1, \cdots, n_\gamma) \leq \binom{n}{2} - \gamma\left(n + \left(\gamma - 5/2\right)\right) + 1.$

In view of the above remarks, this completes the proof of the claim. In order to complete the proof of the theorem, it remains to consider the case where $\gamma = 2, n_1 = n_2 \geq 4, n_1 \text{ and } n_2$ are even $m = f(n_0, n_1, \cdots, n_\gamma)$.

In this case, $G[P_1]$ and $G[P_2]$ are complete graphs in which perfect matchings have been removed and $G[P_1, P_2]$ is a complete bipartite graph in which a perfect matching has been removed.(The graph $G[P_1, P_2]$ has vertex set $P_1 \cup P_2$ and contains all edges of G that join a vertex in $P_1$and a vertex in P_2). If $D' = \{p_1', p_1''\}$ consists of two non-adjacent vertices in P_1 then $(P_1 \cup P_2) \subseteq N[D', G]$ which is a contradiction.

Hence if $\gamma = 2, n_1 = n_2 \geq 4, n_1 \text{ and } n_2$ are even m<=f$(n_0, n_1, \cdots, n_\gamma) - 1$ .In view of the claim, hence the proof.

4. BLOCK GRAPHS WITH UNIQUE MINIMUM DOMINATING SETS

Lemma: Let D be a γ -set of a graph G. If $\gamma(G - x) > \gamma(G)$for every $x \in D$, then D is the unique γ -set of G.

Proof : Let D be a γ-set of the graph G, such that $\gamma(G - x) > \gamma(G)$ for every $x \in D$. Suppose, there is a γ -set D' of G different from D. Then, there is at least one vertex $x \in D - D'$ and D' dominates $G - x$. Hence, $|D'| \geq \gamma(G - x) > \gamma(G)$, which is a contradiction.

Result : Let G be a connected graph with at least one cut vertex. If $B_1, B_2, \cdots, B_t$ are all blocks of G, then the following conditions hold

(i) $|V(B_i) \cap V(B_j)| \leq 1$ for any $1 \leq i < j \leq t$.

(ii) $E(B_i) \cap E(B_j) = \emptyset$ for any $1 \leq i < j \leq t$ and $E(G) = E(B_1) \cup \cdots \cup E(B_t)$.

(iii) If $x \in V(B_i) \cap V(B_j)$ for any $1 \leq i < j \leq t$, then x is a cutvertex of G.

(iv) If x is a cutvertex of G, then x belongs to at least two different blocks of G.

(v) If the vertices a and b do not belong to a common block, then every path from a to b contains a cutvertex $x \neq a$,b of G, such that a and b lie in different $components\ of\ G - x$.

6. CONCLUSION

This paper deals about "The Review on Graphs With Unique Minimum Dominating Sets", for block graphs and maximum graphs. We investigate some of the structural properties of graphs having a unique gamma set. In particular, three equivalent conditions for this property are

given for trees, this leads to a constructive characterization for those trees which have a unique gamma-set.

REFERENCES

[1] S. Arumugam and S. Ramachandran, Invitation to Graph Theory, Scitech Publications (India) Pvt Ltd,Chennai,2006.

[2] M. Fischermann, L. Volkmann, "Unique minimum domination in trees", Australas. J. Combin.vol.25, pp.117–124, 2002.

[3] M. Fischermann, L. Volkmann, "Cactus graphs with unique minimum dominating sets", Utilitas Math., toappear.

[4] M. Fischermann, "Block graphs with unique minimum dominating sets", Discrete Math., 240, pp. 247–251, 2001.

[5] D.L.Grinstead and P.J.Slater,"On minimum dominating sets with minimum intersection, Discrete Math.86,239-254, 1990.

[6] F.Harary, Graph Theory (Addision Wesley,Reading,Mass, 1969).

[7] T.W. Haynes, S.T. Hedetniemi and P.J. Slater, Domination in Graphs:Advanced Topics (Marcel Dekker, New York, 1998).

[8] T.W. Haynes, S.T. Hedetniemi, P.J. Slater, "Fundamentals of Domination in Graphs," Marcel Dekker Inc.New York, 1998.

[9] MirancaFischermann and Lutz Volkmann, Unique minimum domination in trees,Australas. J. Combin.25(2002), 117–124.

[10] NarshingDeo, Graph Theory with Applications to Engineering and Computer Science, PHI Learning Private Limited, New Delhi – 110001,2009.

A Review on Domination in Planar Graphs with Small Diameter	V.Revathi Assistant Professor of Mathematics	Maths	International Journal of Mathematics Trends and Technology (IJMTT)	April 2017	ISSN: 2231-5373 (P:38-41)	**UGC Approved Journal in 2017** https://www.ijmttjournal.org/2017/Volume-44/number-1/IJMTT-V44P506.pdf

A Review on Domination in Planar Graphs with Small Diameter

[1] V.Sangeetha [2] V.Revathi

[1]*Research Scholar, Sakthi College of Arts and Science For Women, Oddanchatram.*
[2]*Assistant Professor, Department of Mathematics, Sakthi College of Arts and Science For Women, Oddanchatram.*

ABSTRACT – Domination and its variations in graphs are now well studied. However, the original domination number of a graph continues to attract attention. Many bounds have been proven and results obtained for special classes of graphs such as cubic graphs and products of graphs. On the other hand, the decision problem to determine the domination number of a graph remains NP-hard even when restricted to cubic graphs or planar graphs of maximum degree 3. In this paper we consider the domination of planar graphs with small diameter.

Keywords: Domination Number, Planar graph, Diameter Graph, Domination set.

1. INTRODUCTION

Domination and its variations in graphs are now well studied. However, the original domination number of a graph continues to attract attention. Many bounds have been proven and results obtained for special classes of graphs such as cubic graphs and products of graphs. On the other hand, the decision problem to determine the domination number of a graph remains NP-hard even when restricted to cubic graphs or planar graphs of maximum degree 3. Hence it is of interest to determine upper bounds on the domination number of a graph.

In this paper we consider the domination of planar graphs with small diameter. It is trivial that a tree of radius 2 and diameter 4 can have arbitrarily large domination number. So the interesting question is what happens when the diameter is 2 or 3.

MacGillivray and Seyffarth "Domination numbers of planar graphs"proved that planar graphs with diameter two or three have bounded domination numbers. In particular, this implies that the domination number of such a graph can be determined in polynomial time. On the other hand, they observed that in general graphs with diameter 2 have unbounded domination number.

We show that there is a unique planar graph of diameter 2 with domination number 3. Hence every planar graph of diameter 2, different from this unique planar graph, has domination number at most 2. We then prove that every planar graph of diameter 3 and of radius 2 has domination number at most 6. We then show that every sufficiently large planar graph of diameter 3 has domination number at most 7.

Theorem : Every planar graph of diameter 2 has domination number at most 2 except for the graph F of Figure 3.1 which has domination number 3.

Proof : To prove Theorem, suppose G is a planar graph of diameter two satisfying $\gamma(G) > 2$. If a and b are two vertices in G, then there is always a vertex not dominated by {a, b}. We Shall denote one such vertex by υ_{ab}. Fix an embedding G*of G in the plane.

From the Jordan Closed Curve Theorem, we Know that a cycle C in G* separates the plane into two regions, which we call the sides of C. Vertices of different sides of C are said to be separated by C. The side of C that consists of the unbounded region we call the outside of C, while the side of C that consists of the bounded region we call the inside of C. If C has length n and there are vertices both inside and outside C, then we say that C is a cut-n-cycle. A cut-3-cycle is also called a cut-triangle. Since a cut-set dominates a graph of diameter 2, it follows that G is 3-connected; therefore G has an essentially unique embedding in the plane and so we may speak of cut-cycles of G rather than of G*,lemma3.1.2 establishes the existence of a 4-cycle. Then we show that this cycle is neither both induced and dominating, nor both non-induced and dominating, and therefore not dominating. Finally, we show that it follows that G is isomorphic to F.

2. DOMINATION IN PLANAR GRAPHS WITH SMALL DIAMETER II

The domination number of G, denoted by (G), is the minimum cardinality of a dominating set, while the total domination number of G, denoted by $\gamma t(G)$, is the minimum

cardinality of a total dominating set. Domination and its variations in graphs are now well studied. To simplify the notation, if X dominates Y we write X ≻ Y while if X totally dominates Y we write X ≻t Y . Further, if a vertex u is adjacent with a vertex υ, we write u ~ v, while if u and v are nonadjacent, we write u≁υ. We denote the eccentricity of a vertex υ in G by $ecc_G(\upsilon)$, or simply ecc(υ) if G is clear from the context. The subgraph induced by a subset S ⊆ V (G) is denoted by G[S].

Theorem : Every planar graph of diameter 3 and of radius 2 has total domination number at most 5.

Proof : The focus is on cut-cycles. Note that in a planar graph of diameter 3,there cannot on both sides of a cut-cycle be vertices not dominated by the cycle. We define a basic cycle as follows.

Let vertex x have eccentricity 2 in G.

Then a basic cycle C is an induced cycle x, $\upsilon_1, \upsilon_2, \ldots, \upsilon_t$, x such that on both sides of the cycle there is a vertex whose neighbors on the cycle are a subset of the two consecutive vertices fartherest from x, specifically υ(r−1)/2 and υ(r+1)/2 if r is odd, and υr/2 and υr/2+1 if r is even. A special basic cycle is one with the added condition that there is on the dominated side of the cycle a vertex with only one neighbor on the cycle and that neighbor is not x. Our strategy is as follows. In Subsection 3.1 we show the existence of aspecial basic cycle of length 3 or 4 or of a basic 5-cycle in G. Thereafter, in Subsection 4.2 we prove some lemmas about how to totally dominate vertices at distance 2 from two or more vertices, in particular the Divider Lemma.

Basic Cycles Exist

Let G be a plane graph of radius 2 and diameter 3 with central vertex x. We say that it is edge-minimal if for every edge e of G, diam(G − e) >3 or ecc(x) > 2 in G − e. Clearly, we may assume that G is edge-minimal in proving Theorem 1 (since removing edges can only increase the total domination number).

Theorem : Let G be an edge-minimal plane graph of radius 2 and diameter 3 with central vertex x. Then, $\gamma_t(G) \leq 5$, or there exists a special basic triangle, special basic 4-cycle, or basic 5-cycle.

Proof : Suppose there is neither a special basic cycle of length 3 or 4 nora basic 5-cycle in G. Let Y = V (G) − N[x]. Let M be a minimal subset of N(x) that dominates Y . The set M exists since ecc(x) = 2. Let |M| = m. Since $\gamma_t(G) \leq m + 1$, we may assume m >=5. Let the vertices of M be $n_0, n_1, \ldots, n_{m-1}$ in cyclic order (clockwise) around x in G. Let Y'_ibe the set of vertices of Y whose only neighbor in M is n_i. By the minimality of M, each Yi is nonempty.

Let $Y_0, Y_1, \ldots, Y_{m-1}$be a partition of Y such that $Y_i \subseteq N(n_i)$ for each i. Necessarily, $Y_i \subseteq Y_i$ for each i. We now choose a vertex $y_i \in Y'_i$ for each i. If there is a vertex of Y'_I adjacent to both a vertex of Y_{i-1} and a vertex of Y_{i+1} (where addition is taken modulo m), then this vertex is unique by the planarity of G and we choose this as y_i.

If there is no such vertex of Y_i , then we let $y_i$be any vertex of Y_i adjacent to a vertex of Y_{i-1} or a vertex of Y_{i+1}, if such a vertex exists, failing which we let y_i be any vertex of $Y_{0\,i}$. We say that two neighbors u_1 and u_2 of x are separated if there is a vertex of M between u_1 and u_2 in both directions around x in the embedding of G. We define type-1, type-2 and type-3 edges as follows.

A type-1 edge joins vertices $u_1, u_2 \in N(x)$ such that u_1 and $u_2$are separated. A type-2 edge joins vertices $u_1 \in N(x)$ and $v_2 \in Y$ with $v_2$dominated by a vertex u_2 of M such that u_1 and u_2 are separated. A type-3 edge joins vertices $v_1, v_2 \in Y$ with v_1 and v_2 dominated by vertices u_1 and u_2 of M, respectively, such that u_1 and u_2 are separated.

Theorem: There is no type-1, type-2 or type-3 edge.

Proof : Let e be an edge. Suppose e = $u_1u_2$is a type-1 edge. Then there is a vertex n_i of M inside the cycle C: x, u_1, u_2, x and a vertex n_j of M outside the cycle C. Since the vertices y_i and y_j are not dominated by x, C is a basic triangle. Without loss of generality, C dominates its inside. By assumption, C is non special. That is, every vertex of Y inside C is adjacent to both $u_1$and u_2. By planarity, y_i is the only vertex of Y inside the triangle C, since each such vertex must be adjacent to all of u_1, u_2 and n_j. But then we can remove the edge n_iy_i, contradicting the minimality of G. Hence, G has no type-1 edge.

Suppose e = u_1v_2 is a type-2 edge. Then again there is a vertex n_i ofM inside the cycle C: x, u_1, v_2, u_2, x and a vertex n_j of M outside the cycle C with vertices y_i and y_j not dominated by {x, u_2}. Furthermore, since there is no type-1 edge, C is induced and hence a basic 4-cycle. Without loss of generality, C dominates its inside. By assumption, C is non-special. That is, every vertex of Y inside C is adjacent to at least two vertices on the cycle. In particular, since $u_2 \in$ M, y_i is adjacent to $u_1$and v_2 (and not to u_2). Hence by planarity,

each vertex of Y inside C is adjacent to at most one of u_1 and u_2, and therefore, since C is non-special, is adjacent to v_2. But then we can remove the edge n_iy_i, contradicting the minimality of G. Hence, G has no type-2 edge. If $e = v_1v_2$ is a type-3 edge, then again there is a vertex y_i both insideand outside the cycle C: x, u_1, v_1, v_2, u_2, x not dominated by {x, u_1, u_2}. Furthermore, since there is no type-1 or type-2 edge, C is induced and hence a basic 5-cycle, a contradiction. Hence, G has no type-3 edge.

3. TOTAL DOMINATION IN GRAPHS WITH DIAMETER 2

A hypergraph H = (V, E) is a finite set V = V(H) of elements, called vertices, together with a finite multiset E = E(H) of arbitrary subsets of V, called hyperedges or simply edges. A k-uniform hypergraph is a hypergraph in which every edge has size k. Every (simple) graph is a 2-uniform hypergraph. Thus, graphs are special hypergraphs. A hypergraph H is called an intersecting hypergraph if every two distinct edges of H have a nonempty intersection.

A subset T of vertices in a hypergraph H is a transversal in H if T has a nonempty intersection with every edge of H. A transversal is also called a hitting set in the literature. The transversal number τ (H) of H is the minimum size of a transversal in H. A transversal of H of size τ (H) is called a τ (H) set.

For a graph G = (V, E), we denote by H_G the open neighbourhood hypergraph, abbreviated as ONH, of G; that is, H_G = (V,C) is the hypergraph with vertex set V and with edge set C consisting of the open neighborhoods of vertices of V in G.

Theorem : Let G be a diameter-2 graph of order n. Then the following hold.

(a) $\gamma_t(G) \leq 1 + \delta(G)$.

(b) If $n \leq 11$, then $\gamma_t(G) \leq 1 + \sqrt{n}$ with equality if and only if $G = G_9$.

(c) If G has girth 5, then $\gamma_t(G) = 1 + \sqrt{n} - 1$.

We next establish an upper bound on the total domination number of a general graph with large minimum degree.

Proof: Let G = (V, E) be a diameter-2 graph of order n. If v is an arbitrary vertex in G, then the diameter-2 constraint implies that N[v] is a TD-set in G. In particular, choosing v to be a vertex of minimum degree proves part (a) of the above Theorem.It is shown that Moore graphs are r-regular and that diameter-2 Moore graphs have an order $n = r^2 + 1$and exist for r = 2, 3, 7, and possibly 57, but for no other degrees.

The Moore graphs for the first three values of r are unique, namely,

(i) the 5-cycle (2-regular graph on n = 5 vertices),

(ii) the Petersen graph (3-regular graph on n = 10 vertices), and

(iii) the Hoffman–Singleton graph (7-regular on n = 50 vertices).

Since G is a diameter-2 graph of girth 5, the graph G is a diameter-2 Moore graph and $n = r^2 + 1$. Hence $r = \sqrt{n} - 1$.

Let D be a γ_t (G)-set. Then $V = \bigcup_{v \in D} N(v)$, implying that $|V| \leq \sum_{v \in D} d_G(v) \leq \Delta(G) \leq (G) \cdot |D|$; or equivalently, $\gamma_t(G) = |D| \geq |V|/(G) = n/\sqrt{n} - 1$. Therefore by Part (a), we have that $n/\sqrt{n} - 1 \leq \gamma_t (G) \leq 1 + \sqrt{n} - 1$, or, equivalently, $\sqrt{n} - 1 + 1/\sqrt{n} - 1 \leq \gamma_t (G) \leq 1 + \sqrt{n} - 1$. Since both γ_t (G) and n − 1 are integers, $\gamma_t (G) = 1 + \sqrt{n} - 1$.Hence the proof.

5. TOTAL DOMINATION IN PLANAR GRAPHS OF DIAMETER TWO

A total dominating set, denoted TDS, of a graph G = (V, E) with no isolated vertex is a set S of vertices of G such that every vertex is adjacent to a vertex in S. Every graph without isolated vertices has a TDS, since S D V is such a set. The total domination number of G, denoted by γ_t (G),is the minimum cardinality of a TDS. A TDS of G of cardinality γ_t(G) is called a γ_t(G)-set. The decision problem to determine the domination number and total domination number of a graph remains NP-hardeven when restricted to cubic graphs or planar graphs of maximum degree 3. Hence it is of interest to determine upper bounds on the domination number and total domination number of a graph. A tree of radius 2 and diameter 4 can have arbitrarily large (total) domination number. So the interesting question is what happens when the diameter is 2 or 3.This restriction is reasonable to impose because planar graphs with small diameter are often important in applications. MacGillivray and Seyffarth proved that planar graphs with diameter two or three have bounded domination numbers.

Theorem: If G is a planar graph with diam.(G)= 2, then $\gamma_t(G) \leq 3$.

Proof : Our aim in this paper is to study the problem of characterizing planar graphs with diameter two and total

domination number three. Such a characterization seems difficult to obtain since there are infinitely many such graphs.

we therefore restrict our attention to planar graphs with certain structural properties. We say that a graph G satisfies the domination-cycle property if there is some $\gamma(G)$-set not contained in any induced 5-cycle of G. We characterize the planar graphs with diameter two and total domination number three that satisfy the domination-cycle property.

Notation : For notation and graph theory terminology we in general follow. Specifically, let G = (V, E)be a graph with vertex set V of order n and edge set E. For a set $S \subseteq V$, the subgraph induced by S is denoted by G[S].

The S-external private neighborhood epn(υ, S) of a vertex $v \in S$ is defined by $pn(\upsilon, S)= \{u \in V \mid N(u) \cap S=\{\upsilon\}\}$, and each element of epn(υ, S)is called an S-external private neighbor of υ. The open neighborhood of vertex $\upsilon \in V$ is denoted by $N(\upsilon)=\{u \in V \mid u_v \in E\}$ while its closed neighborhood is given by $N[\upsilon]= N[\upsilon] U\{\upsilon\}$. For a set $S \subseteq V$, $N(S)=\cup_{\upsilon \in S}N(\upsilon)$ and N[S] U S. If X, Y ⊆ V, then the set X is said to dominate the set Y if
$Y \subseteq N[X]$, while X is said to totally dominate the set Y if $Y \subseteq N[X]$. If $Y =\{\upsilon\}$ and X dominates Y, we simply write that X dominates υ. We note that if X dominates V, then N[X] =V and X is a dominating set of G, and if X totally dominates V, then N(X)= V and X is a total dominating set of G.

For disjoint subsets U and W of V, we let [U,W] denote the set of all edges of G joining a vertex of U and a vertex of W. We denote the degree of a vertex υ in G by $d_{G(\upsilon)}$ or simply by d(υ) if the graph G is clear from the context. For two vertices u and v in a connected graph G, the distance $d_G(u, \upsilon)$ between u and υ is the length of a shortest u-υ path in G.

For a set $S \subseteq V$ and a vertex $v \in V$, the distance $d_G(\upsilon, S)$ between υ and S is the minimum distance between v and a vertex of S. If a vertex u is adjacent to a vertex υ, we write $u \sim v$, while if u and v are nonadjacent, we write $u \nsim \upsilon$. If υ is adjacent to no vertex in a set $A \subseteq V(G)$ then we write $\upsilon \nsim A$ and if υ is adjacent to every vertex in A then we write $\upsilon \sim A$. A plane graph is a planar graph together with an embedding in the plane. From the Jordan Closed Curve Theorem, we know that a cycle C in a plane graph separates the plane into two regions, the interior of C and the exterior of C. If a vertex lies in the interior of C, we simply say that v lies inside C. We denote the set of vertices in the interior and exterior of C by int(C) and ext.(C), respectively. A plane graph divides the plane into regions which we call faces. The unbounded region is called the exterior face and the other regions are called interior faces. If f is a face of a plane graph G, then we can write $f=[u_1, u_2,\ldots, u_k]$ where $u_1, u_{2,\ldots}, u_k$ are the vertices on the boundary walk of f in clockwise order.

6. CONCLUSION

This paper describes about "A Review On Domination in Planar Graphs With Small Diameter". Domination numbers of planar graphs proved that planar graphs with diameter two or three have bounded domination numbers. This implies that the domination number of such a graph can be determined in polynomial time.

REFERENCES

[1] G. MacGillivray and K. Seyffarth, Domination numbers of planar graphs. J. Graph Theory 22 (1996), 213–229.

[2] W. McCuaig and B. Shepherd, Domination in graphs with minimum degree two.J. Graph Theory 13 (1989), 749–762.

[3] S.L.Mitchell and S.T.Hedetniemi, Edge domination in trees. Congr. Numer. 19, 489-509, 1977.

[4] M.H.Muddebihal, T.Srinivas and Abdul Majeed, (2012), Domination in block subdivision graphs of graphs, (submitted).

[5] O. Ore, (1962), Theory of graphs, Amer. Math. Soc., Colloq. Publ., 38 Providence.

[6] Pratima panigrahi and S.B.Rao, Graph theory research directions, Narosa publishing house (2011).

[7] E.Sampathkumar and H.B.Walikar, The Connected domination number of a graph, J.Math.Phys. Sci., 13, 607-613,1979.

[8] G.Suresh singh, Graph theory published by K.Ghosh, PHI learning private limited, New Delhi -110001 (2010).

A Review on Relationship between Domination, Independent Transversal Domination and Equitable Domination in Graphs	S.Maivizhiselvi Assistant Professor of Mathematics	Maths	International Journal of Mathematics Trends and Technology (IJMTT)	April 2017	ISSN: 2231-5373 (P:51-52)	**UGC Approved Journal in 2017** https://www.ijmttjournal.org/2017/Volume-44/number-1/IJMTT-V44P509.pdf

A Review on Relationship between Domination, Independent Transversal Domination and Equitable Domination in Graphs

[1] S.Surya [2] S.Maivizhiselvi

[1]*Research Scholar, Sakthi College of Arts and Science For Women, Oddanchatram.*
[2] *Head & Assistant Professor, Department of Mathematics, Sakthi College of Arts and Science For Women, Oddanchatram.*

ABSTRACT – A set S □ V of vertices in a graph G = (V,E) is called a dominating set if every vertex in V − S is adjacent to a vertex in S. A dominating set which intersects every maximum independent set in G is called an independent transversal dominating set. In this paper we begin an investigation of relationship between domination, independent transversal domination and equitable domination in graphs.

Keywords: Dominating set, independent set, independent transversal dominating set, equitable dominating set.

1. INTRODUCTION

One of the fastest growing areas within graph theory is the study of domination, independent transversal dominating set, equitable dominating set and related subset problems such as independence, covering and matching. An independent dominating set S is a dominating set such that S is an independent set. The independent domination number i(G) is the minimum cardinality of an independent dominating set. The maximum cardinality of an independent set is called the independence number and is denoted by β_0(G). A subset D of V (G) is called an equitable dominating set of a graph G if for every $u \in \langle V - D \rangle$, there exists a vertex $v \in D$such that $uv \in E(G)$ and $|deg(u) - deg(v)| \leq 1$. The minimum cardinality of such a dominating set is denoted by $\gamma_e(G)$ and is called equitable domination number of G. An equitable dominating set which intersects every maximum independent set in G is called an independent transversal equitable dominating set. The minimum cardinality of an independent transversal equitable dominating set is called the independent transversal equitable domination number of G and is denoted by $\gamma_{ite}(G)$.

2. INDEPENDENT TRANSVERSAL DOMINATION IN GRAPHS

Theorem : For any graph G, we have $\gamma(G) \leq \gamma_{it}(G) \leq \gamma(G) + \delta(G)$.

Proof: Since an independent transversal dominating set of G is a dominating set, it follows that $\gamma(G) \leq \gamma_{it}(G)$.Now, let u be a vertex in G with deg u = δ(G) and let S be a γ-set in G. Then every maximum independent set of G contains a vertex of N[u] so that S □ N[u] is an independent transversal dominating set of G. Also, since S intersects N[u], it follows that |S □ N[u]| ≤ γ(G) + δ(G) and hence the right inequality follows.

Theorem: If G is a graph with diam G = 2, then $\gamma_{it}(G) \leq \delta(G) + 1$.

Proof: Let u be a vertex with deg u = δ(G). Then N[u] is a dominating set of G, because diam G = 2.
Now, it follows from the fact that every maximum independent set contains a vertex of N[u].This closed neighborhood itself is an independent transversal dominating set so that $\gamma_{it}(G) \leq \delta(G) + 1$.

Theorem: Let G be a bipartite graph with bipartition (X, Y) such that |X| ≤ |Y | and γ(G) = |X|. Then$\gamma_{it}(G) = \gamma(G) + 1$ if and only if every vertex in X is adjacent to at least two pendant vertices.

Proof: We first claim that δ(G) = 1. Suppose δ(G) ≥ 2. Since γ(G) = |X|, X is a γ-set. Also, since $\gamma_{it}(G) = \gamma(G) + 1$ it follows that β_0(G) = |Y |. Now, let u □ X and v □ N(u). Since _(G) ≥ 2, it follows that S = (X − {u}) □ {v} is a dominating set of G. Now since β_0(G) = |Y | and δ(G) ≥ 2, everyβ_0- set contains either the vertex v or a vertex w ≠ u in X. Hence S intersects everyβ_0 - set so that $\gamma_{it}(G) = |X| = \gamma(G)$, which is a contradiction. Thus δ(G) = 1.Further suppose there exists a vertex u in X such that N(u) contains at most one pendant vertex. Then S = (X−{u})∪{v}, where v∈ N(u), and v is chosen to be a pendant vertex if it exists, is a dominating set of G. Also since β_0(G) = |Y |, it follows that S intersects every β_0-set of G and hence $\gamma_{it}(G) \leq |X| = \gamma(G)$, which is a contradiction. Thus every vertex in X is adjacent to at least two pendant vertices.Conversely, if every vertex in X is adjacent to at least two pendant vertices, then X is the only γ-set of G so that $\gamma_{it}(G) = \gamma(G) + 1$.

3. INDEPENDENT TRANSVERSAL EQUITABLE DOMINATION IN GRAPHS

Theorem: For any graph G, $\gamma(G) \leq \gamma_e(G) \leq \gamma_{ite}(G)$.

Proof: Let G be a graph with minimum independent transversal equitable dominating set D. Then D is an equitable dominating set of G and any equitable dominating set is also dominating set of G.From the definitions of the parameters, $\gamma(G)$, $\gamma_e(G)$ and $\gamma_{ite}(G)$, we get for any $\gamma(G) \leq \gamma_e(G) \leq \gamma_{ite}(G)$ graph G.

Theorem: For any graph G, $\gamma(G) \leq \gamma_{it}(G) \leq \gamma_{ite}(G)$.

Proof : Let G be a graph with minimum independent transversal equitable dominating set S.
From the definition of the independent transversal dominating set of G, S is also independent transversal dominating set, and any independent transversal dominating set is dominating set of G.
Hence $\gamma(G) \leq \gamma_{it}(G) \leq \gamma_{ite}(G)$.

Theorem : For any graph G which all of its edges are equitable, $\gamma_{it}(G) = \gamma_{ite}(G)$.

Proof: Let G be a graph $G = (V,E)$ such that for any edge e ∈ E e is equitable edge. Then any dominating set of G will also be equitable dominating set of G. Suppose that D is an independent transversal dominating set of G with size $|D| = \gamma_{it}(G)$ .Then D is also an independent transversal equitable dominating set, that means $\gamma_{it}(G) = \gamma_{ite}(G)$.Hence $\gamma_{it}(G) = \gamma_{ite}(G)$.

Example

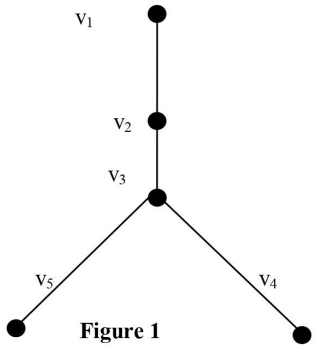

Figure 1

Let G be a graph as in Figure 5.2, we have $\gamma_{it}(G) = \gamma_{ite}(G) = 3$ the maximum independent sets in G are $\{v_1, v_4, v_5\}$ and $\{v_2, v_4, v_5\}$.The minimum independent transversal dominating sets are $\{v_1, v_4, v_5\}$, $\{v_2, v_4, v_5\}$ and $\{v_1, v_2, v_3\}$ and $\gamma_{it}(G) = 3$.

The minimum independent transversal equitable dominating set of G is only $\{v_2, v_4, v_5\}$. So $\gamma_{ite}(G) = 3$.Hence $\gamma_{it}(G) = \gamma_{ite}(G)$, but the edge v_3v_4 and v_3v_5 are not equitable edges in G.

In Figure1 $\gamma_{it}(G) = \gamma_{ite}(G)$ but not all the edges are equitable edges.

4. CONCLUSION

This paper deals about "A Review on relationship between domination, independent transversal domination and equitable domination in graphs". we discuss the relation between domination and independent transversal domination also the relation between independent transversal and equitable domination. So that if we find the domination number we can find the independent transversal domination number. Also we can find the equitable domination number.

REFERENCES

[1] G. Chartrand and L. Lesniak, Graphs and Digraphs Fourth edition, CRC Press, Boca Raton, 2005.

[2] E.J. Cockayne, R.M. Dawes and S.T. Hedetneimi, Total domination in graphs, Networks 10 211–219.

[3] T.W. Haynes, S.T. Hedetniemi and P.J. Slater, Fundamentals of Domination in Graphs (Marcel Dekker, New York, 1998).

[4] T.W. Haynes, S.T. Hedetniemi and P.J. Slater, Domination in Graphs: Advanced Topics ,Marcel Dekker, New York, 1998.

[5] Topics on Domination, Guest Editors: S.T. Hedetniemi and R.C. Laskar, Discrete Math. 86 .

[6] E. Sampathkumar and H.B. Walikar, The connected domination number of a graph, J. Math. Phys. Sci. 13 607–613. Received 19 October 2009.

[7] N. Alon, The strong chromatic number of a graph, Random Structures and Algorithms 3 1–7.

[8] N. Alon, M. R. Fellows, and D. R. Hare, Vertex Transversals that Dominate, Journal of Graph Theory 21 (1) 21–31.

[9] S. K. Ayyaswamy and C. Natarajan, On graphs whose chromatic transversal number is two, Proyecciones 30 (1) 59–64.

[10] E. Boros, M.C. Golumbic, and V.E. Levit, On the number of vertices belonging to all maximum stable sets of a graph, Discrete Applied Mathematics 124 (2002) 17–25.

A Review on Rainbow Edge Colouring and Rainbow Domination	S.Maivizhiselvi Assistant Professor of Mathematics	Maths	International Journal of Mathematics Trends and Technology (IJMTT)	April 2017	ISSN: 2231-5373 (P:53-57)	**UGC Approved Journal in 2017** https://www.ijmttjournal.org/2017/Volume-44/number-1/IJMTT-V44P510.pdf

International Journal of Mathematics Trends and Technology (IJMTT) – Volume 44 Number 1 - April 2017

A Review on Rainbow Edge Colouring and Rainbow Domination

[1] S.Nagalakshmi [2] S.Maivizhiselvi

[1]*Research Scholar, Sakthi College of Arts and Science For Women, Oddanchatram.*
[2]*Head & Assistant Professor, Department of Mathematics, Sakthi College of Arts and Science For Women, Oddanchatram.*

ABSTRACT – In graph theory Edge coloured graph which has the distinct coloured edges are well studied.An Edge coloured graph is t-tolerant if it contains no monochromatic star with t+1 edges.In this paper we consider optimal edge coloured complete graphs.We show that in any optimal edge colouring of the complete graph k_n ,Also we prove that in every proper edge colouring of the complete graph k_n .

Keywords: Rainbow Cycle, edge coloring , edge chromatic number ,Hamilton cycle.

1. INTRODUCTION

An edge-colored graph is rainbow if its edges have distinct colors. Rainbow edge-colored graphs have also been called heterochromatic, polychromatic, or totally multicolored, Within an edge-colored graph G, we consider covering the edges by rainbow matchings or covering the vertices by disjoint rainbow stars.

The existence of a Hamilton cycle with many colors, also the existence of a Hamilton cycle with few colors in any proper edge coloring of a complete graph. A rainbow cycle is a cycle whose all edges have different colors. Given an optimally edge colored complete graph with n vertices, we study the number of colors appearing on its cycles.

The rainbow connection number can be motivated by its interesting interpretation in the area of networking. This new concept comes from the communication of information between agencies of government.

Consider a network G(e.g., a cellular network). To route messages between any two vertices in a pipeline, assign a distinct channel to each link(e.g., a distinct frequency). We need to minimize the number of distinct channels that we use in the network.

The minimum number of distinct channels is called the rainbow connection number and is denoted by rc(G). Let G be an edge-colored graph with n vertices. A rainbow subgraph is a subgraph whose edges have distinct colors. The rainbow edge-chromatic number of G, written $\widehat{\aleph}$ (G), is the minimum number of rainbow matchings needed to cover E(G). An edge- colored graph is t-tolerant if it contains no monochromatic star with t+1 edges.

2. RAINBOW EDGE COLOURING AND RAINBOW DOMINATION

If G is t-tolerant, then $\aleph$ (G) < t (t +1) n ln n, and examples exist with $\widehat{\aleph}$ (G) ≥ t / 2 (n-1). The rainbow domination number, written $\widehat{\gamma}$ (G), is the minimum number of disjoint rainbow stars needed to cover V (G). For t-tolerant edge-colored n-vertex graphs, we generalize classical bounds on the domination number: $\widehat{\gamma}$ (G) $\leq \frac{1+In\ k}{k}$ n (where k = $\frac{\delta(G)}{t}+1$) and $\widehat{\gamma}$ (G) $\leq \frac{t}{t+1}$ n when G has no isolated vertices.

Theorem: There exist infinitely many t-tolerant edge-colored graphs G such that $\widehat{\aleph}$ (G) $\geq \frac{t}{2}(|V(G)|-1) = \frac{t}{2}\Delta(G)$.

Proof: For t, p ∈ N, start with a proper tp-edge-coloring of K_{tp}. Obtain a t-tolerant edge-colored graph G by combining t-tuples s of color classes into single colors.

In G there are only p colors, so $\widehat{\propto}'(G) \leq p$.

Hence $\widehat{\aleph}(G) \geq \frac{1}{p}|E(G)|$

$\geq \frac{t}{2}(tp-1)$

$= \frac{t}{2}(|V(G)|-1)$

$= \frac{t}{2}\Delta(G)$.

Theorem: When n≡ 2 mod 4, there is an edge-colored graph G such that $\widehat{\aleph}$ (G) > Δ(G) + 1 and G is a proper n-edge-coloring of $K_{n,n}$.

Proof: As noted earlier, proper n-edge-colorings of $K_{n,n}$ correspond to Latin squares of order n. Each rainbow matching corresponds to a partial transversal of the Latin

square so $\widehat{\aleph}$ (G) is the minimum number of partial tranversals covering the square.

Latin squares of even order need not have transversals. To construct such squares when n ≡2 mod 4, let k = n/2, and let A and B be latin squares of order k, using disjoint sets of k labels in the two squares.

Let C =$\begin{pmatrix} A & B \\ B & A \end{pmatrix}$.Although C is a Latin square of order n, it has no transversal. A transversal must use each of the 2k labels.Since k is odd, some quadrant must contribute at least $\lceil K/2 \rceil$ positions.

Now each of the other three quadrants is limited to $\lfloor K/2 \rfloor$contributions, so a partial transversal has size at most n−1 .

Thus at least $n^2/(n-1)$ partial transversals are needed to cover C. Since (n−1)(n+1) < n^2

we have $\widehat{\aleph}$ (G) ≥ $n^2/(n-1)$

> (n+1) = Δ(G) + 1.

Theorem: Fix t ∈ N and c ∈ R with c > 0. Every t-tolerant edge-colored graph G with average color degree at least c has an edge-colored t-tolerant subgraph H with $\hat{\delta}$ (H) > $\frac{c}{t+1}$.

Proof : The claim holds with H = G unless $\widehat{d_G}$(v) ≤ $\frac{c}{t+1}$ for some vertex v. Deleting v decreases the color degree of each neighbor by at most 1, but v may have up to t $\widehat{d_G}$(v) neighbors.Thus deleting v reduces the sum of the color degrees by at most (t + 1) $\widehat{d_G}$(v).

Since $\sum_{u\in V(G-v)} \widehat{d_{G-v}(u)} \geq \sum_{u\in V(G)} \widehat{d_G}(u) - (t+1)\widehat{d_G}(v) \geq c\,|V(G)| - c$

deleting v does not reduce the average color degree.

Furthermore, every subgraph of a t-tolerant graph is also t-tolerant. Iteratively deleting vertices with color degree at most c/(t + 1) must end. Since the average color degree never decreases, it ends with a subgraph H having no vertex with color degree at most c/ (t + 1).

3. ON RAINBOW CYCLES IN EDGE COLORED COMPLETE GRAPHS

Graph colorings is one of the most important concepts in graph theory. In the present paper we study the existence of a Hamilton cycle with many colors, also the existence of a Hamilton cycle with few colors in any proper edge coloring of a complete graph. A rainbow cycle is a cycle whose all edges have different colors.

Given an optimally edge colored complete graph with n vertices, we study the number of colors appearing on its cycles. We show that there exists a Hamilton cycle with at most $\sqrt{8n}$ colors and a Hamilton cycle with at least n(2/3 − o(1)) colors. A random Hamilton cycle is also shown to have n(1 − 1/e + o(1)) colors on average.

There are examples of optimal edge colorings that have no Hamilton cycle with less than $\log_2$ n colors. Furthermore, in some optimal edge colorings, there is no Hamilton cycle with n − 1 or n colors. We conjecture that there is always a Hamilton cycle with at most O(log n) colors and a Hamilton cycle with at least n − 2 colors.

For every ∈ > 0 and n > n_0 (∈), any complete graph K_n whose edges are colored so that no vertex is incident with more than $(1-\frac{1}{\sqrt{2}}-\in)$ edges of the same color, contains a Hamilton cycle in which adjacent edges have distinct colors. Moreover, for every k, 3≤ k ≤ n, any such Kn contains a cycle of length k in which adjacent edges have distinct colors.

Let the edges of the complete graph K_n be colored so that no color is used more than k = k(n) times. This coloring it is called a k-bounded coloring. Clearly, if k = 1, every Hamilton cycle is a rainbow cycle.

Theorem:In any optimal edge coloring of the complete graph Kn, there is a Hamilton cycle with at most $\sqrt{8n}$ different colors.

Proof: Our proof relies on the following observation: Let $P_{1,\ldots,}P_k$ be k vertex disjoint paths that cover V (K_n).

For 1 ≤ j ≤ k, let v_j be an endpoint of P_j.

There are $\binom{k}{2}$ edges connecting the v_j 's, and $\aleph'(K_n) \leq n$ colors are used.

We can thus find a set S of at least k(k − 1)/(2n) edges, all of the same color and all connecting the v_j 's Evidently, adding S to P_1, …., P_k decreases the number of paths by at least k(k − 1)/(2n) and increases the number of distinct colors that appear on the paths by at most one. In addition, the paths are still vertex-disjoint and cover V (K_n).To begin, let Pi be the path of length zero formed by the ith vertex of Kn for 1 ≤ i ≤ n.

Clearly, P_1 ,…,P_n cover V (K_n) and are vertex-disjoint. Let us set x_0 = n.

By the above observation and induction on $i \geq 0$, there are x_i vertex-disjoint paths that use at most i colors and cover V (K_n), and

$x_{i+1} \leq x_i - x_i(x_i - 1)/(2n)$.

Clearly, the function $1/(x(x-1))$ is decreasing in the range $x > 1$. Hence if m is a nonnegative integer and $x_m > 1$, we have

$$m \leq \sum_{i=0}^{m-1} \frac{2n(x_i - x_{i+1})}{x_i\,(x_i-1)} \leq \int_{x_m}^{x_0} \frac{2n}{x(x-1)}dx \leq \int_{x_m}^{x_0} \frac{2n}{(x-1)^2}dx = \frac{2n}{x_m - 1} - \frac{2n}{n-1},$$

which implies that $x_m \leq 1+2n/(m+2)$ for all nonnegative integers m.

Recall that there are x_m vertex-disjoint paths with at most m colors on the edges which cover V(K_n).We can connect these paths to form a Hamilton cycle by adding x_m edges; the resulting Hamilton cycle has at most $m + x_m$ colors.

For $m = \lceil\sqrt{2n}\rceil - 2$,we have $x_m \leq \sqrt{2n}+1$.

thus atmost $(\lceil\sqrt{2n}\rceil - 2) + (\sqrt{2n} + 1) \leq 2\sqrt{2n}$ colors appear on the Hamilton cycle.

Theorem: Given an optimal edge coloring of the complete graph K_n, the expected number of different colors that appear on the edges of a random Hamilton cycle of K_n is approximately equal to $(1 - e^{-1})n$, for large enough n.

Proof:Let c be an arbitrary color used in the given optimal edge coloring of K_n and let C be the set of edges whose colors are c. The edges in C are a matching of size $\lfloor n/2 \rfloor$. Clearly K_n has (n − 1)!/2 Hamilton cycles.

Assume S is a subset of C with size k. We can count the number of Hamilton cycles that contain S by considering the following transformation. For each edge in S, contract its two endpoints into a single vertex.

If H is a Hamilton cycle of K_n that contains S, its transform is a Hamilton cycle of the graph K_{n-k}. Furthermore, every Hamilton cycle of K_{n-k} is the transform of exactly 2^k Hamilton cycles of K_n that contain S, because the directions of the alignments of the edges of S in H have no impact on the transform of H.

Consequently, there are $2^{k-1}(n - k - 1)!$ Hamilton cycles in K_n that contain S.Thus the probability that a random Hamilton cycle contains S is $2^k (n - k - 1)!/(n - 1)!$.The principle of inclusion and exclusion now implies that the probability of the event that a random Hamilton cycle avoids all edges in C is $P=\sum_{K=0}^{\lfloor \frac{n}{2} \rfloor}(-1)^k a_k$

Where , $a_k=\binom{\lfloor \frac{n}{2} \rfloor}{k}\frac{2^k(n-k-1)!}{(n-1)!} = \frac{1}{k!}\prod_{j=0}^{k-1}\frac{2\left(\lfloor \frac{n}{2} \rfloor - j\right)}{n-j-1}$.

It is not hard to see that $a_k \leq 1/k!$ for $k \geq 3$. For any real number x, we have $1 + x \leq e^x$; hence for $k \leq n^{1/3}$ we have

$$\begin{aligned} a_k &= \frac{1}{k!}\prod_{j=0}^{k-1}\left(1 + \frac{(n-j-1)-2\left(\lfloor \frac{n}{2} \rfloor - j\right)}{2\left(\lfloor \frac{n}{2} \rfloor - j\right)}\right)^{-1} \\ &\geq \frac{1}{k!}\prod_{j=0}^{k-1}\left(1 + \frac{j}{2\left(\lfloor \frac{n}{2} \rfloor - k\right)}\right)^{-1} \\ &\geq \frac{1}{k!}\prod_{j=0}^{k-1}\exp\left(-\frac{j}{2\left(\lfloor \frac{n}{2} \rfloor - k\right)}\right) \\ &= \frac{1}{k!}exp\left(-\frac{k(k-1)}{4\left(\lfloor \frac{n}{2} \rfloor - k\right)}\right) \\ &\geq \frac{1}{k!}\exp\left(-\frac{n^{2/3}}{4\lfloor \frac{n}{2} \rfloor - n^{1/3}}\right) \\ &= \frac{1}{k!}(1 + o(1)), \end{aligned}$$

where o(1) is a function in terms of n and k that becomes arbitrarily small as n gets large.

Splitting the right hand side of Equation into two sums as in

$p = \sum_{k=0}^{\lfloor n^{1/3} \rfloor}(-1)^k a_k + \sum_{k=\lfloor n^{1/3} \rfloor}^{\lfloor \frac{n}{2} \rfloor}(-1)^k a_k$,

we note that the Taylor expansion of e^x for $x = -1$ yields

$$\sum_{k=0}^{\lfloor n^{1/3} \rfloor}(-1)^k a_k = \sum_{k=0}^{\lfloor n^{1/3} \rfloor}\frac{(-1)^K}{k!}(1 + o(1))$$

$$= \sum_{k=0}^{\lfloor n^{1/3} \rfloor}\frac{(-1)^K}{k!} + \sum_{k=0}^{\lfloor n^{1/3} \rfloor}\frac{(-1)^k o(1)}{k!}$$

$$= (e^{-1} + o(1)) + o(1) = e^{-1} + o(1)$$

On the other hand, we have

$$\left|\sum_{k=\lfloor n^{1/3} \rfloor+1}^{\lfloor \frac{n}{2} \rfloor}(-1)^k a_k\right| \leq \sum_{k=\lfloor n^{1/3} \rfloor+1}^{\lfloor \frac{n}{2} \rfloor}\frac{1}{k!} = o(1),$$

since the series $\sum_{k=0}^{\infty}\frac{1}{k!}$ is convergent.

Thus we get $p = e^{-1} + o(1)$. We known $n - 1 \leq \aleph'(Kn) \leq n$, and the color c appears on a random Hamilton cycle with probability 1−p.

Thus we expect that $\aleph'(Kn)(1-p) = n(1-e^{-1})(1+o(1))$ different colors appear on a random Hamilton cycle on average.

Theorem: In any optimal edge coloring of K_n, there is a Hamilton cycle with at least n(2/3 − o(1)) colors.

Proof: Suppose n is even. Without loss of generality assume {1, 2, ⋯ , n − 1} is the set of colors used.

Let A be an n × n square matrix where $A_{ij} = c(v_iv_j)$ if 1≤ i , j≤ n and i ≠ j, and A_{ii} = n if 1 ≤ i ≤ n. Clearly, A is a Latin square.

By a result , we can select n −$O(\log^2 n)$ entries of A that have different values, and are located on distinct rows and columns. Of these entries, only one can be on the diagonal.

Furthermore, if A_{ij} is selected then A_{ji} can not be selected since values appearing on the selected entries should be distinct.

This means that we can select n−$O(\log^2 n)$−1 edges of K_n such that the selected edges have different colors, and the degree of each vertex is at most two in the graph induced by these edges.

That is, the selected edges consist of vertex-disjoint paths and cycles. Every cycle has at least 3 edges.

Thus we can delete one edge of every cycle to get (2/3)(n − $O(\log^2 n)$ − 1) edges forming vertex-disjoint paths.We can connect these paths to get a Hamilton cycle with at least (2/3)(n − $O(\log^2 n)$ − 1) = (2/3 − o(1))n colors.

When n is odd, K_n is colored using n colors. Moreover, for any of these n colors, exactly one vertex is not an endpoint of an edge of that color. Thus, we can extend the optimal edge coloring of K_n to an optimal edge coloring of K_{n+1}.Since n+1 is even, K_{n+1} has a Hamilton cycle with at least (2/3 − o(1))(n + 1) colors. We can now trivially construct a Hamilton cycle for K_n that has (2/3 − o(1))n colors.

4. AN EDGE COLOURING PROBLEM FOR GRAPH PRODUCTS

The edges of the Cartesian product of graphs G×H are to be colored with the condition that all rectangles ,i.e, $k_2 \times k_2$ subgraphs,must be colored with four distinct colours.The minimum number of colors in such colorings is determined for all pairs of graphs except when G is 5-chromatic.

A rectangle in the Cartesian product G×H of two graphs is a four-cycle in the form $k_2 \times k_2$ .The term **Good coloring** is used for edge coloring of G×H such that all rectangles are colored with four distinct colours.We determine rb (G,H) , the minimum number of colours needed for a Good coloring of G×H (rb stands for rainbow).The minimum number colours needed for a Good colouring of $k_m \times k_n$.this number is denoted by
rb (m,n)and rb (n,n).

Theorem :rb (G,H)≤ rb($\aleph(G), \aleph(H)$).
Proof: Assume that V(G) is partitioned into k independent sets *A,* and V(H) is partitioned into l independent sets B_i where k =ℵ (G) and 1 = ℵ (H) Contract each set $A_i \times B_j$ in $G \times H$ into a single vertex v_{ij} and view this As M = K_k x K_l by adding all horizontal and vertical edges.

There is a good coloring of M with rb (k, 1) colors. Transfer this coloring to G x H by coloring each edge between $A_i \times B_j$ and $A_i \times B_t$ with the color of $v_{ij}v_{it}$ in *M,* similarly by coloring each edge between $A_i \times B_j$ and $A_i \times B_t$ with the color of $v_{ij}v_{it}$.This is a good coloring of $G \times H$.

Theorem :rb (G,H)≥max ($\aleph(G), \aleph(H)$).
Proof: Assume that rb(G, H) = *t* and let ∝ be a good coloring of $G \times H$ with *t* colors.Fix an arbitrary edge e of *G,* and for each vertex v in *H* color *v* with ∝ (e × v). Since ∝ is a good coloring of $G \times H$, we obtain a proper coloring of the graph *H* with at most *t* colors. Therefore $\aleph(H) \leq t$. A similar argument $\aleph(G) \leq t$.

Theorem: For each n ≥6 there exist weak decompositions of K_n which are complementary.
Proof: Set m = ⌊n/2⌋ and define A = {0,1,. . . , m - 3, m - 2, m}.For odd n, define *B* as B = {2,3,. . . , m - 1, *m,* m + 2},and for even n, define *B* as B = {1,2,. . . ,m - 2,m - 1,m+ 1}. In both cases A∩B= ∅ holds. Therefore defining G_o and H_o as complete graphs with vertex sets A and *B,* respectively, the condition of complementary decompositions is satisfied. Furthermore, if $n \geq 6$ the edges of the complete graphs G_o + i and H_o + i both cover the edges of k_n on [n] because the differences of elements in both A and B give all elements of [n] .

Therefore recursively defining the edge set *E,* for i = 1,2,. . . , *n* - 1 of the graph *G,* as E_{i+1}=$\{\cup pq: p, q \in V(G_o) + i, pq \notin E_j, 0 \leq j \leq i\}$
(with *Eo* = *E(Go)),*th e graphs *G,* form a weak decomposition.The graphs H_i can be defined similarly,writing H instead of G.

5. CONCLUSION

This paper describes about "A Review On Rainbow edge colouring and rainbow domination" edge coloured graph is tolerant if it contains no monochromatic star. Also every proper edge colouring of the complete graph k_n .

REFERENCES

[1] M. Albert, A. Freize, B. Reed, Multicoloured Hamilton cycles, Electron. J. Comb.
research paper 10, 1995.

[2] N. Alon. Transversal numbers of uniform hypergraphs. Graphs and Combinatorics, vol. 6, pp.1 {4, 1990.

[3] N. Alon, G. Gutin, Properly colored Hamilton Cycles in edge colored complete
graphs, Random Structures Algorithms 11 (1997) No. 2, 179-186.

[4] J. Bos& Decompositions of graphs, Vol. 47 in Mathematics and Its Applications, Kluwer Academic Publishers (1990).

[5] R. J. Faudree, A. Gykfis, L. Lesniak, and R. H. Schelp, Rainbow coloring of the cube, J.Graph Theory 17 (19931, 607-612.

[6] R. J. Faudree, A. Gykfas, and T. Szonyi, Projective spaces and colorings of $K_{,,} \times K_{,}$, Coll. Math. Soc. J. Bolyai 60, Sets Graphs and Numbers (1991), 273-278.

[7] [Chakraborty et al., 2009] Chakraborty, S., Fischer, E., Matsliah, A., and Yuster, R.(2009). Hardness and algorithms for rainbow connection. Journal of Combinatorial Optimization, pages 1–18.

[8] A. M. Frieze, B. A. Reed, Polychromatic Hamilton cycles, Disc. Math. 118 (1993) 67-54.

A Review on Global Domination Number of a Graph	R.Jeyamani Assistant Professor of Mathematics	Maths	International Journal of Mathematics Trends and Technology (IJMTT)	April 2017	ISSN: 2231-5373 (58-60)	**UGC Approved Journal in 2017** https://www.ijmttjournal.org/2017/Volume-44/number-1/IJMTT-V44P510.pdf

A Review on Global Domination Number of a Graph

[1] S. Kalaiselvi [2] R.Jeyamani

[1]*Research Scholar, Sakthi College of Arts and Science For Women, Oddanchatram.*
[2]*Associate Professor, Department of Mathematics, Sakthi College of Arts and Science For Women, Oddanchatram.*

ABSTRACT – Adominating set is called a global dominating set if it is a dominating set for a graph G and its complement $\bar{G}$. We investigate some general results for global dominating sets corresponding to the graphs Pn. In the present work we investigate some general results which relate the concept of global domination and duplication of a vertex. In this paper sharp bounds for γ_{gn}, are supplied for graphs whose girth is greater than three. Exact values of this number for paths and cycles are presented as well.

Keywords: Domination, global domination, global sets domination, global neighborhood domination.

1. INTRODUCTION

Graph theory can be defined as the study of graphs. Graphs are mathematical structures used to model pair-wise relations among objects from a certain collection. Graph can be defined as a set V of vertices and set of edges. Where V is collection of $|V| = n$ abstract data types. Vertices can be any abstract data types and can be represented with the points in the plane. These abstract data types are also called nodes. A line segment connecting these nodes is called an edge. Again, more abstractly saying, edge can be abstract data type that shows relation among the nodes.

In this document , I would briefly go over through how and what led to the development of the graph theory which revolutionized the way to many complicated problems to be solved.

The " Konigsberg bridge " problem originated in the city of Konigsberg , formerly in the Germany but , now known as Kaliningrad and part of Russia , located on the river Preger. The city had seven bridges, which connected two island with the main land Via seven bridges. People staying there always wondered whether was there any way to walk over all the bridges once and only once and return to the starting place. The below picture is the map of Konigsberg during Euler's time showing the actual layout of the seven bridges, highlighting the river Preger and the bridges.

2. THE GLOBAL DOMINATION NUMBER OF A GRAPH

Theorem: (i) For a graph G with p vertices , $\gamma_g(G) = p$ if and only iff $G = K_p$ or $\bar{K}_p$.
(ii) $\gamma_g(K_{m,n}) = 2$ for all $m, n \geq 1$
(iii) $\gamma_g(C_4) = 2$, $\gamma_g(C_5) = 3$ and $\gamma_g(C_n) = \{ n / 3 \}$ for all $n \geq 6$.
(iv) $\gamma_g(P_n) = 2$ for $n = 2, 3$ and $\gamma_g(P_n) = \{ n / 3 \}$ for all $n \geq 4$.
Proof: We prove only (i) and (ii)- (iv) are obvious.Clearly , $\gamma_g(K_p) = \gamma_g(\bar{K}_p) = p$. Suppose $\gamma_g(G) = p$ and $G = K_p . \bar{K}_p$ Then G has at least one edge uv and a vertex w not adjacent to , say v. Then $V - \{v\}$ is a global dominating set and $\gamma_g(G) \leq p - 1$.For some graphs including trees, γ_g is at most equal to γ.

Theorem: Let S be a minimum dominating set of G. If there exists a vertex v in V- S adjacent to only vertices in S, then $\gamma_g \leq \gamma+1$
Proof: This follows since $S \cup \{v\}$ is a global dominating set.

Theorem: For a (p, q) graph G without isolates.
$(2q - p(p-3)) / 2 \leq \gamma_g \leq p - \beta_0 + 1$
Proof : Let S be a minimum global dominating set.
Then every vertex in V–S is not adjacent to at least one vertex in S. This implies $q \leq (p/2) - (p-\gamma_g)$ and the lower bound $(2q - p(p-3)) / 2 \leq \gamma_g$ follows. To establish the upper bound, let B be an independent set with β_0 vertices. Since G has no isolates, $V - B$ is a dominating set of G. Clearly, for $v \in B$,$(V - B) \cup \{v\}$ is a global dominating set of G, and upper bound follows.Since $\alpha_0 + \beta_0 = p$ for any graph of order p without isolates , We have from $(2q - p(p-3)) / 2 \leq \gamma_g \leq p - \beta_0 + 1$.

3. THE GLOBAL SET - DOMINATION NUMBER OF A GRAPH

Theorem: In a tree T with p vertices and e end vertices , that is not a star , the set of non end vertices forms a minimum global set domination-set and $\gamma_{sg} = p - e$
Proof: It is known that the set D of all cut vertices of T forms a γ_s set of T and $\gamma_s = p - e$. Clearly, the sub graph $\langle V(T) -$

$D\rangle$ in $\bar{T}$ is complete. Since $T \neq K_{1,n}$, in $\bar{T}$, each vertex in V(T) – D is adjacent to some vertex in D.
This implies that D is an set domination set of $\bar{T}$ also, and $\gamma_{sg} = p - e$.

Theorem: Let G be a connected graph of order $p \geq 4$. Then, $2 \leq \gamma_{sg} \leq p - 2$.
Proof: Let u and v be adjacent vertices of degree at least two(such vertices clearly exist).Then V – { u , v } is a global s d – set of G .so $\gamma_{sg} \leq p-2$. The bounds in $2 \leq \gamma_{sg} \leq p - 2$ are sharp . The upper bound is attained by paths of length at least 3 and the 5- cycle. All graphs for which the lower bound is attained can be determined.

Theorem: For a graph G of order p , $\gamma_{sg} = 2$ if and only if diam G = diam $\bar{G}$ = 3 and either G or $\bar{G}$ has a bridge which is not an end edge.
Proof: Assume $\gamma_{sg} = 2$. Since diam $G \leq \gamma_s + 1$, We have diam $G \leq 3$ and diam $\bar{G} \leq 3$, Now let D = { u , v } be a γ_{sg} - set of G. Suppose u and v are adjacent in G . All vertices in V(G) – D are adjacent to either u or v (but not to both).
If all such vertices are adjacent to only u (or v) in G, then $\bar{G}$ is disconnected. Hence, some vertices of V(G) – D are adjacent to u and some are adjacent to v. If $x \in N(u) - \{v\}$ and $y \in N(v)-\{u\}$, then x and y are not adjacent in G , for otherwise, {u ,v } will not be an set domination set in $\bar{G}$. Thus, uv is a bridge in G that is not an end edge, and d(x , y) – 3 – diam G. Also in G , d(u , v) = 3 and hence , diam $\bar{G}$ =3. Conversely, if G has a bridge uv that is not an end edge, and diam G = diam $\bar{G}$ =3 , then every vertex in G is adjacent to u or to v and hence { u , v } is a γ_s – set in G. let $N_G(u)$ be the set of all neighbours of u in G.Then, $N_G(u) = N_G[v]$, Since uv is a bridge in G, every vertex of $N_G(u) - \{v\}$ is adjacent to every vertex of $N_G(v) - \{u\}$ in $\bar{G}$.
Hence {u, v} is an set domination set of $\bar{G}$, and $\gamma_{sg} = 2$.

4. SOME NEW RESULTS ON GLOBAL DOMINATING SET

Lemma: For cycle C_n, let C_n' be the graph obtained by duplication of a vertex x by x' where $x \in V(C_n)$. If S is a dominating set of C_n containing either of the vertices which are adjacent to x, then S is also a dominating set of C_n'.
Proof : If $x \in V(C_n)$ is duplicated by a vertex x' then $V(C_n') = V(C_n) \cup \{x'\}$. Now if S is a dominating set of C_n and $a \in S$ $(a \neq x)$ dominates x then a is adjacent to x' in C_n'.
Thus, a dominates x' in C_n'. That is, S is a dominating set of C_n'.

Theorem: Let C_n' be the graph obtained by duplication of a vertex x of C_n by x'. If S is a global dominating set of C_n containing either of the vertices which are adjacent to x then S is also a global dominating set of C_n'.
Proof: If S is a global dominating set of C_n then S is a dominating set of C_n as well as $\bar{C}_n$. As S is a dominating set of C_n then according to above Lemma , S is also a dominating set of C_n'.
To prove the required result it remains to show that S is a dominating Set of $\bar{C}_n'$. For that if $a \in S$ is adjacent to x in C_n' then it is not adjacent. to x in $\bar{C}_n'$. Now, S being a dominating set of $\bar{C}_n$ $\exists$ a vertex $b \in S$, $a \neq b$ such that b is not adjacent to x in C_n but dominates x in C_n. As $a \in S$ is adjacent to both x and x' in C_n' implies that it is not adjacent to both x and x' in $\bar{C}_n'$. Moreover, $V(\bar{C}_n') = V(\bar{C}_n) \cup \{x'\}$ and S is a dominating set of $\bar{C}_n$ then above referred vertex $b \in S$ must dominate x' in $\bar{C}_n'$. Hence, S is also a dominating set of $\bar{C}_n$. Thus, S is a dominating set of both C_n' as well as $\bar{C}_n'$. Therefore, S is a global dominating set of C_n'.

Theorem: If S is a γ-set of P_n $(n \geq 6)$ then S is a global dominating set of P_n. Also $\gamma(P_n) = \gamma_g(P_n)$.

Proof For P_n, $n \geq 6$, consider a γ-set, $S = \{v_2, v_5, \ldots, v_{3j+2}\}$ if $n \equiv 0$ or 2(mod 3) and $S = \{v_2, v_5, \ldots, v_{3j+2}\} \cup \{v_{n-1}\}$ if $n \equiv 1$(mod 3) where $0 \leq j \leq [n-2/3]$. In P_n, there are two vertices of degree 1 and (n − 2) internal vertices are of degree 2. Now, let $v_i \in S$ and $v_j \in S$ be any two vertices such that $v_j \notin N[v_i]$.Then we claim that these two vertices are sufficient to dominate remaining vertices of $\bar{P}_n$. Since the vertices which are not in $N(v_i)$ must belong to $N(v_j)$, any $S \subset V$ containing v_i and v_j will be a dominating set of $\bar{P}_n$. Thus, S is a dominating set of both P_n as well as $\bar{P}_n$. Hence, S is a global dominating set of P_n. Since, S being a γ-set, it is of minimum cardinality. Therefore, $\gamma(P_n) = \gamma_g(P_n)$ for $n \geq 6$.

Theorem: S is a global dominating set of P_n if and only if it is a global dominating set of P_n'.
Proof: For P_n $(n \geq 4)$, consider the global dominating set $S = \{v_2, v_5, v_8, \ldots, v_{3j+2}\}$ if $n \equiv 0$or2(mod 3) and $S = \{v_2, v_5, v_8, \ldots, v_{3j+2}\} \cup \{v_{n-1}\}$ if $n \equiv 1$(mod 3) where $0 \leq j \leq [n-2/3]$. There are three possibilities when duplication of a vertex of P_n takes place. (i) Duplication of a pendant vertex. (ii) Duplication of an internal vertex not belonging to S. (iii) Duplication of an internal vertex belonging to S.
Case-I: Either a pendant vertex or an internal vertex of P_n not belonging to S is duplicated.

Here, a duplicated vertex v' is adjacent to a vertex in above referred S and $V(P_n') = V(P_n) \{v'\}$.Hence, S is a global dominating set of P_n'

Case-II An internal vertex of P_n belonging to S is duplicated. For P_n ($n \geq 4$), consider the global dominating set $S = \{v_1, v_4, v_7, \ldots, v_{3j+1}\}$if $n \equiv 1$ or 2(mod 3) and $S = \{v_1, v_4, v_7, \ldots, v_{3j+1}\} \cup \{v_n\}$ if $n \equiv 0$(mod 3) where $0 \leq j \leq [n-1/3]$. Here the duplicated vertex v' is adjacent to a vertex in above referred S and $V(P_n') = V(P_n) \cup \{v'\}$. Hence S is a global dominating set of P_n'. Conversely, suppose that S is a global dominating set of P_n'. Therefore, S is a dominating set of both as in P_n' and $\overline{P}_n'$. But $V(P_n') = V(P_n) \cup \{v'\}$ and $V(\overline{P}_n') = V(\overline{P}_n') \cup \{v'\}$. Moreover, S being a global dominating set of P_n' a vertex in S which will dominate both the vertices v and v' in P_n' as well as in $\overline{P}_n'$. Hence, S is a dominating set of both P_n and $\overline{P}_n$. Therefore, S is a global dominating set of P_n. Hence, we have proved that S is a global dominating set of P_n if and only if it is a global dominating set of P_n'.

5.GLOBAL NEIGHBORHOOD DOMINATION NUMBER

Theorem: D be a minimum dominating set of G. Then $\gamma_{gn}(G) \leq 1 + \gamma(G)$ iff there is a vertex υ in V – D satisfying:(i)$N(\upsilon) \subset D$, each of the vertices in $N(\upsilon)$is isolated in $< D >$.(ii) $\upsilon_1 \in V - D$ ($\upsilon \neq \upsilon_1$) satisfies (i) then $N(\upsilon) \cap N(\upsilon_1) \neq \emptyset$.

Proof: Assume that $\gamma_{gn}(G) = 1 + \gamma(G)$. Then there is a vertex υ in V – D satisfying (i) and (ii), otherwise $\gamma_{gn}(G) = \gamma(G)$ which is a contradiction. Assume that the converse holds. Then $D \cup \{v\}$ is a gnd – set in G and D is not a gnd – set in G. Thus $D \cup \{v\}$ is a minimum gnd – set in G. Hence $\gamma_{gn}(G) = |D \cup \{\upsilon\}| = \gamma_c(G)+1$.

Theorem:G be a connected graph, the $\gamma(G) \leq \gamma_{gn}(G) \leq \gamma_c(G)$.

Proof: Clearly $\gamma(G) \leq \gamma_{gn}(G)$. Since any connected dominating set for G is a gnd – set for G, $\gamma_{gn}(G) \leq \gamma_c(G)$. Hence $\gamma(G) \leq \gamma_{gn}(G) \leq \gamma_c(G)$.

Theorem: G be a connected graph with $g(G) > 3$, then $\gamma_g(G) \leq \gamma_{gn}(G)$.

Proof: By hypothesis, every gnd – set is a global dominating set in G. Hence $\gamma_g(G) \leq \gamma_{gn}(G)$.

Theorem:(Characterization Result): G be a connected graph. $D \subset V$ is a gnd – set of G iff each vertex in V – D lies on an edge whose end points are totally dominated by the vertices in D.

Proof: Assume that D is a gnd – set for G. Let $\upsilon_1 \in V - D$.Since D is a dominating set for G there is a $\upsilon_2 \in D$ such that $\upsilon_1 \upsilon_2 \in E(G)$. Since D is dominating set for G^N there is a $\upsilon_3 \in D$ such that $< \upsilon_1 \upsilon_4 \upsilon_3 >$ is a path in G for some $\upsilon_4 \in V(G)$. If $\upsilon_4 \neq \upsilon_2$ then υ_1 lies on the edge $\upsilon_1 \upsilon_4$, where υ_1 is dominated by υ_2 and υ_4 is dominated by υ_3 ($\upsilon_2, \upsilon_3 \in D$). If $\upsilon_4 = \upsilon_2$, then υ_1 lies on the edge $\upsilon_1 \upsilon_2$, where υ_1 is dominated by υ_2 and υ_2 is dominated by υ_3($\upsilon_2, \upsilon_3 \in D$). So in either case υ_1 lies on the edge whose end points are totally dominated by the vertices in D. Assume that the converse holds.

Let $\upsilon_1 \in V - D$. Then by our assumption there is a $\upsilon \in V(G)$, $\upsilon_3, \upsilon_4 \in D$ such that $\upsilon_1\upsilon_3, \upsilon_2\upsilon_4 \in E(G)$.

Case(i): Suppose $\upsilon_2 = \upsilon_3$

Then $<\upsilon_1 \upsilon_2 \upsilon_4>$ is a path in G.

$\Rightarrow \upsilon_1\upsilon_4 \in E(G^N), \upsilon_4 \in D$.

Case(ii): Suppose $\upsilon_2 \neq \upsilon_3$

Then $< \upsilon_3\upsilon_1\upsilon_2\upsilon_4 >$ is a path in G.

$\Rightarrow \upsilon_1\upsilon_4 \in E(G^N), \upsilon_4 \in D$

Therefore υ_1 is dominated by υ_3 in G and by υ_4 in G^N.Since υ_1 is arbitrary, D is a gnd – set of G.

6 CONCLUSION

In This paper deals about "A Review on global domination number of a graph".We discuss some structural properties corresponding to the concept of global dominating sets. Analogous results can be obtained for other graph families and in the context of various types of dominating sets in graphs.

REFERENCE:

[1] E. Sampathkumar, The global domination number of a graph, J. Math. Phys.Sci., 23.

[2] S. K. Vaidya and R. M. Pandit, Some new results on global dominating sets, ISRN Discrete Mathematics,vol. 2012

[3] E.J.Cockayne and S.T.Hedetnimi, Towards a theory of Domination in graphs,networks7.

[4] F.Harary, Graph theory , Addition Wesley, Reading, M.A.

[5] S.T.Hedetniemi and R.Laskar, Connected Domination in Graphs, Graph Theory and Combinatorics,B.Bollabas,Ed. Academic Press, London.

[6] S.T.Hedetniemi, R.Laskar and J.Pfaff, Irredundance in Graphs; A Survey Technical Report, Clemson University.

[7] Bondy J. A. and Murthy, U. S. R., Graph theory with Applications, The Macmillan Press Ltd.

[6] R. C. Brigham, R. D. Dutton,On Neighbourhood Graphs, J. Combin. inform. System Sci, 12.

[8] G. S. Domke, etal., Restrained Domination in Graphs, Discrete Mathematics,203.

[9] T. W. Haynes, S. T. Hedetneimi, P. J. Slater, Fundamentals of Dominations in Graphs Marcel Dekker, New York.

[10] I. H. Naga Raja Rao, S. V. Siva Rama Raju, On Semi-Complete Graphs, International Journal Of Computational Cognition, Vol.7(3).

[11] D. F. Rall, Congr. Numer., 80.

[12] E. Sampathkumar, H. B. Walikar,The connected Domination Number of a Graph, J. Math. Phy. Sci, Vol.13.

A Review on Lower Bounds for the Domination Number	A.Praveenkumari Assistant Professor of Mathematics	Maths	International Journal of Mathematics Trends and Technology (IJMTT)	April 2017	ISSN: 2231-5373 (P:89-93)	**UGC Approved Journal in 2017** https://www.ijmttjournal.org/2017/Volume-44/number-2/IJMTT-V44P518.pdf

A Review on Lower Bounds for the Domination Number

[1] G.Geetha [2] A.Praveenkumari

[1]*Research Scholar, Sakthi College of Arts and Science for Women, Oddanchatram.*

[2]*Assistant Professor, Department of Mathematics, Sakthi College of Arts and Science for Women, Oddanchatram.*

ABSTRACT – *We prove several Lower bounds on the domination number of simple connected graph. In this paper we prove that* $(2k+1)\ \gamma_k(T) \geq |v| + 2k - kn_1$ *for each tree.* $T=(V,E)$ *with* n_1 *leafs, and we characterize the class of tree that satisfy the equality* $(2k+1)\ \gamma_k(T) \geq |v| + 2k - kn_1$.

Keywords: *Domination, Distance domination number, Tree.*

1. INTRODUCTION

Domination in graphs has been studied extensively in recent years. The study of domination in graphs originated around 1850 with the problems of placing minimum number of queens on an n × n chessboard so as to cover or dominate every square. With very few exceptions these problems still remain unsolved today. The theory of domination in graphs introduced by Ore and Berge is an emerging area of research in graph theory today

Berge presents the problem of five queens, namely, place five queens on the chess board so that every square is covered by at least one queen. The solution to these problems are nothing but dominating sets in the graph, whose vertices are the queens of the chessboard and vertices u,v are adjacent if a queen move from u to v in one move. This leads to domination in graphs.

2. APPLICATION OF GRAPH THEORY

Graph theoretical concepts are widely used to study and model various applications, in different areas. They include, study of molecules, construction of bonds in chemistry and the study of atoms. Similarly, graph theory is used in sociology for example to measure actors prestige or to explore diffusion mechanisms.

Graph theory is used in biology and conservation efforts where a vertex represents regions where certain species exist and the edges represent migration path or movement between the regions. this information is important when looking at breeding patterns or tracking the spread of disease, parasites and to study the impact of migration that affect other species. Graph theoretical concepts are widely used in Operations Research. For example, the travelling salesman problem, the shortest spanning tree in a weighted graph, obtaining an optimal match of jobs and men and locating the shortest path between two vertices in a graph. It is also used in modeling transport networks, activity networks and theory of games.

The network activity is used to solve large number of combinatorial problems. The most popular and successful applications of networks in OR is the planning and scheduling of large complicated projects. The best well known problems are PERT(project Evaluation Review Technique)and CPM(Critical Path Method). Next, Game theory is applied to the problems in engineering, economics and war science to find optimal way to perform certain tasks in competitive environments to represent the method of finite game a digraph is used. Here, the vertices represent the positions and the edges represent the moves. Everything in our world is linked cities are linked by street, rail and flight networks. Pages on the internet are linked by hyperlinks. The different components of an electric circuit or computer chip are connected and the paths of disease outbreaks form a network. Scientists, engineers and many others want to analyze, understand and optimize these networks. And this can be done using graph theory. For example, mathematicians can apply graph theory to road networks, trying to find a way to reduce traffic

congestion. An idea which, if successful, could save millions every year which are lost due to time spent on the road as well as mitigating the enormous environmental impact. it could also make life safer by allowing emergency services to travel faster and avoid car accidents in the first place.These intelligent transportation systems could work by collecting location data from smart phones of motorists and telling them where and how fast to drive in order to reduce overall congestion.

Graph theory is already utilized on flight networks. Airlines want to connect countless cities in the most efficient way, moving the most passengers with the fewest possible trips a problem very similar to the travelling Salesman. At the same time, air traffic controllers need to make sure hundreds of planes are at the right place at the right time and donot crash an enormous task that would be almost impossible without computers and graph theory. One area where speed and the best connections are of crucial importance is the design of computer chips. Integrated circuits(ICs) consist of millions of transistors which need to be connected. Although the distances are only a few millimeters, it is important to optimize these countless connections to improve the performance of the chip. Graph theory also plays an important role in the evolution of animals and languages, crowd control and the spread of diseases.

3. LOWER BOUNDS FOR THE DOMINATION NUMBER

Several lower bounds on the domination number of simple connected graphs. Among these are the following: the domination number is at least two-thirds of the radius of the graph, three times the domination number is at least two more than the number of cut-vertices in the graph, and the domination number of a tree is at least as large as the minimum order of a maximal matching.

Theorem: Let G be a connected graph with n > 1 and diameter d. Then,

$$\gamma \geq \frac{d+1}{3}$$

Proof : Since the diameter can actually equal the radius, it is sometimes twice as good as a lower bound on the domination number (take cycles for instance). Moreover, it is similar to the well known result that the independence number is at least the radius – originally a conjecture of Graffiti and proven independently several times. In addition, it is that the total domination number (that is, the cardinality of a set of minimum order having the property that every vertex in the graph is adjacent to a vertex in the set) is at least the radius.

Theorem: Let G be a connected graph with n > 1. Then, $\gamma \geq \frac{2}{3}r$ Moreover, this bound is sharp.

Proof : Let D be a minimum dominating set of G. Form a spanning tree T of G, as prescribed in statement, so that D is also a minimum dominating set of T. Since $r(G) \leq r(T)$, $2r(T) - 1 \leq d(T)$ (because T is a tree) and $\gamma(T) = \gamma(G)$,we can apply to T and obtain the following chain of inequalities:

$2r(G) - 1 \leq 2r(T) - 1 \leq d(T) \leq 3\gamma(T) - 1 = 3\gamma(G) - 1.$

Equality holds in the bound above for cycles with orders congruent to 0 modulo 6. On the other hand, the tree obtained by algamating a pendant vertex to each vertex of a path has radius about n/3 while it has domination number of $\frac{n}{2}$ – thus showing that the difference between these two expressions can be made arbitrarily large.

Theorem 3.1.3

For any connected graph G with x cut-vertices,

$$\gamma \geq \frac{x+2}{3}$$

Moreover, this bound is sharp.

Proof

Let D be a minimum dominating set of G. Form a spanning tree T of G, as prescribed in statement. So that D is also a minimum dominating set of T. Let x(T) denote the number of cut-vertices of T and note that $x(T) \geq x$, since any cut-vertex of G is also a cut-vertex of T. Now, applying Theorem to T we find,

$$\gamma(G) = \gamma(T) \geq \frac{n-1(T)+2}{3} = \frac{x(T)+2}{3} \geq \frac{x+2}{3}$$

If T is a tree such that the distance between any two leaves is congruent to 2 modulo 3. Since for trees, the number of cut-vertices is exactly n − l, equality

holding in The sufficient condition for equality holding in the above Theorem. An example of a graph here equality holds in this Theorem that is not necessarily a tree is a graph with a cut-vertex of degree n − 1. Since cycles have no cut-vertices, the difference between the expressions in Theorem can be made arbitrarily large.

4. LOWER BOUNDS ON THE DISTANCE DOMINATION NUMBER OF A GRAPH

Let k ≥ 1 be an integer and let G be a graph. In 1975, Meir and Moon introduced the concept of a distance k-dominating set (called a "k-covering") in a graph. A set S is a k-dominating set of G if every vertex is within distance k from some vertex of S; that is, for every vertex v of G, we have d(v, S) ≤ k. The k-*domination number* of G, denoted $\gamma_k(G)$, is the minimum cardinality of a k-dominating set of G. When k = 1, the 1-domination number of G is precisely the domination number of G; that is, $\gamma_1(G) = \gamma(G)$.

Lemma: For k ≥ 1, every connected graph G has a spanning tree T such that $\gamma_k(T) = \gamma_k(G)$.

Proof : Let S = $\{V_1, \ldots, V_l\}$ be a minimum k-dominating set of G. Thus, |S| = ℓ = γ_K(G). We now partition the vertex set V (G) into ℓ sets $V_1, \ldots, V_l$ as follows.

Initially, we let $V_i = \{V_i\}$ for all i ∈ [ℓ]. We then consider sequentially the vertices not in S. For each vertex v ∈ V (G) \ S, we select a vertex V_i ∈ S at minimum distance from v in G and add the vertex v to the set V_i. We note that if v ∈ V (G) \ S and v ∈ V_i for some i ∈ [ℓ], then d_G (v, v_i) = d_G (v, S), although the vertex V_i is not necessarily the unique vertex of S at minimum distance from v in G. Further, since S is a k-dominating set of G, we note that d_G(v, V_i) ≤ k. For each i ∈ [ℓ], let T_i be a spanning tree of G[V_i] that is distance preserving from the vertex v_i; that is, V (T_i) = V_i and for every vertex v ∈ V (T_i), We have d_{T_i} (v, V_i) = d_G (v, V_i). We now let T be the spanning tree of G obtained from the disjoint union of the ℓ trees $T_1, \ldots, T_l$ by adding ℓ − 1 edges of G. We remark that these added ℓ − 1 edges exist as G is connected. We now consider an arbitrary vertex, v say, of G. The vertex v ∈ V_i for some i ∈ [ℓ]. Thus d_T (v, V_i) ≤ d_{T_i} (v, V_i) = d_G(v, V_i) = d_G (v, S) ≤ k. Therefore, the set S is a k-dominating set of T, and so γ_K (T) ≤ |S| = γ_K (G). However, by Observation , γ_K (G) ≤ γ_K (T).

Lemma :

Let G be a connected graph that contains a cycle, and let C be a shortest cycle in G. If v is a vertex of G outside C that k-dominates at least 2k vertices of C, then there exist two vertices u,w ∈ V (C) that are both k-dominated by v and such that a shortest (u, v)-path does not contain w and a shortest (v,w)-path does not contain u.

Proof : Since v is not on C, it has a distance of at least 1 to every vertex of C. Let u be a vertex of C at minimum distance from v in G. Let Q be the set of vertices on C that are k-dominated by v in G. Thus, Q ∈ V (C) and, by assumption, |Q| ≥ 2k. Among all vertices in Q, let w ∈ Q be chosen to have maximum distance from u on the cycle C. Since there are 2k − 1 vertices within distance k − 1 from u on C, the vertex w has distance at least k from u on the cycle C. Let P_u be a shortest (u, v)-path and let P_w be a shortest (v,w)-path in G. If w ∈ V (P_u), then d_G (v,w) < d_G (v, u),contradicting our choice of the vertex u. Therefore w ∉ V (P_u). Suppose that u ∈ V (P_w). Since C is a shortest cycle in G, the distance between u and w on C is the same as the distance between u and w in G. Thus, d_G (u,w) = d_C (u,w), implying that d_G (v,w) = d_G (v, u) + d_G (u,w) ≥ 1 + d_G (u,w) = 1 + d_C (u,w) ≥ 1 + k, a contradiction. Therefore, u ∉ V (P_w).

4.1 Lower bound

We provide various lower bounds on the k-domination number for general graphs.

Theorem: For k ≥ 1, if G is a connected graph with diameter d, then $\gamma_K G) \geq \frac{d+1}{2K+1}$

Proof : Let P : u_0 u_1 . . . u_d be a diametral path in G, joining two peripheral vertices u = u_0 and v = u_d of G. Thus, P has length diam(G) = d. We show that every vertex of G k-dominates at most 2k+1 vertices of P. Suppose, to the contrary, that there exists a vertex in the q ∈ V (G) that k-dominates at least 2k +2 vertices of P. (Possibly, vertax q ∈ V (P).

Let Q be the set of vertices on the path P that are k-dominated by the vertex q in G. By

supposition, $|Q| \geq 2k + 2$. Let i and j be the smallest and largest integers, respectively, such that $u_i \in Q$ and $u_j \in Q$. We note that $Q \subseteq \{u_i, u_{i+1}, \ldots, u_j\}$. Thus, $2k + 2 \leq |Q| \leq j - i + 1$. Since P is a shortest (u, v)-path in G, we therefore note that vertax $d_G(u_i, u_j) = d_P(u_i, u_j) = j - i \geq 2k + 1$.

Let P_i be a shortest (u, q)-path in G and let P_j be a shortest (q, v)-path in G. Since the vertex q k-dominates both u_i and u_j in G, both paths P_u and P_v have length at most k. Therefore, the (u_i, u_j)-path obtained by following the path P_i from u_i to q, and then proceeding along the path P_j from q to u_j, has length at most 2k, implying that $d_G(u_i, u_j) \leq 2k$, a contradiction.

Therefore, every vertex of G k-dominates at most 2k + 1 vertices of P.

Let S be a minimum k-dominating set of G. Thus, $|S| = \gamma_K(G)$. Each vertex of S k-dominates at most 2k + 1 vertices of P, and so S k-dominates at most |S|(2k + 1) vertices of P. However, since S is a k-dominating set of G, every vertex of P is k-dominated the set S, and so S k-dominates |V (P)| = d + 1 vertices of P. Therefore, $|S|(2k + 1) \geq d + 1$, or, equivalently, $\gamma_K(G) = (d + 1)/(2k + 1)$. That the lower bound of Theorem 4.3.3 is tight may be seen by taking G to be path, $v_1 v_2 \ldots v_n$, of order $n = \ell(2k + 1)$ for some $\ell \geq 1$.

Let that the d = diam(G), and so $d = n - 1 = \ell(2k + 1) - 1$. By Theorem such that $\gamma_K(G) \geq \frac{(d+1)}{(2K+1)} = \ell$. The set

$$s = \bigcup_{i=0}^{l-1} \{v_{k+1+i(2k+1)}\}$$

is a k-dominating set of G, and so $\gamma_K(G) \leq |S| = \ell$.

Consequently, $\gamma_K(G) = \ell = \frac{(d+1)}{(2K+1)}$.

5. A LOWER BOUND FOR THE DISTANCE K-DOMINATION NUMBER OF TREES

A subset D of vertices of a graph G = (V,E) is a distance k-dominating set for G if the distance between every vertex of V − D and D is at most k. The minimum size of a distance k-dominating set of G is called the distance k-domination number $\gamma_K(G)$ of G. In this paper we prove that $(2k + 1)\gamma_K(T) \geq |V| + 2k - kn_1$ for each tree T = (V,E) with n1 leafs, and we characterize the class of trees that satisfy the equality

$$(2k+1)\gamma_K(T) = |V| + 2k - kn_1.$$

Lemma: Let T be a tree with $\gamma_K(T) > 1$. Then there exists an edge uv in T such that

$$\gamma_K(T) = \gamma_K(T_u) + \gamma_K(T_v).$$

Proof :

Let $P = v_0 v_1 \ldots v_l$ be a longest path in T. Since $\gamma_K(T) > 1$, we have $l \geq 2k + 1$. Now let D be a minimum distance k-dominating set of T such that (1) $v_K \in D$ and (2) $\sum_{x \in d} d(x, p)$ is minimal.

For $1 \leq i \leq l-1$ let T_i be the component of $T - \{v_{i-1}v_i, v_i v_{i+1}\}$ that contains the vertex v_i. Note that condition (2) implies that all verticesx $\in V(T_i) \cap D$ satisfy the inequality $d(v_i, x) \leq i - k$ for $i \geq k$.

Let the a $0 \leq p \leq k$ be the greatest integer such that v_K has at least one private k-neighbor in $T_K + p$.

We will now show that $d(v_{K+p}, v) \leq k - p$ for all vertices $v \in V(T_{K+p})$, i.e., $V(T_{K+p}) \in N^k[v_K]$.

Let the theorem of the $y \in PN^k[v_K, D] \cap V(T_{K+p})$ be a private k-neighbor of v_K In T_{K+p} and suppose that $z \in V(T_K + p) - N_K[v_K]$ Is not a k-neighbor of v_K.

Then $d(v_{K+p}, y) \leq k - p$ and $k - p + 1 \leq d(v_{K+p}, z) \leq k + p$ (the latter inequality holds because P is a longest path in T). In addition, there exists a vertex $v_K \neq x \in D$ such that $Z \in N^k[x]$. y is also a k-neighbor of x.

Suppose first that $x \notin V(T_{K+p})$. Since $d(x, v_{K+p}) \overset{(2)}{\leq} p$ and $d(v_{K+p}, y) \leq k - p$, it follows that $d(x, y) \leq d(x, v_{K+p}) + d(v_{K+p}, y) \leq k$, a contradiction. Suppose second that $x \in V(T_{K+p})$, i.e., $x \in V(T_j)$ for an integer of a $1 \leq j \leq l - 1$.

Then d(x, y) = d(x, v_j) + d(v_j , v_{K+p}) + d(v_{K+p}, y) ≤ d(x, v_j) + d(v_j , v_{K+p}) + d(v_{K+p}, z) = d(x, z) and thus, since z ∈ N_K [x], we conclude that y ∈ N^k [x], a contradiction.

Let us now remove the edge uv =$v_{k+p}v_{k+p+1}$. We shall show now that {v_k} is a distance k-dominating set of T_u and that D−v_k is a distance k-dominating set of T_v which completes the proof.

Since v_k has no private k-neighbor in T_v, it is immediate that D − v_k is a distance k-dominating set of T_v. Now assume that there exists a vertex y ∈ V (T_u) that is no k-neighbor of v_k.

Then y ∈ V (T_k+q) for an integer 1 ≤ q ≤ p − 1 and d(v_{k+q}, y) ≥ k − q + 1.

Let v_k ≠ x ∈ D be a k-neighbor of y. We shall now conclude a contradiction to the assumption that v_K has a private k-neighbor in T_{K+p}. Let x ∈ V (T_{K+j}) for an integer 1 ≤ j ≤ l − 1 and let z be an arbitrary vertex of T_{K+p}.

Then

d(x, z) ≤ d(x, v_{K+j}) + d(v_{K+j} , v_K+$_p$) + d(v_{k+p}, z) ≤ j + (p − j) + (k-p)=k

6. CONCLUSION

In this paper, "A review on Lower Bounds for the Domination Number" can make an in depth study in graphs and its related works. We also discussed about the properties of the Lower bounds for the domination number. We also arrived out Lower bounds on The distance domination number of a Graph. Also we preliminary Lemmas of Lower bound on the distance domination and we obtain certain direct Product graph on connection with other lower bounds on the distance domination.

REFERENCES

1. F.Haray, Graph Theory (Addison Wesley, Reading, Mass, 1969).
2. T.W.Haynes, S.T. Hedetniemi and P.J. Slater, Fundamentals of domination in Graphs, Marcel Dekker, New York, 1998
3. B.Bollobas and E.J. Cockayne, J.Graph Theory 3(3),241 (1979) http://dx.doi.org/10.1002/jgt.3190030306
4. S. Arumugam and S.Velammal, Taiwanese J.Math 2(2),173 (1998).
5. M.Lemanska, Lower Bound on the domination Number of a graph, Discuss Math Graph Theory 24 (2004), 165-170.
6. J.Cyman, M.Lemanska and J.Raczek, Lower Bound on the distance k-domination number of a tree, math Slovaca 56(2) (2006), 235-243.
7. A.Henning, Caleb Fast and Franklin Kenter, Lower Bound on the distance domination Number of a Graph.
8. D.F.Rall, Total domination in Categorical Product of graphs. Discuss Math Graph Theory 25 (2005) 35-44.
9. M.Valencia Pabon, Idomantic Partitions of direct product of complete graphs Discrete Math 310 (2010) 1118-1122.
10. B.Bresar, S. Klavzar, D.F.Rall, Dominating direct products of graphs. Discrete Math 307 (2007) 1636-1642